Understanding the Role of the PALB2-BRCA1 Interaction in Tumor Suppression

by

AMAR HEKMAT MAHDI

A Dissertation submitted to the Graduate School-New Brunswick

Rutgers, The State University of New Jersey

and

The Graduate School of Biomedical Sciences

In partial fulfillment of the requirements for the degree of

Doctor of Philosophy

Graduate Program in Physiology and Integrative Biology

Written under the direction of

Dr. Bing Xia

And approved by

_____

_____

_____

_____

_____

New Brunswick, New Jersey

May 2017

ABSTRACT OF THE DISSERTATION

Fundamental role of the PALB2-BRCA1 Interaction in Tumor Suppression

By Amar Hekmat Mahdi

Dissertation Director: Dr. Bing Xia

Homologous recombination (HR) is the only error-free pathway for the repair of DNA double strand breaks (DSBs). BRCA1 and BRCA2, the two major breast cancer suppressor proteins, play essential roles in HR-mediated repair of DSBs by promoting the recruitment of RAD51, the recombination enzyme, to DNA damage sites for the initiation of HR. PALB2 (partner and localizer of BRCA2) plays a key role in this pathway by acting as a chromatin adaptor for BRCA2 and a linker between BRCA1 and BRCA2. Like *BRCA1* and *BRCA2*, *PALB2* is a tumor suppressor gene itself. Germline, heterozygous mutations in the gene increase the risk of breast, ovarian and pancreatic cancers. However, its mechanism is not fully understood. To investigate the *in vivo* role of the PALB2-BRCA1 interaction, we previously generated a *Palb2* knockin mouse strain that contains a mutation that disrupts BRCA1 binding. This mouse model also allows us to bypass the embryonic lethality of the *Palb2* KO mice.

In this study, we hypothesized that the direct communication between the two proteins is critical for proper DNA damage repair and response *in vivo* and for suppression of tumorigenesis. Indeed, both immunohistochemistry (IHC) and immunofluorescence (IF) demonstrated that different tissues of the *Palb2* mutant mice have higher levels of endogenous DSBs (γH2AX foci) and slower DSB

repair kinetics after ionizing radiation (IR). Yet, mutant cells were more resistant to cell death. When aged under normal conditions, mutant mice showed increased tumor incidence in multiple tissues, particularly in the liver. Upon challenging of these mutant mice with carcinogen administration or gamma irradiation, they showed accelerated tumor development as compared with wild-type (wt) mice. When crossed with *Trp53* mutant mice, the compound mutant mice showed greatly accelerated development of tumors typically associated with mutations in p53, i.e. thymic lymphoma, osteosarcoma and soft tissue sarcoma, etc.

Whole exome sequencing (WES) of the tumors arising from *Palb2m/m;Trp53*+/- mice revealed loss of the wt allele of *Trp53* in the majority of tumors, with at least some tumors showing focal deletions of the wt gene, suggesting that disruption of BRCA1-PALB2/BRCA2 axis promotes regional genomic deletions that may lead to loss of other tumor suppressors such as p53. These results underscore the importance of the BRCA1-PALB2/BRCA2 pathway for tumor suppression and suggest a potentially novel mechanism for BRCA/PALB2-mediated tumor suppression, which is by preventing *Trp53*/*TP53* loss of heterozygosity (LOH), which would allow for tumor development.

Finally, we also found constitutively elevated levels of reactive oxygen species (ROS) and activation of NF-κB, a redox sensitive transcription factor, in tissues and cells from the mutant mice. Given its established pro-survival function, NF-κB activation could explain why cells in the mutant mice are resistant to apoptosis upon irradiation despite having increased and prolonged

DNA damage. This finding also suggests that the NF-κB pathway may be a potential target for treatment of *PALB2* and *BRCA1*-associated cancers.

ACKNOWLEDGEMENTS

First of all, I am grateful to my thesis advisor, Dr. Bing Xia for his welcoming, supervising, guiding, and teaching me how to design an experiment and how to critically analyze the results. I am greatly honored to be under his supervision, many thanks.

I want to thank all the former and current members in Dr. Bing Xia lab for their support and encouragement that they provided to me during my PhD years. Srilatha Simhadri, Hong, Allen, Tzeh Keong Foo, Dr.Gabriele Vincelli, Bola Olayanju, Susan Zwyea, Kevin Lu and particularly, I appreciate the great help from Dr. Yanying Huo for her enormous technical support for my projects. To Gabriele- Thank you for your FACS help.

Next, I am sincerely grateful to my thesis advisors committee, Dr. Huizhou Fan, Dr. Shrider Ganesan, Dr. Samuel Bunting, and Dr. Chang S. Chan for their suggestions, guidance, brilliant input and feedback.

I also want to thank all vivarium and CINJ core staff for their collaboration; in particular, Shafiq Bhat from histopathology department for his help in tissues processing and blocking.

Finally, I would like to thank the Higher Committee for Education Development in Iraq (HCED) for their financial support during whole my PhD. Without their support, I would not be here today, my special thanks to my beloved wife for being on my side throughout the completion of my study all these years. And I want to thank my lovely children, Zeanab, Yaser, and Sara for providing me so much power and motivation.

TABLE OF CONTENTS

LIST OF FIGURES

LIST OF ABBREVIATIONS

Apaf-1: Apoptotic protease activating factor 1

AMPK: AMP activated protein kinase

AREs antioxidant response elements

Bad: Bcl2-associated agonist of cell death

Bak: Bcl2-antagonist/killer 1

Bax: Bcl2-associated X protein

BCL-2: B-cell lymphoma 2

BCL-XL: B-cell lymphoma extra large

Bid: BH3 interacting domain death

BIF-1: Bax-interacting factor 1

Bim: Bcl2-like 11

BRCA1: breast cancer 1, early onset

BRCA2: breast cancer 2, early onset

BrdU: Bromodeoxyuridine

DCFH-DA: 2', 7'-dicholorofluorescein-diacetate

DMBA: 7,12-dimethylbenz[α]anthracene

DMA: dimethylacetoacetamide

EMT: epithelial-mesenchymal transition

ER: endoplasmic reticulum

FOXO: forkhead box O

GADD45B: growth arrest DNA damage 45B protein

GEMMs: genetically engineered mouse models

Gy: gray

H&E: Hematoxylin and Eosin

HR: homologous recombination

IACUC: Institutional Animal Care and Use Committee

IL-6 interleukin-6

KEAP1: Kelch-like ECH-associated protein

LOH: loss of heterozygosity

MEF: mouse embryonic fibroblast

MeOH: methanol

min: minute

MOMP: mitochondrial outer membrane permeabilization

MUT: palb2 m/m Knockin mouse

NF-κB: nuclear factor kappa-light-chain-enhancer of activated B cells

NHEJ: non-homologous end joining recombination

Noxa: Phorbal-12-myristate-13-acetate-induced protein 1

NRF2: NF-E2 related factor 2

PAH : polycyclic aromatic hydrocarbon

PE: phosphotidylethanolamine

P53-binding protein 1: 53BP1, a key regulator for NHEJ

PI3P: phosphatidylinositol-3-phosphate

PINK1: PTEN-induced putative kinase 1; a Ser/Thr kinase

PUMA: p53 up-regulated modulator of apoptosis

RA: retinoic acid

RBC: red blood cells

ROS: reactive oxygen species

Smac: mitochondria derived activator of caspase

TCGA: The Cancer Genome Atlas

TFEB: transcription factor EB

TNFR1: tumor necrosis factor

TPCA-1: 2-[(Aminocarbonyl)amino]-5-(4-fluorophenyl)-3-thiophenecarboxamide

*Trp*53: transformation related protein 53

TUNEL Terminal deoxynucleotidyl transferase-mediated dUTP nick-end labeling

w: week

WDR45: WD repeat domain 45

WT: wild type mouse

CHAPTER 1

GENERAL INTRODUCTION

1.1 Role of the BRCA1-PALB2-BRCA2 complex in homologous recombination

BRCA1 and *BRCA2* are the two most frequently mutated genes found in hereditary (or familial) breast cancer. Inherited (heterozygous) mutations in these genes make the carriers more susceptible to different kinds of cancers, particularly in the breast. These two genes encode very large proteins that play critical roles in the repair of DNA double-strand breaks (DSBs) by homologous recombination (HR), as well as in DNA damage-induced cell cycle checkpoint control (1, 2). PALB2 was discovered and cloned as a major BRCA2 binding partner that controls the localization and stability of BRCA2, anchors it in the chromatin, recruits it to DNA damage sites and enables its functions in HR-repair (3). Later, PALB2 was found to also directly bind BRCA1 (4-6). Importantly, like BRCA1 and BRCA2, PALB2 itself is also a tumor suppressor mutated in breast and other cancers. To date, truncating mutations in *PALB2* have been identified in cancer families around the world. Moreover, breast cancer risk of *PALB2* mutation carriers may overlap with that of *BRCA*2 mutation carriers (7). Combined, germline mutations in the 3 genes (BRCA1, BRCA2 and PALB2) may account for ~5% of all breast cancer (8). Moreover, various studies have found hyper-methylation of *BRCA1* and *PALB2* promoters in 9-30% and 7% of sporadic breast cancer cases, respectively (9-11). Germline mutations in these genes also

increase the risk of ovarian (12), pancreatic (13) and prostate (14) cancers. Thus, understanding the molecular and genetic mechanisms as to how tumors develop following the loss of these proteins has major implications in cancer prevention and treatment.

Since the discovery of PALB2 11 years ago through its interaction with BRCA2 (3), its involvement and mechanism in HR repair have been subject to significant amount of studies. It has been shown that N terminus of PALB2 contains a coil- coil domain that directly binds to a similar coil- coil motif in BRCA1, while the C terminal WD40 repeats domain of PALB2 forms a seven bladed β-propeller structure that directly interacts with BRCA2 (Figure 1) (15, 16). As such, PALB2 acts as a liker between BRCA1 and BRCA2 to form what is called the BRCA complex (5). PALB2-deficient cells show a decrease in HR activity, intra S checkpoint defect and inability of RAD51 to form foci following DNA damage (17).

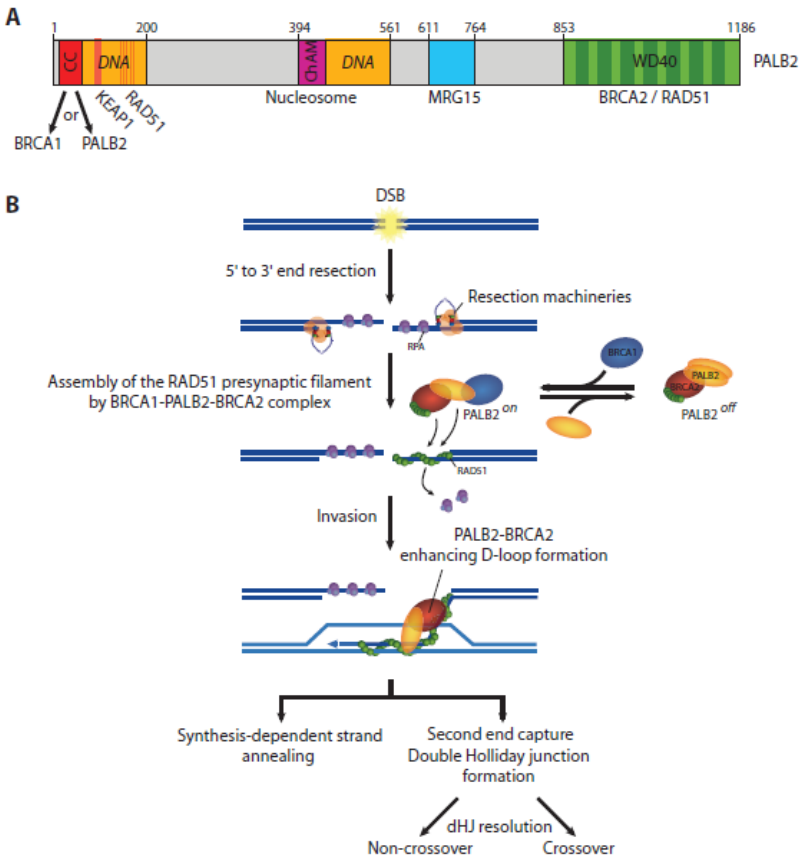

Figure1. Domain structure of PALB2 and a model of the BRCA complex in HR repair. (A&B) (adapted from Remi Buisson et al, 2012). A. PALB2 domains. **B**. Model for PALB2 in HR for DNA double stands break repair.

Complete knockout of each of the three genes in the mouse results in embryonic lethality with the induction of the cyclin-dependent kinase inhibitor p21 (18, 19), suggesting an activation of p53. Consistent with this notion, loss of p53 partially rescues the embryonic lethality and developmental defect caused by the knockout of each of the 3 genes (19, 20). Conditional knockout (CKO) of each gene in the mammary gland results in mammary tumor formation with long latency, and most of the tumors contain somatic mutations in *Trp*53 (the mouse p53 gene) (21-23). Therefore, p53 is a barrier to cell proliferation and tumorigenesis following the loss of BRCA and PALB2 proteins, and an

inactivation of p53 or other part(s) of its pathway may be a prerequisite for their associated tumorigenesis. Indeed, *BRCA1/2*- and *PALB2*-associated human breast cancers have a high frequency of somatic mutations in the *TP*53 gene (24-26). The virtually identical tumor phenotypes of human FA-D1 (BRCA2) and FA-N (PALB2) patients and the highly similar spectrum of tumor development in *PALB2* and *BRCA2* heterozygous carrier families strongly indicate that BRCA2's tumor suppressive function largely depends on its association with PALB2. However, how much of BRCA1's tumor suppressive function is transmitted by PALB2 and to what extent PALB2's function is dependent on BRCA1 have not been tested.

To understand the role of the BRCA1-PALB2 interaction in vivo, we generated a Palb2 knockin mouse strain, which contains a mutation in the coiled-coil domain that disrupts BRCA1 binding (27). Cells derived from the mutant mice displayed greatly increased chromosomal breakage following treatment with a DNA interstrand crosslinker mitomycin C (MMC) and hypersensitivity to the agent (26), indicating a significant HR and interstrand crosslink repair defect in vivo. Homozygous mutant (MUT) mice were viable without any gross developmental defects. Thus, this mouse model allows us to bypass the embryonic lethality of the *Palb*2 KO mice (18, 28) to further study PALB2 function in vivo, such as its potential roles in development, metabolic regulation and cellular hemostasis.

1.2 Apoptosis

Apoptosis by definition is programmed cell death, which occurs normally to maintain cellular homeostasis in the tissues. Apoptosis inhibits malignant transformation and a failure of apoptosis can lead to cancer development. Apoptosis is typically characterized by nuclear fragmentation, chromatin condensation, cellular shrinkage, and membrane blebbing (29). Another morphological feature of apoptosis is that the plasma membrane is intact all over the whole process without inducing the inflammatory response because apoptotic cells are well enclosed within vesicles and rapidly phagocytosed, so do not induce anti-inflammatory cytokines that distinguishes it from necrosis (30, 31). Apoptosis is activated in response to a large range of stimuli throughout development and in the event of severe cellular stress or damage. Dysregulation of apoptotic cell death mechanisms has been connected to a large numbers of physiological and pathological conditions, and deficiency in apoptosis is considered one of the hallmarks of carcinogenesis and metastasis (32).

Biochemical features of apoptosis include membrane changes, caspase activation, and DNA breakdown. At early stage of apoptosis , there is a flipping out of phosphatidylserine (PS) from the inner to outer layer of the cell membrane (33). This PS flipping out enables macrophage to recognize the apoptotic cell resulting in phagocytosis. Then, DNA of the cell starts to break down into 180-200 base pair pieces by endonucleases (34). Finally, there is activation of a class of cysteine protease named as caspases. Activated caspases not only cleave

and break down many proteins and cytoskeleton inside the cell but also activate DNases, which further digest the fragmented DNA (35).

There are three pathways for apoptosis in which caspases, upon activation, play an essential role as initiators and executioners (31)**,** namely the extrinsic or death receptor pathway, the intrinsic or mitochondrial pathway, and the intrinsic endoplasmic reticulum pathway. Eventually, these pathways unite in the activation of caspases that result in proteolytic and nuclear digestion of the cell. Caspases are divided into the upstream initiator caspases (caspase-9, caspase-2, caspase-8, and caspase-10) and the downstream executioner caspases (caspase-3, caspase-6, caspase-7, and caspase-12). Activation of caspases results in the cleavage of downstream executioner substrates that cause apoptosis.

1.2.1 The extrinsic death receptor pathway

The extrinsic apoptotic pathway triggers apoptosis in response to the binding of a death ligand with specific death receptors on the cell surface. The most well-known death receptors are members of the tumor necrosis factor receptor (TNFR) gene superfamily and Fas-associated death domain (FADD) and their ligands (36). These receptors through their intracellular domain recruit adaptor proteins like TNF receptor associated death domain (TRADD) and Fas associated death domain (FADD) (37). Activation of the death receptor by their corresponding ligands results in the formation of a complex from ligand/receptor/adaptor proteins known as the death inducing signaling complex

(DISC) as shown in the Figure 1-2. After that, DISC cleaves procaspase 8 or procaspase 10 to an active form (initiator caspase), which subsequently cleaves and activates downstream caspases 3 (executioner or effector caspase) (36).

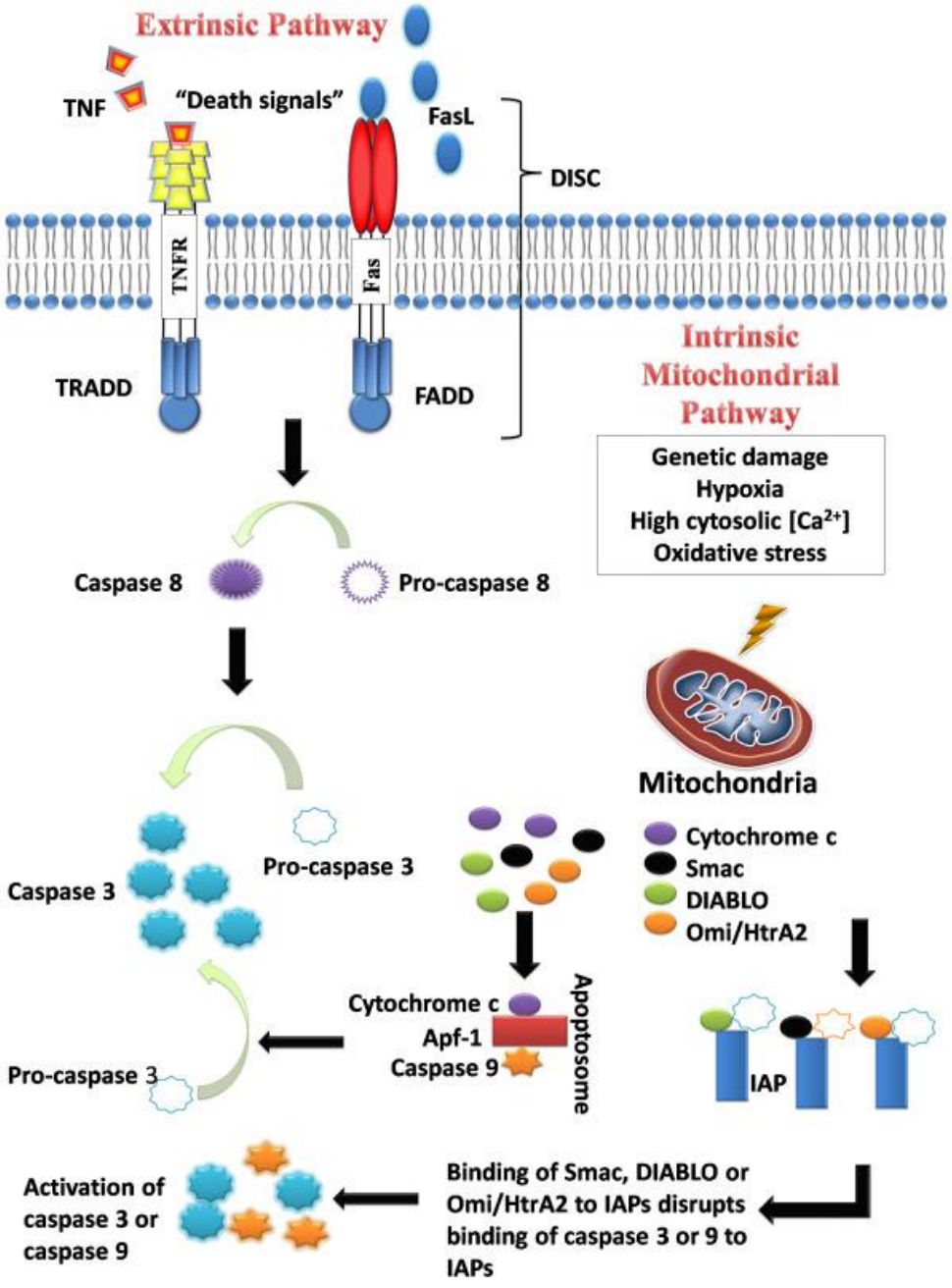

Figure 1-2 The extrinsic and intrinsic pathways of apoptosis, Adapted from Apoptosis in cancer: from pathogenesis to treatment (32).

1.2.2 The Intrinsic mitochondrial pathway

This pathway is not induced by receptor-mediated stimuli but by intracellular stimuli such as hypoxia, high cytosolic concentration of Ca^{2+}, DNA damage, radiation, toxins, and high levels of oxidative stress (38, 39). All of these triggering factors produce a signaling cascade that ultimately results in increased mitochondrial outer membrane permeabilization (MOMP) to release proapoptotic factors, such as cytochrome c, into cytosol (Figure 1-2). This leads to caspase activation through the formation of a complex known as apoptosome. Apoptosome is formed by binding of cytochrome c to the C terminal region of Apaf-1 (Apoptotic protease activating factor 1), a cytosolic protein with an N-terminal caspase-recruitment domain (CARD) (40). Upon formation of apoptosome, it binds caspase 9, which cleaves and activates the executioner caspase-3. In addition to cytochrome c, other apoptotic molecules are also released from mitochondria into cytosol, which include apoptosis inducing factor (AIF), direct inhibitor of apoptosis protein (IAP), second mitochondria derived activator of caspase (Smac), direct IAP Binding protein with Low pI (DIABLO), and others as shown in (Figure 1-2). IAPs efficiently bind to caspases and block their activation, thereby stopping the proteolytic cascade that leads to cell death. All other molecules including Smac, DIABLO, and Omi induce caspase activation by binding to IAPs and abrogating the interaction of IAPs with caspase 9 or 3 to perform their apoptotic function (32). In addition, another factor will be released from inner mitochondrial space after MOMP, namely Endonuclease G (EndoG),

which is a nuclear DNA-encoded nuclease that moves to the nucleus where it is involved in nuclear DNA degradation (41).

In general, the intrinsic pathway is controlled by a group of proteins collectively known as the Bcl-2 family, which consists of both pro-apoptotic and anti-apoptotic proteins (42). The pro-apoptotic members include BaX, Bak, Bcl-Xs, Bid, and Bim, while the anti-apoptotic members include Bcl 2, Bcl-Xl, Bcl-W, Bfl-1, and Mcl-1. The balance between these pro- and anti-apoptotic proteins will determine whether the cell should undergoes apoptosis or not (42).

After the activation of caspase-3 whether through intrinsic or extrinsic pathways, they will converge into a common executioner pathway. Activated caspase 3 then will be responsible for cleavage of many cell proteins, such as kinase, DNA repair, cytoskeletal and other proteins in charge of the maintenance of cellular hemostasis. Caspase-3 also stimulates the apoptotic chromatin condensation inducer in the nuclease (ACINUS) and the cytosolic helicase (HELI-CARD), which promotes chromatin condensation and DNA disintegration (41). All of these effects together are responsible for the characteristic features of apoptosis such as chromatin condensation, DNA fragmentation, and cellular shrinkage (33).

1.2.3 The intrinsic endoplasmic reticulum pathway

This third pathway of apoptosis is caspase-12 dependent and is believed to be triggered by cellular stresses such as ROS, tissue hypoxia, or nutrient deprivation. Caspase-12 becomes activated when its adaptor protein known as

TNF receptor associated factor 2 (TRAF2) dissociates from it (43). This dissociation is induced or promoted when endoplasmic reticulum (ER) is stressed by any of the above cellular stressors, resulting in protein unfolding and activation of caspase-12 (43).

1.3 Regulation of Apoptosis

Apoptosis has many regulators through a number of cellular and signaling pathways, among these are p53, NF-κB, Phosphatidylinositol 3-kinase (PI3K), etc. (44, 45).

1.3.1 The p53 pathway

p53, known as “cellular gatekeeper”, is one of the prominent regulators of apoptosis (46). It transmits a variety of stress-induced signals, such as DNA damage, hypoxia, or ROS, to induce anti-proliferative cellular responses, such as cell-cycle arrest, senescence, autophagy regulation and apoptosis (47)**.** Upon activation, nuclear p53 can induce the transcription of numerous pro-apoptotic genes including Bax, PIG3, Killer/DR5, CD95 (Fas), Noxa, and p53 up-regulated modulator of apoptosis (PUMA), which induce apoptosis (48). Additionally**,** p53 activation has (transcription-independent) cytosolic activity, where it localizes to the mitochondria and enhances mitochondrial outer membrane permeabilization leading to the release of cytochrome c (47). It has been demonstrated that PUMA plays a fundamental role in this pathway (48). p53 can transactivate PUMA, which in turn moves to the mitochondria, where it interacts with Bcl-Xl protein,

leading to with Bax activation. On the other hand, p53 has been suggested to not only negatively regulate Bcl-2 through its role in processing microRNAs (miR) that suppress Bcl-2, but also cytoplasmic p53 can inhibit Bcl-2 causing dissociation of Bax, Bak, and Bim to induce mitochondrial cytochrome c release to initiate apoptosis (49). Taken together, p53 has a critical role in regulation of apoptosis in both transcription-s dependent and independent manners.

1.3.2 The NF-κB pathway

The NF-κB transcriptional factors are another class of regulators of apoptosis that act through the induction of apoptosis-related proteins. One of the earliest experiments showed that mice deficient in RelA, an NF-κB subunit, died at day 15 postconception due to extensive liver apoptosis (50). Moreover, RelA-/- fibroblasts isolated from mutant mice revealed an increased sensitivity to pro-apoptotic stimuli such as tumor necrosis factor-α (TNF-α). Later on, NF-κB was shown to induce anti-apoptotic factors through transcription activation; these factors include caspase 8-c-FLIP (FLICE inhibitory protein), A1 (Bf11), TNFR-associated factor 1 and 2 (TRAF1/2) and cellular inhibitor of apoptosis (c-IAPs), as shown in Figure 1-3.

All of the above factors act synergistically to inhibit apoptosis at multiple levels, including mitochondrial, apoptotic pathways activation, or death receptor levels (51). C-IAPs can inhibit caspases 3 and 7, the effector caspases, through direct binding. C-IAPs can also act on mitochondrial membrane preventing cytochrome c release (52). C-FLIP, a different inhibitor of apoptosis, interacts

with pro caspase 8 through its two death effector domains (DED), restricting its activation, thereby inhibiting apoptosis (53). Upon DNA damage, through transcription induction of A1, a Bcl-2 family member, NF-κB can inhibit apoptosis by prevention of mitochondrial depolarization (54). NF-κB can regulate another group of anti-apoptotic factors, TRAF1 and TRAF2, through modulating of cell death receptors. TRAF2 has an activating effect on inhibitor of NF-κB (IκB) kinase (IKK), thereby activating NF-κB and c-Jun NH2-terminal kinase (JNK) pathways to activate activator protein 1 (AP-1), a downstream target of Bim (55). However, JNK activation has been reported to have weak anti-apoptotic function, so its main role in apoptosis remains controversial (56). Finally, the anti-apoptotic effect of growth arrest DNA damage 45B protein (GADD45B) in response to DNA damage is also regulated by NF-κB (57), adding another layer of NF-κB anti-apoptotic effects (Figure 1-3).

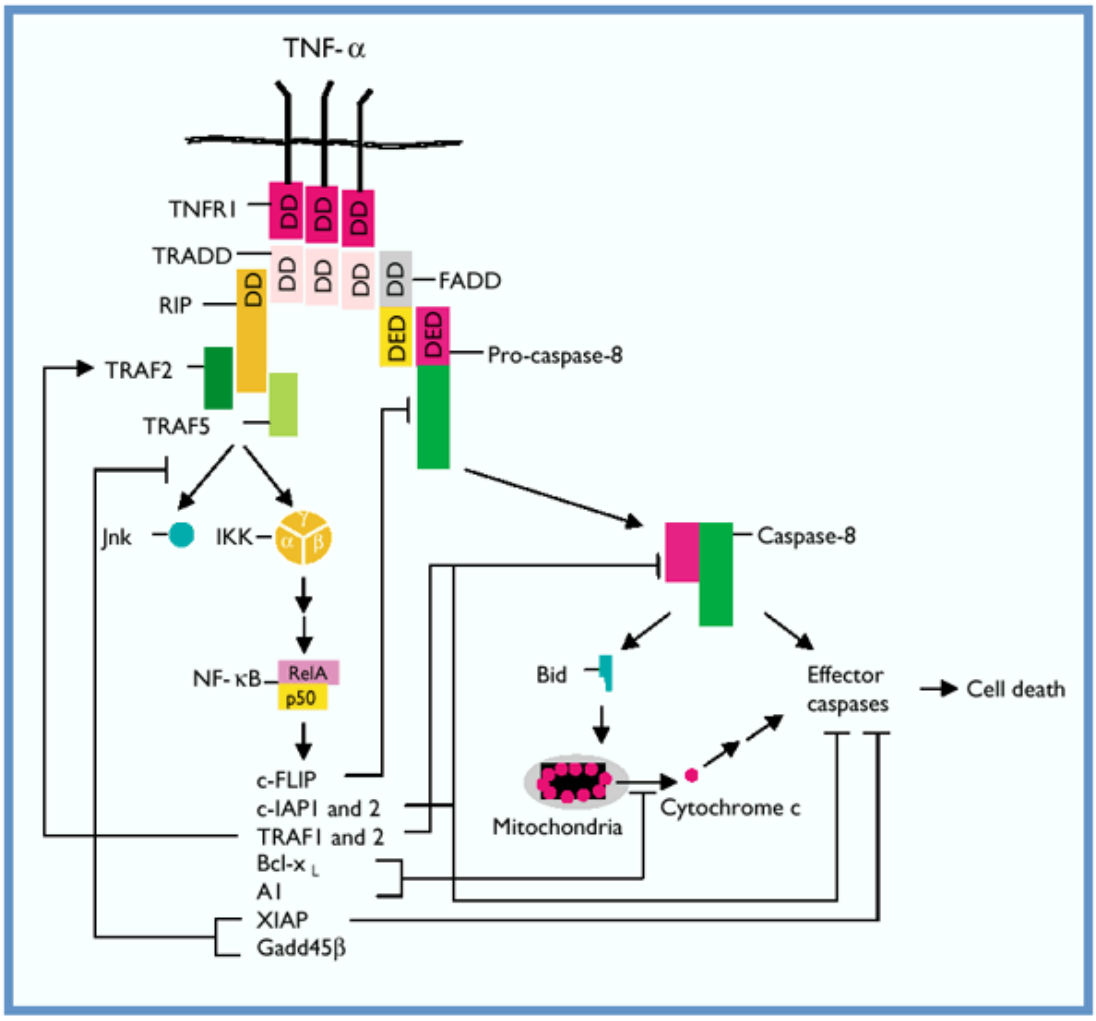

Figure 1-3. A model for NF-κB and anti-apoptotic factors. Adapted from Karin M and Lin A., 2002 (51).

1.4 Apoptosis in Cancer

The capability of cancer cells to grow in size and population is controlled not only by the speed of their proliferation but also by the speed of their death. Apoptosis is critical mechanism of this death and its dysregulation is a characteristic of most, if not all types of cancer (32). Therefore, apoptosis has a critical effect on

tumor survival, growth and even regression. Moreover, targeting of apoptosis is a powerful therapeutic strategy for treating tumors (58-60). p53, which is mutated in about 55% of tumors, was first recognized to link apoptosis with treatment resistance (61). Cancer cells can acquire resistance to apoptosis through many different ways. Indeed, the most frequently observed mutations in p53 lead to a loss of its pro-apoptotic function (62). Mutations in the p53 protein eliminate a critical part of the DNA damage sensor that activates the apoptotic effector cascade, and the attenuation or loss of p53 increases chromosomal instability and cellular lifespan (63). Therefore, p53 helps to preserve genomic stability and to block the accumulation of genetic aberrations that can cause carcinogenesis (46). Further insight into the role of apoptosis in cancer came from the discovery of the *Bcl-2* oncogene from a chromosomal translocation in follicular lymphoma and its anti-apoptotic function (64). Another example supporting the notion that apoptosis is a fundamental block to carcinogenesis that must be defeated is the retinoblastoma gene (*Rb*)**.** The Rb pathway is another significant tumor suppressor that regulates DNA replication and cell proliferation (65), and aberrations in the Rb pathway have been associated with many human cancers (66)**.** Rb targets E2F, a transcriptional factor, to stimulate expression of pro-apoptotic genes such as caspases and Apaf-1, thus alterations in the RB pathway can inhibit apoptosis and affect tumor cell sensitivity to cytotoxic agents (65). Studies on p53, Bcl-2 and Rb have provided critical insights into the importance of dysregulated apoptosis in carcinogenesis**.** We can now attribute

aberrant apoptosis into loss of balance between pro- and anti-apoptotic proteins, diminished caspase activity, and/or compromised death receptor signaling (32).

The Bcl2 family, p53, and IAPs are considered to be the main factors that determine the balance between pro- and anti-apoptotic activities. The Bcl-2 family consists of both anti- and pro-apoptotic proteins: Bcl-2, Bcl-xL, A1/BfI-1, Bcl-w, and Bcl-B/Bcl2L10 are anti-apoptotic, while Bim, pNoxa, Bad, Bax, Bak, Bok/Mtd, Bmf, and Bik play pro-apoptotic functions (67). Any disruption in this balance, such as upregulation of anti-apoptotic or downregulation of pro-apoptotic proteins, or a combination of both, can lead to aberrant apoptosis and resistant to death. For example, chronic lymphocytic leukemia (CLL) patient exhibits high level of Bcl-2, an anti-apoptotic protein, and low levels of Bax, a pro-apoptotic protein, causing reduced apoptosis and leukaemogenesis (68). Another report showed that in CLL patients with an increased Bcl2/Bax ratio are more drug resistant with poorer prognosis, while those with lower ratio exhibit better prognosis and drug response (69). In addition, disregulation of caspases can also lead to carcinogenesis (35). For instance, caspase-3 activity has been found downregulated in many ovarian and breast cancers, including the MCF-7 breast cancer cell line (70).

Finally, abnormality in the death-signaling pathway can lead to circumvention of the apoptosis through the extrinsic pathway. Down-regulation of death receptors or reduction in death signal lead to reduction in apoptosis. It has been indicated that a reduction in expression of CD95, a death receptor also known as Fas, plays a role in therapy-resistant leukemia through attenutation of

death signaling pathways and hence reduced apoptosis (71). Another example is dysregulation of Fas ligand (FasL), which has been implicated in the pathogenesis of cervical intraepithelial neoplasia (CIN) (72).

1.5 Targeting apoptosis for cancer therapy

The majority of human diseases involve apoptosis dysregulation, either excessive apoptosis as in neurodegenerative disorders like Alzheimer disease or diminished apoptosis in cancer (73). Therefore, development of specific therapeutics to restore apoptosis pathways is essential. Cancer cells find ways to downregulate or circumvent apoptosis to enable survival and avoid death. For example, alterations in the p53 protein are found in greater than 55% percent of human tumors (74), and loss of wild type p53 function is associated with defective apoptosis and therapy resistance. This suggests that restoration of p53 activity in a tumor could restore apoptosis and therefore tumor regression. This can be achieved by transfer of the *TP53* gene with adenovirus vectors, using monoclonal antibodies to stimulate transcriptional activity, or by inhibiting p53-mdm2 binding to stabilize p53 (75, 76). However, the major challenge and side effects of such treatment are cancer target specificity and drug delivery (77). Modulation of caspase inhibitors such as IAPs represents another promising avenue, among other strategies to induce apoptosis. Antagonists of IAPs could also help to restore caspase activity and improve radio- and chemo-sensitivity of cancer cells (78, 79). For example, a small molecule known as polyphenylurea, an XIAP inhibitor, has been shown to overwhelm the inhibitory effects of XIAP on

executioner caspases 3 and 7 and induce apoptosis in leukemia cells (80). Similarly, pan-IAP inhibitors that are similar to the endogenous inhibitor of the IAPs, known as Smac, can bind to IAP's to not only abolish their activity but also sensitize tumor cells to TNF and apoptosis (81).

Mitochondria, a major regulator of apoptosis, represent another target site for cancer therapy. Since overexpression of Bcl-2 is responsible for resistance of many cancer cells to apoptosis, targeting Bcl-2 may have good potential for cancer treatment (82, 83). For example, gene therapy targeting Bcl-2 pro-apoptotic peptide through adenovirus delivery of Bax to mitochondria can resume apoptosis (84).

Apoptosis can also be prompted by triggering death receptor activation. Activating the extrinsic pathway elicits apoptosis independent of p53 and has the ability to activate apoptosis in cancer cells with poor responsiveness to conventional therapies. In addition, usage of NF-kB inhibitor in treatment of multiple myeloma showed promising results through redirecting abnormal myeloma cells to apoptosis (85). However, a major challenge is the immunity suppression side effects, and, in the same vein, chronic TNF use also showed side effects such as hepatotoxicity (86). Finally, TRAIL, a direct caspase activator, can mediate apoptosis through bypassing Bcl-2 overexpression in a p53-independent manner (86). TNF-related apoptosis-inducing ligand (TRAIL) agonist, a caspase activator, can promote apoptosis with high specificity in tumor cells (87).

CHAPTER 2

The PALB2-BRCA1 Interaction Is Required for the Suppression of both Spontaneous and Induced Tumorigenesis

2.1 Summary

In brief, we found that γH2AX background level is higher in multiple tissues of the *Palb2* mutant mice than in the same tissues of WT mice. After radiation, γH2AX levels were further induced in both mice, with the MUT mice showing a greater extent of induction in all issues tested and in both genders. In WT mice, γH2AX levels returned to background levels by 24 hr post radiation, whereas the decline in the numbers of γH2AX positive cells in the MUT mice was slower and there were still positive cells at this time. By analyzing BrdU incorporation, we found higher DNA synthesis rates in mutant mice at different time points after gamma irradiation. Similarly, more phospho-histone H3 positive cells were found in various tissues of the mutant mice after radiation. These results are consistent with the known function of PALB2 as a key regulator of the intra-S and G2/M checkpoints (88). Additionally, we found more p53 and p21 positive cells in the mutant mice. Thus, cells expressing the mutant PALB2 inefficiently repair DNA after exposure to IR yet continue to replicate after exposure, even though p21 is also induced. Finally, by TUNEL assay we found less apoptotic staining in some tissues like intestinal, mammary, prostatic and ovarian tissues in the mutant mice, while it is almost the same for other tissues such as lung, seminal vesicle and kidney. Defect in the apoptotic pathway plays a critical role not only in initiation and progression of cancer but also in resistance to treatment (89). When *Palb2* mutant mice were challenged by IR, they quickly developed thymic lymphoma. More interestingly, we found an upregulation and persistent accumulation of 53BP1 in mutant *Palb2* tissues, particularly at 6 hr post IR, which

could be the underlying mechanism for thymic lymphoma development through increased mutagenic NHEJ repair.

2.2 Introduction

2.2.1 Radiation and DNA damage

DNA double strand breaks (DSBs) can be induced by either exogenous sources as in ionizing radiation (IR) or by endogenous sources as reactive oxygen species as a byproduct of metabolic processes (90). Upon DSBs induction by IR, cells repair the breaks through NHEJ and HR. NHEJ represents the faster process and is responsible for repairing more than 75% of the DSB within 30 min, and it occurs in all phases of cell cycle (91). In contrast, HR, which is significantly more complex, represents a relatively slower process and is responsible for repairing the rest of DSBs, mainly in S and G2 cell cycle phases. This slower kinetics of HR repair could also be partially due to checkpoint response, which does not appear to effect on NHEJ, suggesting that NHEJ is checkpoint independent repair pathway (92).

Radiation exposure can increase risk of different kinds of malignancy such as breast, thyroid, lung, hematological and many others (93-95). An early event after IR is phosphorylation of histone H2AX in the chromatin adjoining DSB ends at serine 139 producing γH2AX (96). This phosphorylation is achieved through different kinase, that is, ataxia telangiectasia mutant (ATM), AT and Rad3-related protein (ATR), or DNA-dependent protein kinase (DNA-PK) (97). Afterward, γH2AX helps to recruit DNA damage response proteins, such as 53BP1, BRCA1,

MDC1, phospho-ATM and many others, to start chromatin relaxation and subsequent repair choice pathway (98).

Tumor cells that have lost BRCA1 function exhibit defect in HR pathway, leading to increased usage of NHEJ pathway and genomic instability (99). 53BP1 (p53-binding protein 1), a key regulator for NHEJ, was initially identified as a p53 interacting protein and later found to be a key player in DNA repair independent of p53. Upon induction of DSBs, ATM and ATR phosphorylate 53BP1, which enables 53BP1 to be recruited to DNA damage sites. It has been suggested that 53BP1 counteracts with BRCA1 to inhibit HR and favor NHEJ by blocking DNA end resection (100). On the other hand, BRCA1 can inhibit 53BP1 activity, by yet unclear mechanism, allowing resection of the DNA breaks and eventually repair through HR pathway (100). However, another report showed that BRCA1 can displace 53BP1 from DNA damage sites during S-phase (101). 53BP1-/- mice are viable and show an increase in apoptosis, loss of T-cell receptor, and lymphopenia, suggesting a critical role of this DNA damage response protein in the maturation and maintenance of lymphocytes. In addition, homozygous mice lacking the transcriptional activation domain of c-Rel showed impaired lymphocytes proliferation with severe lymphocytopenia (102). Furthermore, aberrant amplification expression of human RelA gene has been implicated in pathogenesis of leukemia and lymphoma (103, 104).

2.2.2 Liver tumor

Hepatocellular carcinoma (HCC) is the third leading cause of death from cancer and the fifth most common human men cancer, with approximately 20K new cases/year in USA (105). Since more than half of these liver tumor cases are due to chronic hepatitis B and C infection, vaccination is still the most effective preventing method for this cancer. Unfortunately, until recently no chemotherapy has been discovered to be effective in HCC (106). Many reports showed potential of targeting Nrf2 for the treatment of liver tumor, indicating a key role of oxidative stress in HCC pathogenesis (107, 108). This tumor causation or association between oxidative stress and carcinogenesis has been established (109). This association is likely through the activation of many signal transduction and gene expression cascades such as MAPK, Erk, JNK, AKT, NF-κB, and other kinases (110-112). Other possible association is through direct effects of ROS on DNA resulting in sequence alteration and consequently oncogene mutations due to the mutagenic nature of 8 Oxo-dG (113, 114). Likewise, mice lacking SOD1-/- (superoxide dismutase, a cytoplasmic superoxide scavenger) exhibit shorter life span with persistently high ROS level and develop HCC at around 18 months of age (115). It has been reported that RANKL is up regulated and promotes HCC invasion and migration, suggesting a fundamental role of NF-kB not only in pathogenesis of liver tumor but also enhancement of epithelial-mesenchymal transition (EMT) (116). This EMT is reportedly implemented through up-regulation of N-cadherin (mesenchymal marker) and down-regulation of E-cadherin (epithelial marker) at both protein and mRNA levels (116).

2.2.3 DMBA Carcinogenesis

7,12-dimethylbenz(a)anthracene (DMBA) is a polycyclic aromatic hydrocarbon (PAH) and a carcinogenic chemical that have been shown to induce ovarian cancer (117), dermatological malignancy (118), hematological malignancy (119), and breast cancer (120), in addition to its ability to induce premature ovarian failure (121). Humans can be exposed to this carcinogen through environmental pollution and burning of organic materials, such as from cigarette smoke or car exhausts that contain significant amount of PAH chemicals (122-124). Oxidation of this carcinogen by the induction of P450 enzymes produces metabolites such as epoxide that can cause covalent adducts on DNA and the formation of depurinated abasic sites (125, 126). Induction of cytochrome P450 enzymes also generates ROS, predominantly hydroxyl radicals and H_2O_2, through uncoupling reactions (127). Moreover, other reports have shown that DMBA can induce oncogenic mutation in H-Ras and c-Myc promoting mouse mammary tumor formation, suggesting another mechanism of action for this carcinogen (128, 129). Either way, there will be more oxidized and modified DNA products (8-Oxo-dG) caused by either hydroxyl radical or ROS in general (130).

2.2.4 Anemia and PALB2

Bi-allelic germline mutations in PALB2 result in Fanconi anemia (FA), subtype N (4, 131). Fanconi anemia is an autosomal recessive disease manifested by high susceptibility to cancer, hypersensitivity to mitomycine C (DNA cross linker), pancytopenia with bone marrow failure, and developmental retardation with bone

abnormality (131). Hypersensitivity to interstrand cross-links (ICLs) upon mitomycin C challenging indicates that a defect in the repairing of DNA damage underlies FA. There are 19 FA genes that have been discovered so far: FANCA, FANCB, FANCC, FANCD1 (BRCA2), FANCD2, FANCE, FANCF, FANCG, FANCI, FANCJ (BRIP1), FANCL, FANCM, FANCN (PALB2), FANCP (SLX4), FANCS (BRCA1), RAD51C, and XPF (132, 133). These proteins are not only involved in DNA repair but also in checkpoint activation upon induction of DSBs in S phase (17, 134). Some of these proteins can be activated upon phosphorylation of FACD2 and FANCI by the ATR kinase (135). Following the recognition and processing of the ICLs into DSBs by the “upstream” FA proteins, the breaks are eventually repaired by HR, for which PALB2 plays a key role.

2.2 Material and methods

2.3.1 *Palb2* knockin mice

In this study, I used our recently generated *Palb2-cc6* knockin mouse model in which a mutation in the N terminus of PALB2 abolishes its interaction with BRCA1 (27). The *Palb2* genomic locus and the generation of the strain are shown in Figure 2-1. Unlike the *Palb2* conventional knockout (KO) mice that show embryonic lethality, our knockin mice are viable, allowing for study of tumor/disease development in different tissues.

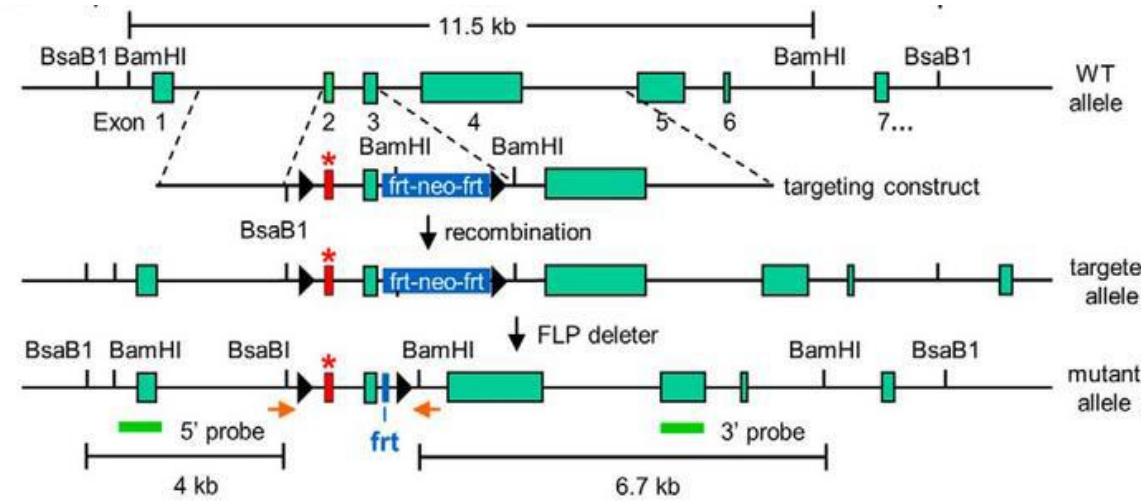

Figure 2-1 Schematic diagram for *Palb2* knock-in mice generation. Adapted from Simhadri al et, 2014 (27)

2.3.2 Animals and experimental procedures: C57BL/6

All animal care and treatments were conducted in compliance with Institutional Animal Care and Use Committee (IACUC) guidelines. Genotyping was carried out by PCR amplification of genomic DNA extracted from the tails from 3-week-old mice. To prepare genomic DNA, tails were first digested at 56°C overnight in 500 μl of TNES buffer with 0.5 mg/ml proteinase K (Sigma Aldrich). Then, 220 μl of 6M NaCl was added to precipitate digested proteins, which were then removed by centrifugation at 15K rpm. Subsequently, an equal volume of 2-propanol was added to the supernatant to precipitate DNA, which was then spun down at 15K rpm. Finally, DNA pellets were dissolved in TE buffer, pH8.0 at 65°C for 20 min.

Genotyping was carried out by PCR amplification of the region surrounding exons 2 and 3, using forward primer Arm1short F (GCCTGCTGGGCACTGTATCCATTCTCTCTGTTCT) and reverse primer

Arm2LongR2

(CTGGCAATCCAATTGAAGGCACTGGGTATTGCTTGAATTGTATAACATG), which yield a 200bp product for the wt allele and a 350 bp product for the mutant allele.

The reaction mix for single reaction consisted of:

Hotmaster Taq DNA polymerase	0.1 μl
10 mM dNTP (promega)	0.1 μl
10X HotMaster Taq buffer	1.0 μl
Forward primer	12 pmol
Reverse primer	12 pmol
DNA	1.0 μl
H_2O to	10 μl

The PCR cycling parameters were: 94°C 3 min; 94°C 30 sec, 65°C 3 min, 68°C 5 min X 35 cycles; 72°C 5 min, 4°C forever.

2.3.3 Mouse Irradiation (experimental design)

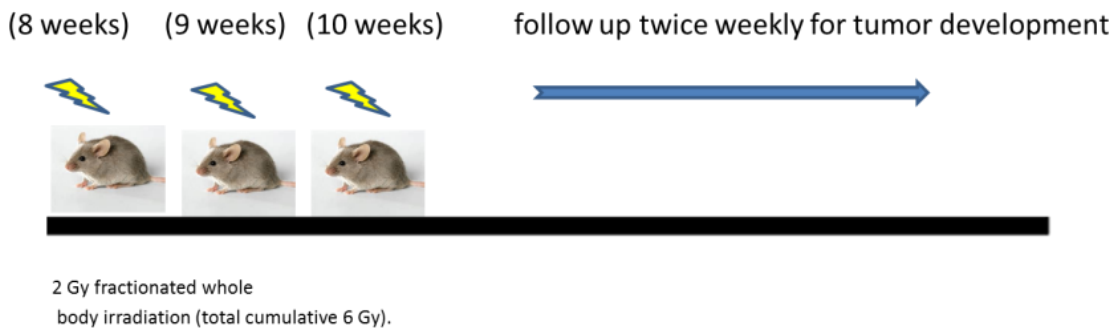

At 8 weeks of age, mice were treated with 2 Gy of γ-radiation from a Cesium137 source (Gammacell 40 Exactor) at a dose rate of 0.97 Gy/min once a week for 3

times. Animals were then monitored twice weekly for tumor development. For both WT and MUT genotypes, 25 mice of each gender were irradiated and monitored.

For short-term tissue analysis, mice were irradiated with 3 Gy in a single dose (whole body irradiation) and dissected at 30 min, 3 hr, 6 hr, and 24 hr post-irradiation.

2.3.4 Histopathological analyses

Mouse tissues were fixed in 10% buffered formalin solution. Intestine, mammary gland (MG), spleen, and liver were fixed for 24 hours. Fixed tissues were then transferred to 70% ethanol and sent to The Histopathology Shared Resources of Rutgers Cancer Institute of New Jersey for paraffin-embedded block production and tissue sectioning. Tissue sections mounted on slides were stained with hematoxylin & eosin (H&E) for histopathological analysis.

We used Elston grade for histopathological breast cancer grading, which evaluates the following three parameters:

A- Tubule formation: 1 point is assigned when ≥75% of the area is composed of definite tubules, 2 points if it is 10-75%, and 3 points if less than 10%.

B- Nuclear pleomorphism: 1 point is given when tumor nuclei that are small with little increase or variation in size compare to normal nuclei and have regular outline. 2 points is given when nuclei are larger than normal and usually with single nucleoli and moderate variation in size and shape,

and 3 points when variation is marked in size and shape and often with multiple nucleoli.

C- Mitotic count per 10 high power fields; 1 point for up to 7 mitoses, 2 points for 8-16, and 3 points for more than 17 mitoses.

3-5 points mean grade I (well differentiated)

6-7 points mean grade II (moderate differentiated)

8-9 points mean grade III (poor differentiated)

For immunohistochemistry (IHC), paraffin-embedded sections were stained with antibodies against γH2AX (Millipore, pSer139, 1:200 dilution), p53 (Leica, NCL-p53-CM5p, 1:1000 dilution,) 53BP1 (Cell signal,1:5,000 dilution), phospho-Histone H3 (Cell Signaling, pSer10, 1: 200 dilution,), active Caspase-3 (Abcam, ab13847), P21 (Santa Cruz, F-5, 1: 50), BrdU (BECTON DICKINSON, 1:100 dilution).

For quantification of IHC for γH2AX and active Caspase-3, the most representative whole field was analyzed by quantifying at least 10 images at 40X magnification. A minimum of 300 cells from each slide were scored for each genotype.

2.3.5 Western blotting

Tissues were homogenized with homogenizer ground and lysed with NETNG-400 (400mM NaCl, 1 mM EDTA, 20 mM Tris-HCl [pH7.5], 0.5% Non-Idet P-40, and 10% glycerol) with protease inhibitor (Roche). The protein samples were separated on 4-12% Tris-glycine gels and transferred to a nitrocellulose

membrane (0.45 micro m Bio-RAD). The membranes were blocked with 5% milk in PBST buffer for 1 hr and then incubated with the appropriate primary antibody solutions overnight at 4C. Membranes were then washed with PBST, and incubated with horseradish peroxidase conjugated secondary antibody solutions for 1 hr at room temperature. Protein bands were visualized using Immobilon Western Chemiluminescent HRP Substrate (Millipore). The primary antibodies used were as follows: NFκB p65 (Abcam, ab16502, at 1:1000 dilutions), 53BP1 (A300-272A, Bethyl Laboratories 1:10000), and β-Actin (Santa Cruz, Ac-15 at 1: 5,000). The secondary antibodies used were Amersham ECL HRP Conjugated Antibodies purchased from GE Healthcare Life Sciences

2.3.6 BrdU injection

BrdU (5-Bromo-2'-deoxyuridine, CAS 59-14-3 – Calbiochem) was purchased from Sigma Aldrich. Mice were intraperitoneally injected at dose of 100 mg/kg.

2.3.7 Measurements of apoptosis

Paraffin-embedded tissue sections were fixed in 4% paraformaldehyde, permeabilized using proteinase K solution (20 µg/ml), and stained using Terminal deoxynucleotidyl transferase-mediated dUTP nick-end labeling (TUNEL) staining kit purchased from Promega (Madison, WI, USA). After counterstaining with DAPI (VECTASHIELD Antifade Mounting Medium with DAPI, Catalog Number: H-1200), slides were examined under a Nikon Eclipse TE200-4 fluorescent

microscope. Images were captured with NIS Elements BR 4.40 software Infinity capture for IHC.

2.3.8 DMBA carcinogen administration

DMBA (7,12-Dimethylbenz[a]anthracene) was purchased from Sigma Aldrich (Cat # 57-97-6). We dissolved it in olive oil and then thoroughly vortexed the mix to make it completely dissolved. *Palb2* MUT and WT female mice were each given a single dose of DMBA in 0.2 ml volume by oral gavage at 5 week of age. Due to the unknown toxicity of this carcinogen on our mice, we tested 3 different doses, 1 mg, 0.5 mg and 0.1 mg per mouse. Mice were mated one week after drug treatment to provide an oscillating hormonal effect and then monitored twice weekly for tumor development. At the same time, we performed short-term experiment after oral gavage of 1 mg DMBA, in which we dissected the mice one and two days after treatment for different tissues analysis.

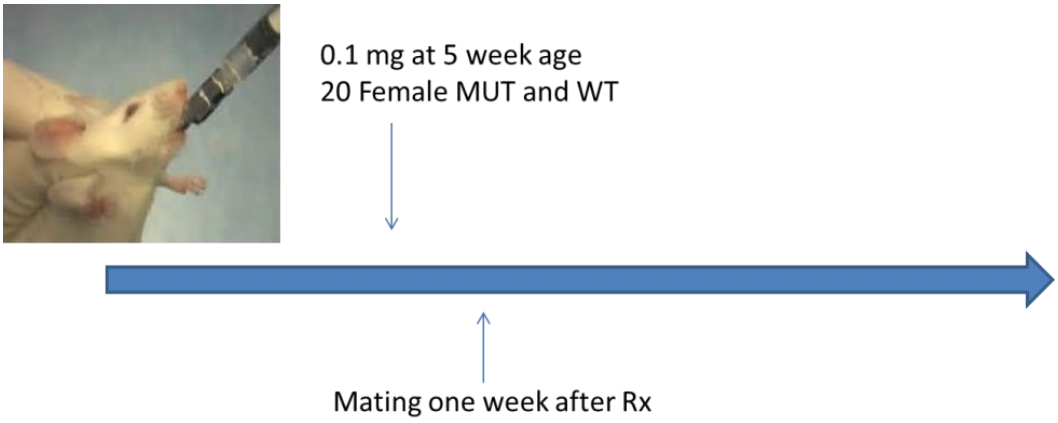

2.4 Results and discussion

2.4.1 Mutant *Palb*2 mice display smaller body weight

As mentioned before, our homozygous *Palb2* knockin mutant mice are viable. However, they were smaller in body size and weight as compared with wt mice at the same age (~25% less) (Fig. 2-2A&B). This observation is consistent with that act that the majority of Fanconi anemia patients show growth retardation (131). It is interesting that *Trp53* heterozygosity partially rescued the growth retardation of the homozygous *Palb2* mutant mice to statistically nonsignificant (Fig.2-2C). It has been shown that loss or mutation of p53 can partially rescue the developmental defect of *Palb2* knockout mouse embryos (19). Also it is well-known that wild type p53 activation through oncogene activation or DNA damage lead to cell cycle arrest, apoptosis or senescence (136). Given the key role of p53 in DNA repair, it is likely that p53 is activated in the *Palb2* knockin mice due to increased endogenous DNA damage, and this might explain why partial loss of p53 (*Trp53*+/-) can rescue the growth retardation of the *Palb2* knockin mice. This is also consistent with our finding that baseline p53 levels are higher in mutant than control MEFs (Fig 4-5 A). Furthermore, it has been reported that *Trp53*+/- fibroblasts showed higher growth rate and HR following IR than *Trp53*+/+ fibroblasts (137). This manifested as loss of G1 arrest, higher proportion of cells in the S phase and a reduction in p21 staining in the p53-/- cells (138).

A-

B-

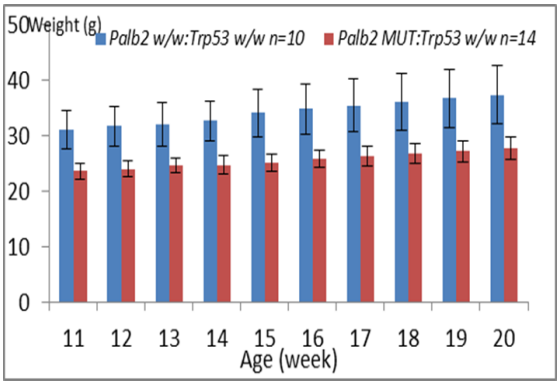

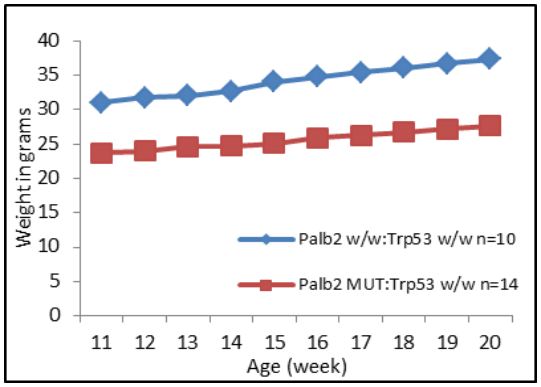

C-

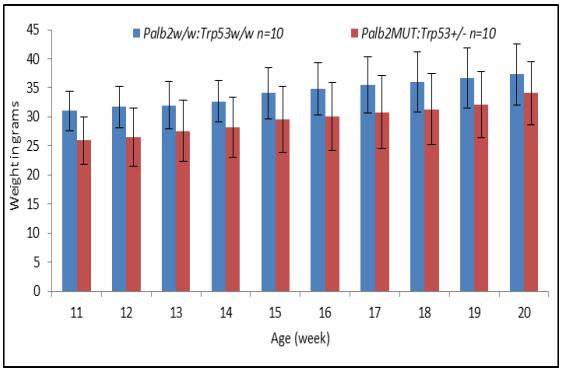

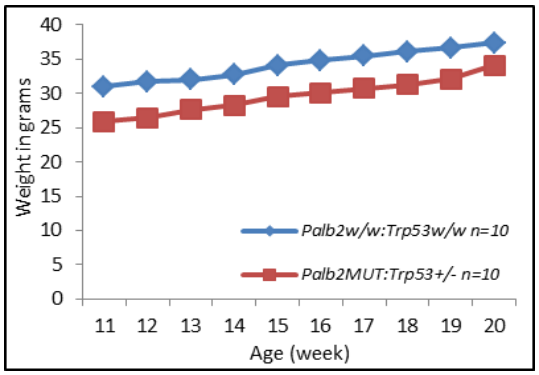

Figure 2.2 Body weight of *Palb*2 mutant and *Trp53*+/- adult mice at the indicated times. (A-C)

A- Representative image showing body size difference between WT and MUT littermate males; Black, WT, Brown.
B- Body weights (in grams) of WT and MUT males (in *Trp53* wt background) from 11 to 20 weeks of age. $p<0.05$.
C- Body weights (in grams) of WT and *Palb2*m/m;*Trp53*+/- males from 11 to 20 weeks of age. $p>0.05$.

2.4.2 *Palb*2 mutant males have propensity for liver tumor development

Compared with wt mice, our *Palb2* mutant mice showed increased spontaneous tumor development with median tumor latency (T_{50}) of 582 days (Figure 2-3A). Unexpectedly, liver tumor was the most common maligancies, with approximately 30% of the mice affected by the disease. A gender difference was also noted; among the mice that did develop tumor within the 800-day observation period, 9/15 (60%) of the males but only 2/14 (14%) of females were affected by liver cancer (Fig 2-3 A&B). Grossly, the tumors had a large single outgrowth mass and were largely uniform in shape (Fig.2-3 C). Tumor histopathology are anaplastic, pleomorphic, dis-cohesive, with multiple prominent nucleoli, some giant large anaplastic hepatocyte cells, loss of overall hepatic architectural arrangement with solid nest pattern, and a lot of fibrosis with scant stroma (poorly differentiated hepatocellular carcinoma) (Fig 2-3 D). Many dead cells were also observed (Fig 2-3 D, right panel).

It has been shonw that reactive oxygen species (ROS) stimulate human hepatoma cell proliferation via cross talk between PI3-K/PKB and JNK signaling pathways (159). However, despite the fact that ROS have been elevated in our *Palb*2 mutant MEFs, it will be interesting to examine SOD1 expression in these liver tumors (162).

A-

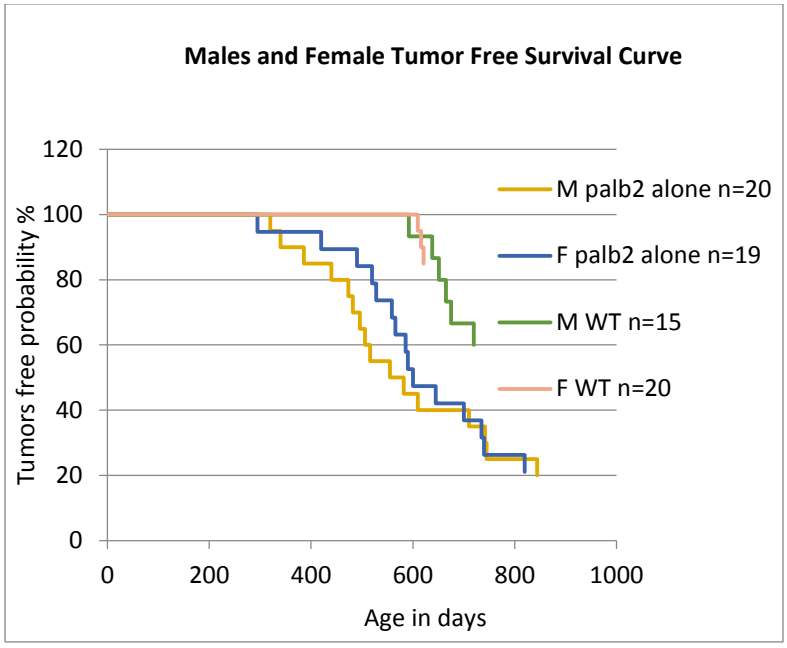

B-

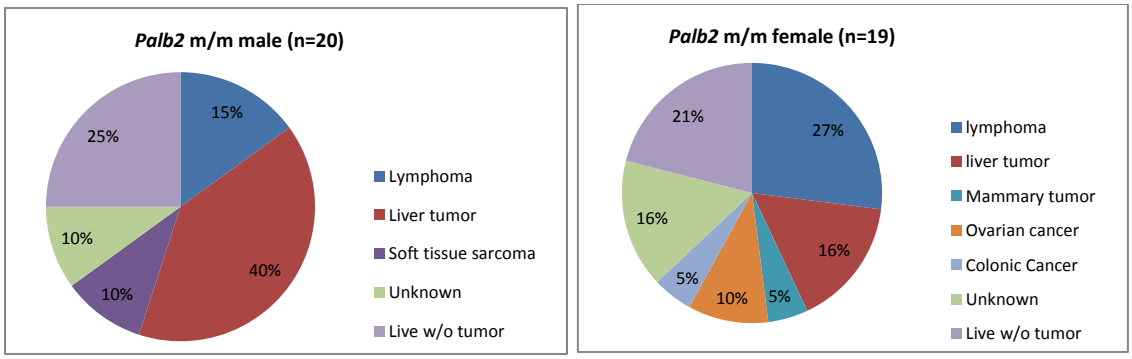

Figure 2-3 Spontaneous tumor formation in *Palb*2 mutant mice.

A- Kaplan-Meier tumror free survival curves wt and *Palb*2 knockin mice. Males and females are showen separately.

B- Tumor spectrums of male and female *Palb*2 mutant mice.

C-

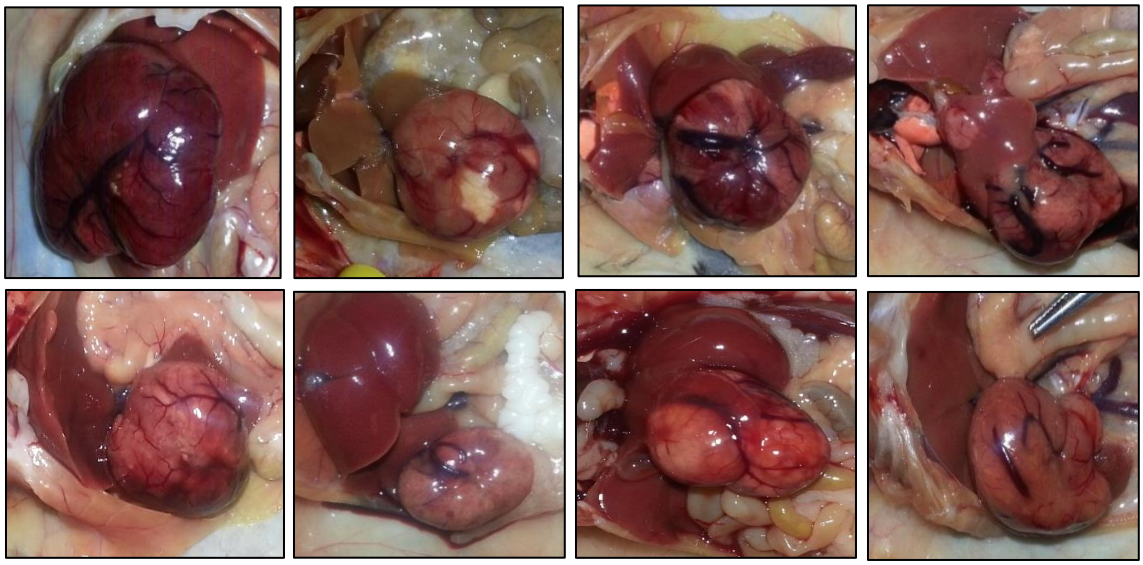

D-

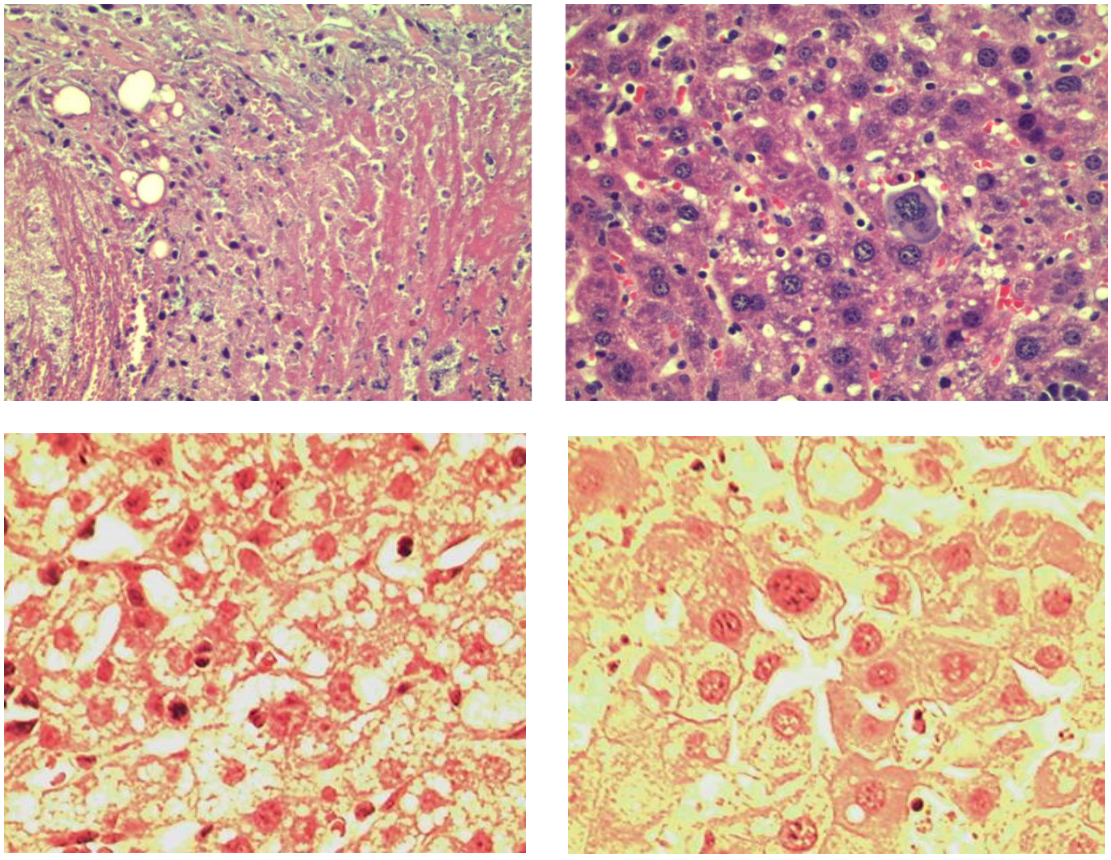

Figure 2-3 Spontaneous tumor formation in *Palb*2 mutant mice (A-D)

C, Liver tumors gross appearance. D. Histopathology of liver tumors.

2.4.3 Mutant mice show accelerated tumor development after radiation

Since our knockin mice showed a mild phenotype with a relatively long latency to develop tumors or hematological malignancy, we challenged them with gamma irradiation to induce DSBs in order to accelerate tumor development and explore DNA damage response in vivo and the mechanism of tumor suppression. To assess the consequence of irradiation on tumorigenesis, a cohort of 25 wt and mutant mice of both genders were irradiated (2 x 3 Gy with one-week interval) and followed as described in material and methods. The median tumor latency for irradiated *Palb*2 mutant mice was 255 days versus >700 days for the corresponding wild-type control mice, demonstrating that the PALB2-BRCA1 interaction is not only critical for suppression of spontaneous tumor development but also for radiation-induced tumor formation (Fig. 2-4A). Since more than two thirds of wt mice did not develop any tumor, we decided to terminate observation at 700 days of age. In both wt and mutant mice, the majority of tumors that developed were thymic lymphomas (Fig 2-4B). Interestingly, the mutant mice developed 2 ovarian cancers, for which *PALB2* is a susceptibility gene in humans. Collectively, the above data suggested that the PALB2-BRCA1 interaction is critical for tumor suppression in the thymus, which are known to be particularly prone to radiation-induced tumorigenesis, due presumably to intense cell proliferation. In consistent with these results, a recent report showed for the first time two patients who presented with non-Hodgkin’s lymphoma carrying biallelic *PALB2* mutations, underscoring a fundamental role of PALB2 in

lymphoma suppression (139). These two patients both have one truncated allele and the second being a deletion of exon 6 (139).

A-

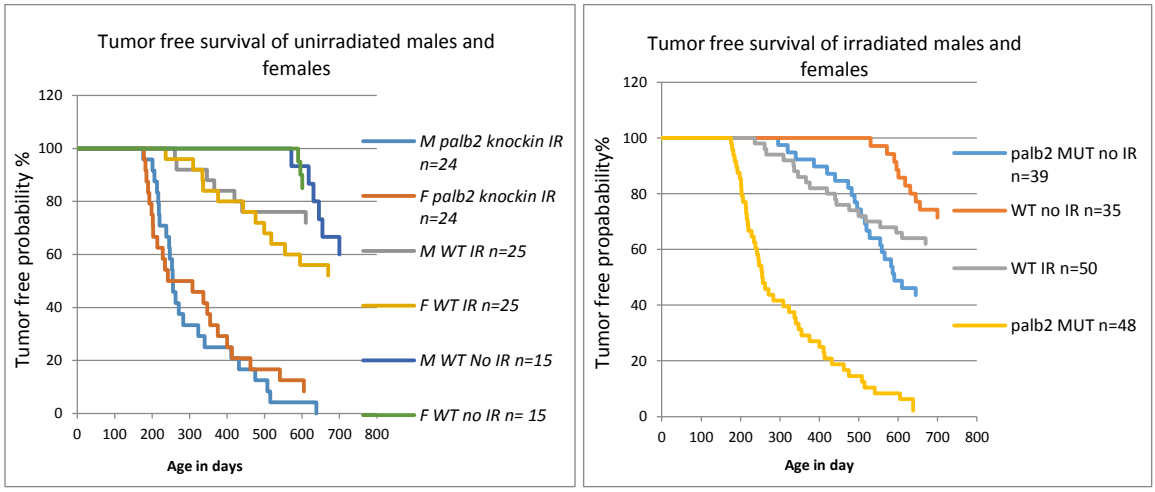

Figure 2-4 Tumor formation in *Palb*2 knockin and control irradiated mice.

A. Kaplan-Meier tumor free survival curve of irradiated and non-irradiated *Palb*2 m/m and wt adult mice of both genders, separated (left one) and merge (right one).

B-

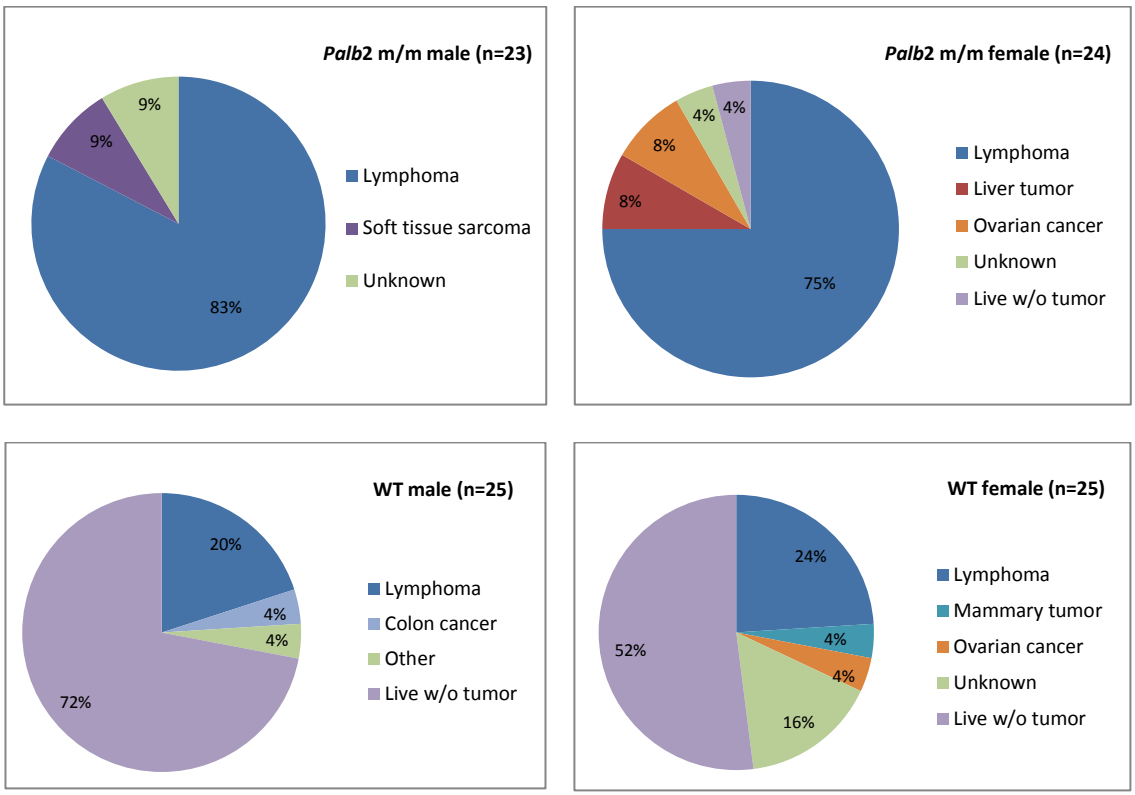

Figure 2-4 Tumor formation in *Palb*2 knockin and control irradiated mice.

B. Tumor spectrum for irradiated *Palb*2 m/m (upper) and wt (lower) (male right and female left) adult mice.

2.4.4 Increased endogenous DNA damage and impaired DNA repair in the *Palb*2 mutant mice

To determine the importance of the interaction between PALB2 and BRCA1 for the repair of radiation induced DSBs in vivo, we irradiated another group of mice with 3 Gy and dissected them at different time points post IR (as mentioned in the material and method). To understand the DSB repair kinetics in these mice, we measured the levels and foci formation of DNA damage marker γH2AX and

the DNA damage response protein 53BP1 through IHC. For γH2AX the decline in the numbers of γH2AX positive cells was much slower in MUT tissues, as 24 hr after IR they still showed positive staining (Fig. 2-5 A&C). Quantitation of the foci showed that even before IR the background level of γH2Ax was higher in MUT than in WT cells (Fig.2-5B&D). γH2AX background foci levels for the intestine and mammary gland were 40% and 38% with >1 foci in mutant tissues vrsus 10% and 15% for wt tissues). By 30 min post IR, γH2AX was induced in both mutant and wt tissues, but the mutant showed a higher induction. In wt tissues, γH2AX positive cells started to decline 30 min after IR approaching background level by 24 hr post IR. However, in mutant inestine and mammary gland, the decline of γH2AX positive cells was slower (50% and 60% mutant cells with >1 foci versus 10% and 30% for wt cells at 24 hr post IR).

These finding indicate that with the abrogation of BRCA1-PALB2 interaction, cells inefficiently repair damaged DNA. DSBs have detrimental effect to the cell if not repaired properly and can endanger genomic integrity. Failure of repair may end with cell death or instability of the genome, while misrepair can lead to rearrangement or loss of genetic information (140).

A-

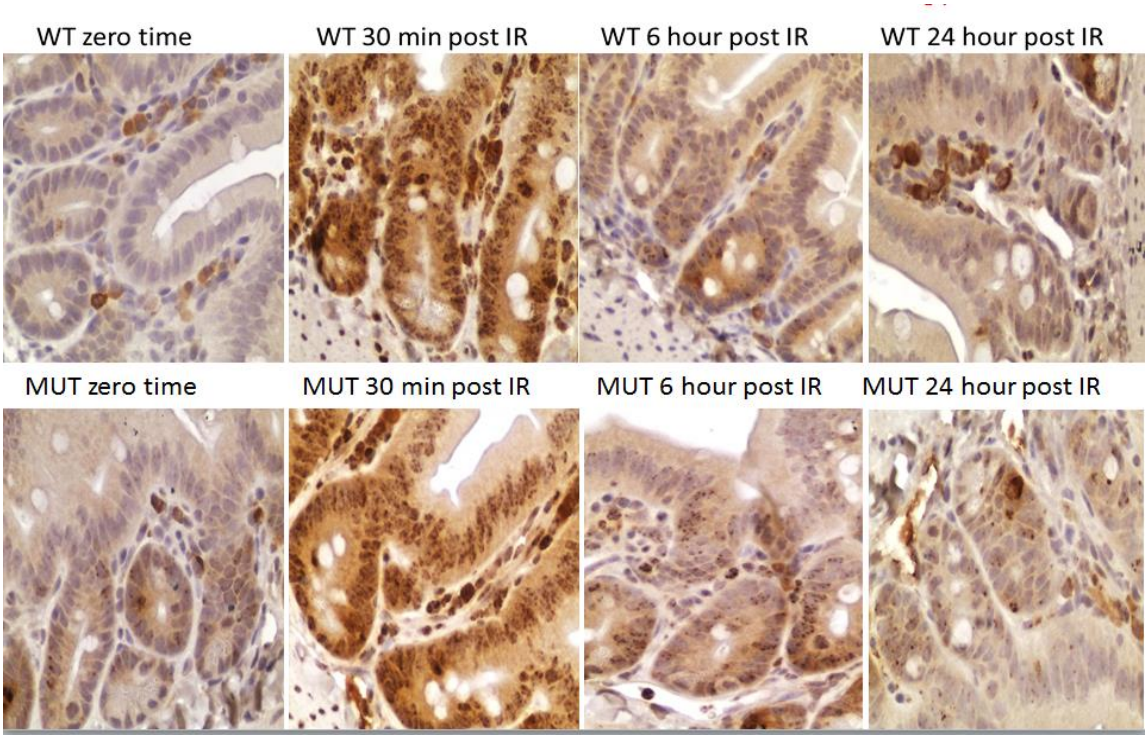

B-

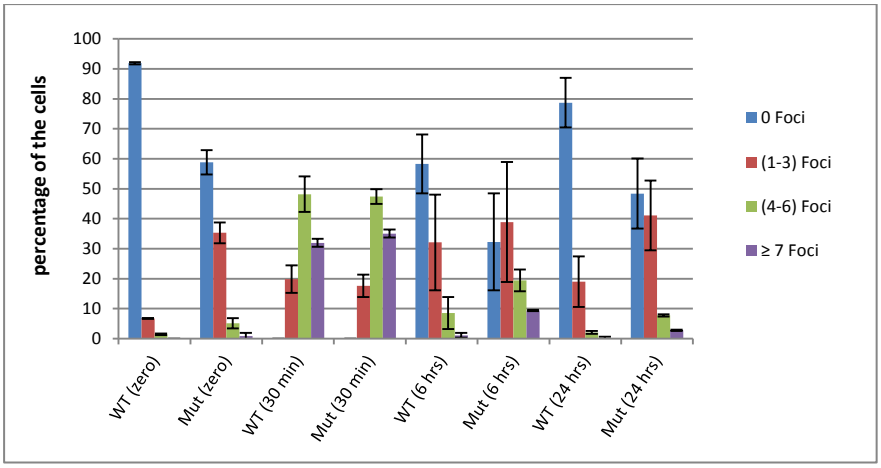

Figure 2-5. *Palb*2 MUT mice tissues show impaired DNA repair after irradiation. (A-D)

A. Representative IHC images for γH2AX of the intestinal sections from 8 weeks old *Palb*2 m/m and control mice at the indicated time points post 3 Gy IR.

B. Quantification of IHC for intestine γH2AX in panel A.

C-

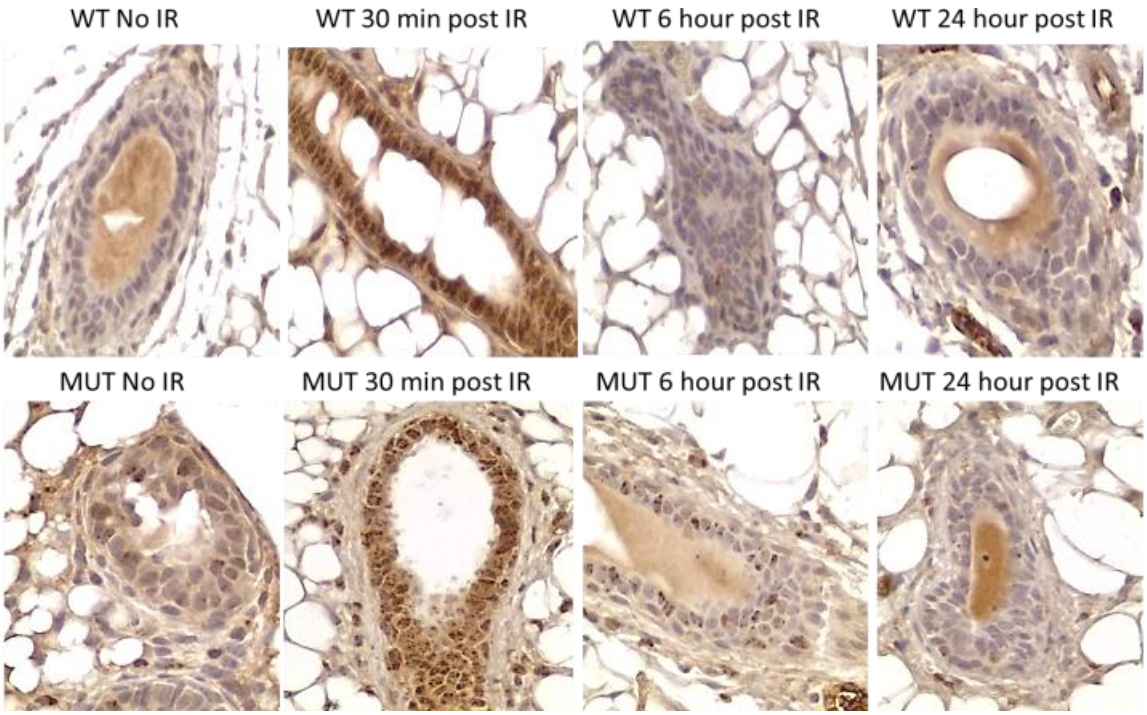

D-

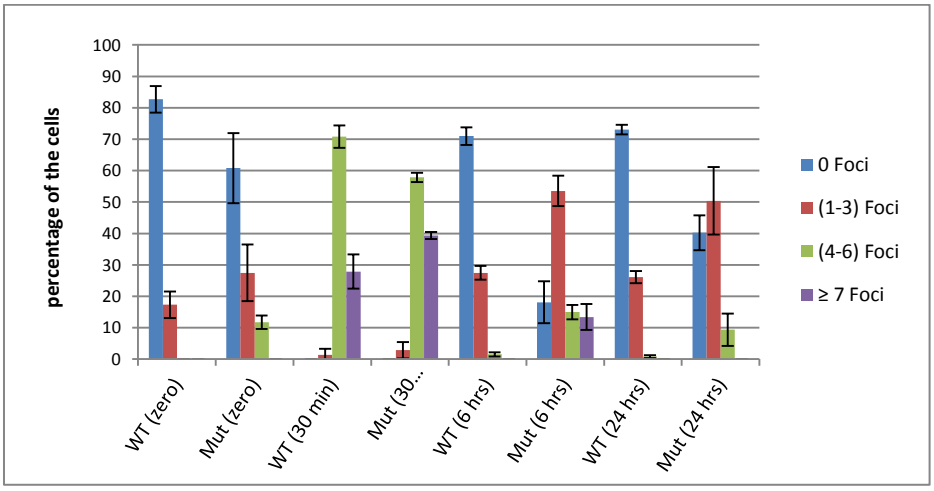

Figure 2-5 *Palb*2 MUT mice tissues show impaired DNA repair after irradiation.

C. Representative IHC images for γH2AX of the mammary gland sections of 8 weeks old *Palb*2 m/m and wt mice at the indicated time points post 3 Gy IR.

D. Quantification of IHC for mammary gland γH2AX in panel C.

It has been shown that 53BP1 is upregulated in BRCA1 deficient cells and promotes DSB repair through the NHEJ pathway, thereby protecting cell from death (141). Nonetheless, it will shift the balance towards the mutagenic pathway in the context of HR deficiency. However, it is still unclear or debatable if 53BP1 can inhibit BRCA1 recruitment to the damage site thus directing repair choice to NHEJ pathway (100). In addition, it has been shown that 53BP1 can be markedly reduced and degraded as early as 15 min post IR (142). To test whether our mutant tissues have any alteration of 53BP1 response, we performed IHC for detecting 53BP1. Surprisingly, we observed a resistance of 53BP1 to degradation in our mutant mice relative to control, suggesting that these cells may be dependent on this protein for repairing DNA damage (143, 144) (Fig. 2- 6 A & C). This difference was especially evident at 6 hr post IR, when the mutant intestine and mammary gland showed 55% and 58% cells with positive staining, versus 20% and 22% cells in corresponding wt tissues (Fig. 2-6 C & D).

Collectively, these finding suggest that in the context of HR deficiency there is an up-regulation of 53BP1 protein that enables the cells to repair its damage and survive.

Cells with high levels of DNA breaks but defective in HR are expected to undergo apoptosis, but those survive with mutagenic repair pathway have a potential to progress and become cancerous.

A-

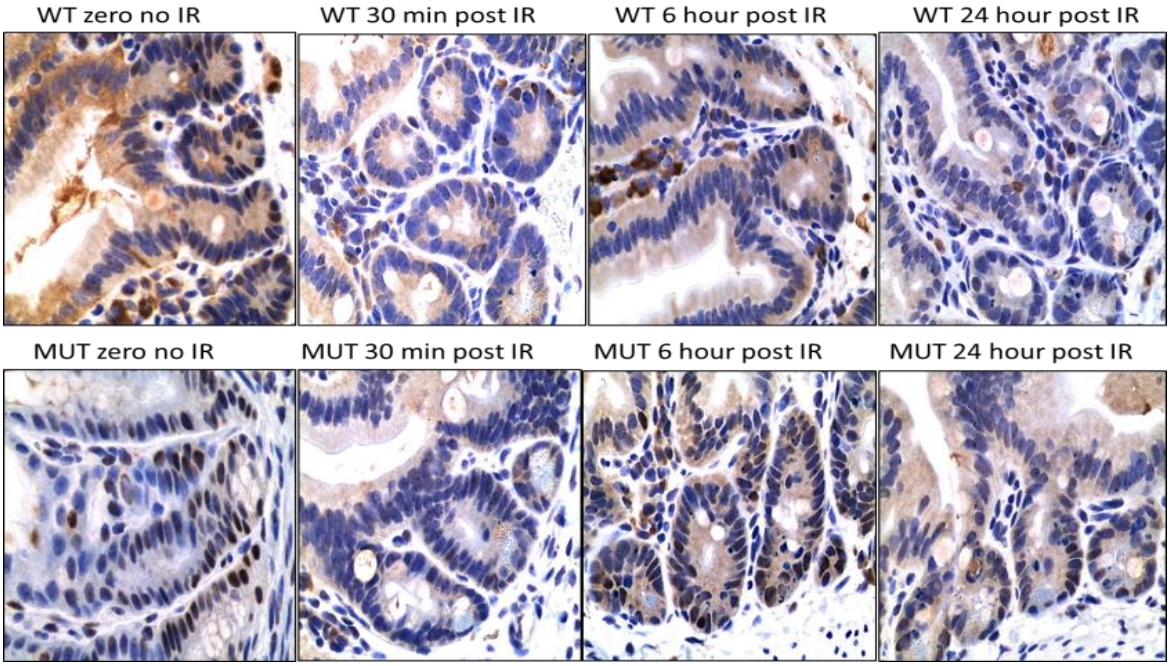

B-

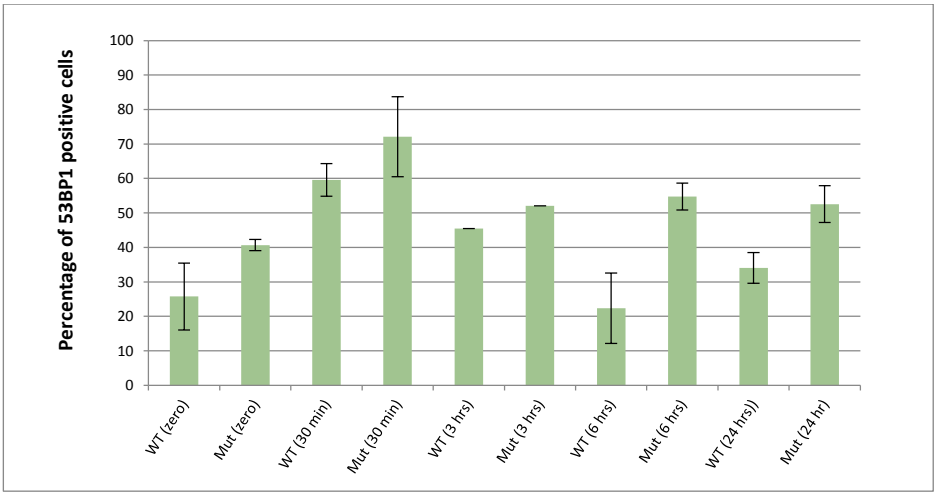

Figure 2-6 53BP1 is resistant to degradation after 6 hrof IR in *Palb2* mutant mice. (A-D)

A. Representative IHC images for 53BP1 in the intestinal sections from 8 weeks *Palb*2 m/m and wt mice at the indicated time points post 3 Gy IR.

B. Quantification of IHC for intestine 53BP1 in panel A above.

C-

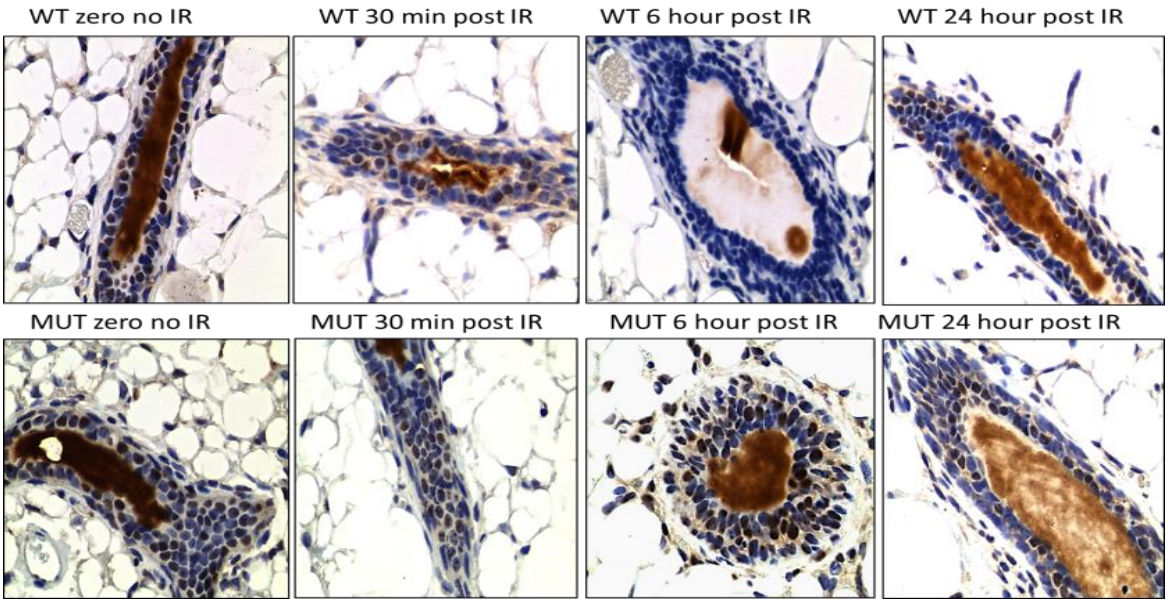

D-

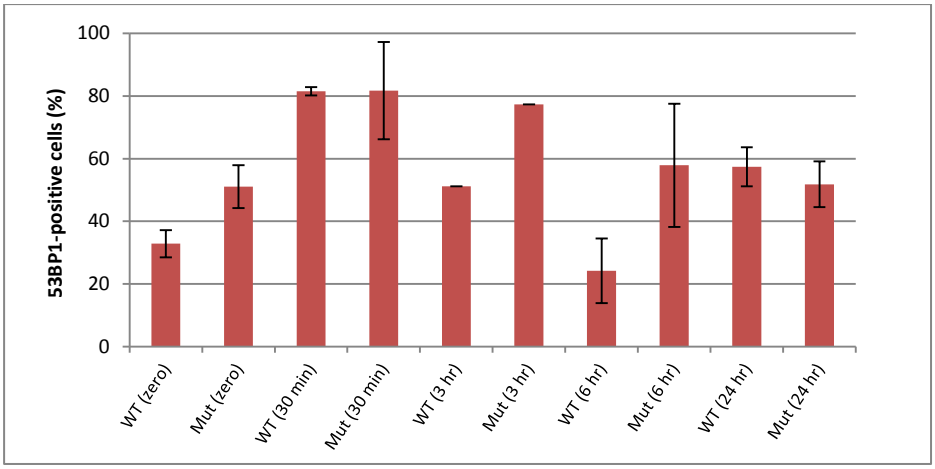

Figure 2-6 53BP1 is resistant to degradation after 6 hr of IR in *Palb2* mutant mice. (A-D)

C. Representative IHC images for 53BP1 in the mammary gland sections from 8 weeks old *Palb*2 m/m and control mice at the indicated time points post 3 Gy IR.

D. Quantification of IHC for mammary gland 53BP1 in panel C above.

2.4.5 Mutant mice tissues exhibit radio-resistant DNA synthesis, defective G2/M checkpoint, and resistant to apoptosis upon irradiation

The next questions we asked were whether abrogation of the PALB2-BRCA1 interaction would afford the mutant cells a potential proliferative advantage after irradiation and, if so, what was the fate of these cells - apoptosis or cell cycle arrest? These two questions were addressed by doing BrdU (Bromodeoxyuridine) incorporation and TUNEL (Terminal deoxynucleotidyl transferase end labeling) assays, respectively.

To assess proliferation, we analyzed BrdU incorporation in intestines and mammary glands. WT tissues showed a decrease in BrdU incorporation as compared to baseline levels without irradiation (Fig. 2-7), indicating an intact intra-S phase checkpoint in these tissues. In contrast, tissues in the mutant mice showed more proliferating cells after irradiation, suggesting that mutant cells have a defect in the intra-S check point that might give the cells a potential proliferative advantage over wt cells (17) or it could be driven by another pro-proliferation factor (will be discussed later). Mutant intestine and mammary gland showed increase in BrdU positive cells especially at 6 hr post IR (42% and 20% in mutant tissues versus 23% and 5% in wt tissues) (Fig.2-7 B and D).

Then next question is whether this interaction is crucial for the G2/M checkpoint in vivo? If more cells showed incorporation with BrdU in MUT, we would expect that a higher numbers of cells enter into mitosis (cell cycle progression). Similarly, more phospho-histone H3, an M phase marker, positive cells were found in various tissues of the mutant mice after radiation (Fig. 2-8 A

and C). This provides further evidence that a larger number of mutant cells will divide after IR; in contrast, little pH3-positive cells were detected in tissues of wt mice, suggestive of a G2 arrest.

A-

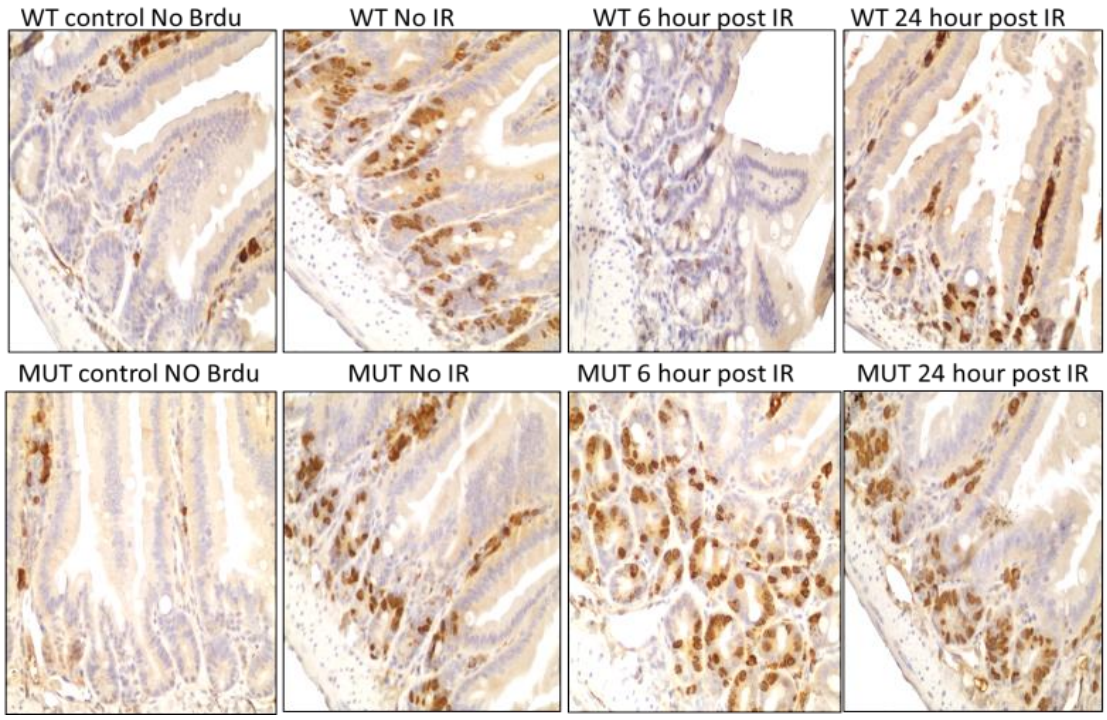

B-

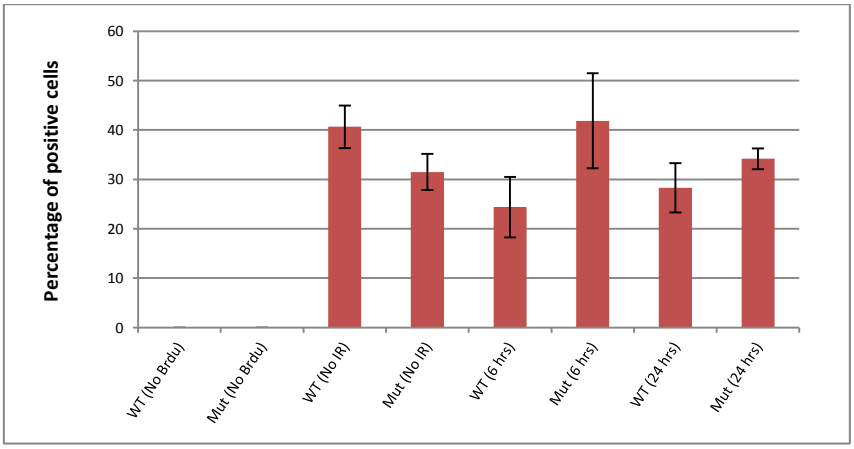

Figure 2-7 *Palb*2 MUT mice tissues show higher levels of BrdU incorporation than control after irradiation. (A-D)

A. Representative IHC images for BrdU incorporation of the intestinal sections from 8 weeks old *Palb*2 m/m and control adult mice at the indicated time points post 3 Gy IR.

B. Quantification of IHC results for intestine BrdU incorporation in panel A above.

C-

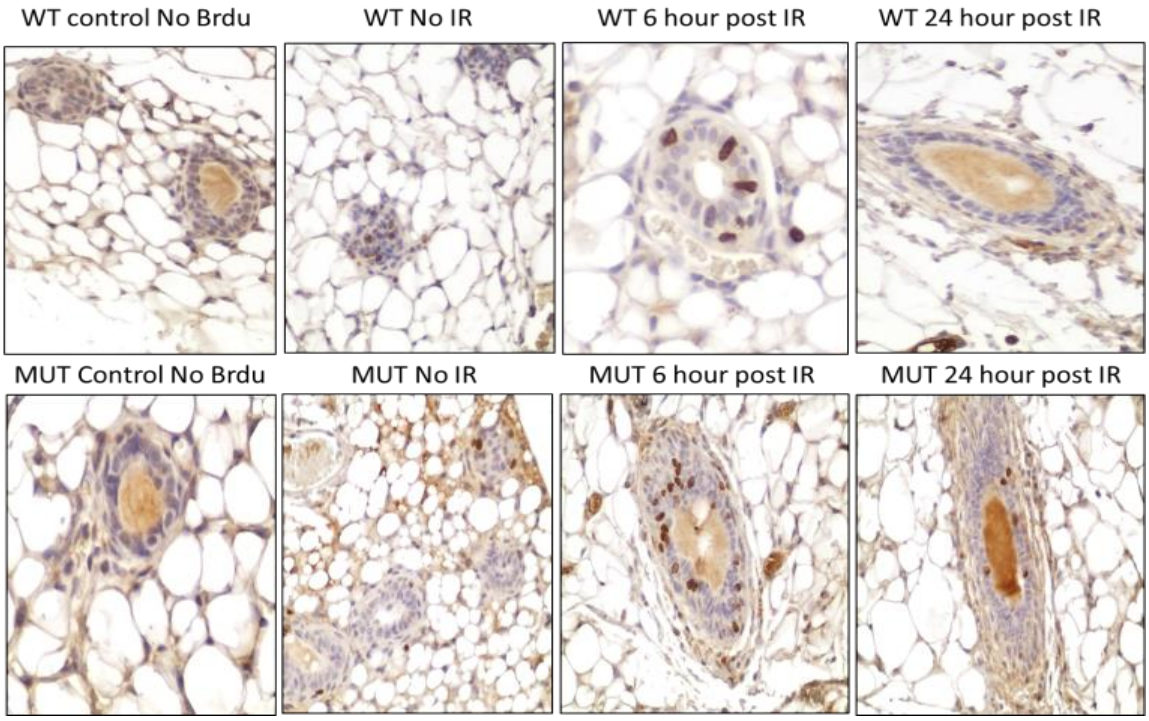

D-

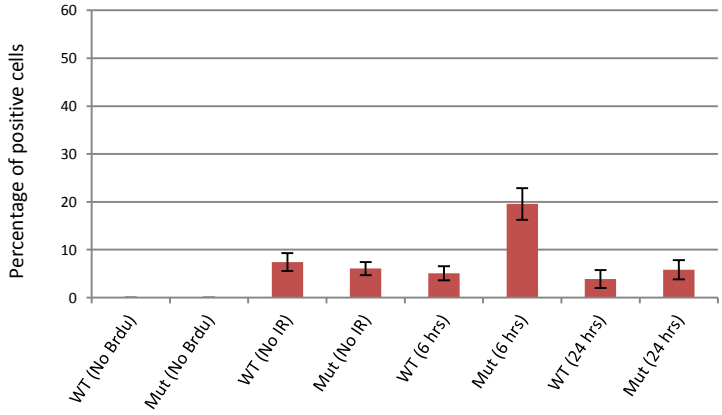

Figure 2-7 *Palb*2 MUT mice tissues show higher levels of BrdU incorporation than control after irradiation. (A-D)

C. Representative IHC images for BrdU incorporation in the mammary glands of 8 weeks old *Palb*2 m/m and control adult mice at the indicated times post 3 Gy IR.

D. Quantification of IHC for mammary gland BrdU incorporation in panel C above.

A

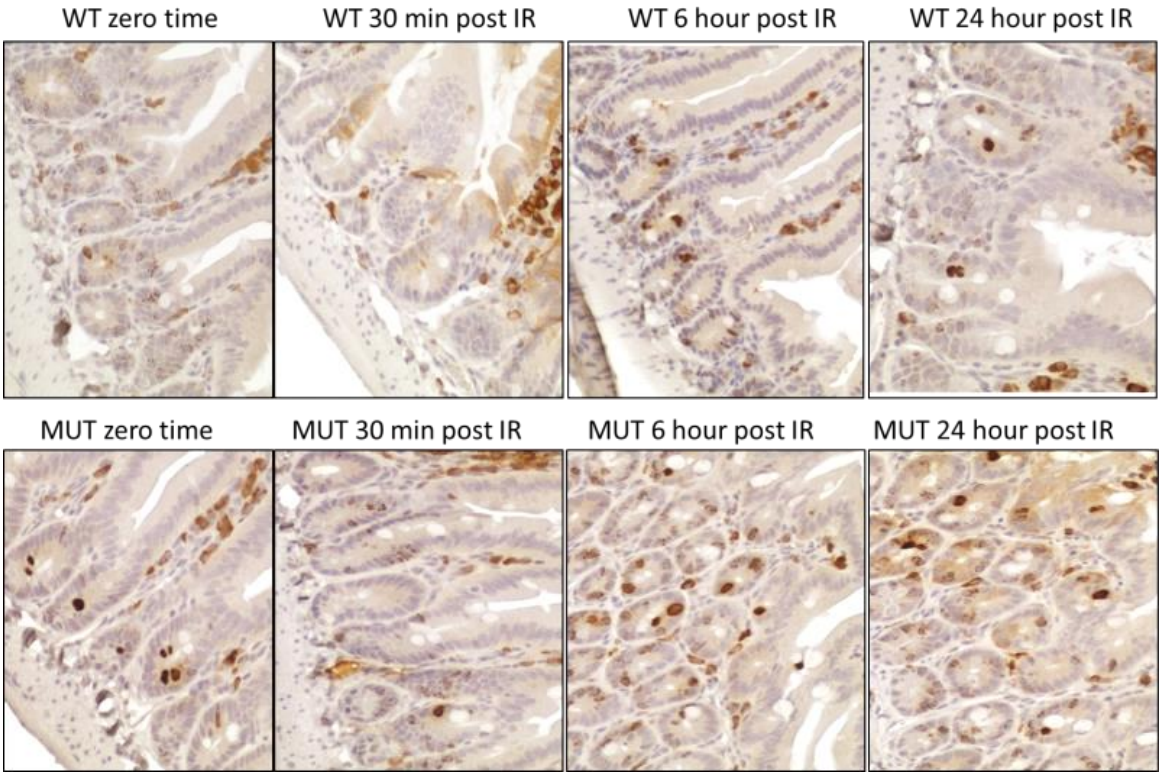

B-

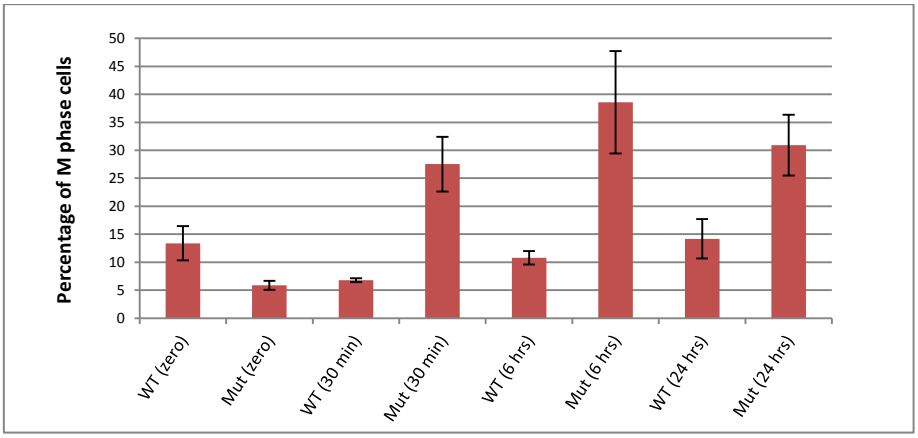

Figure 2-8 G2/M checkpoint activation defect in *Palb*2 MUT tissues. (A-D)

A. Representative IHC images for phospho-histone H3 in the intestinal sections from 8 weeks old *Palb*2 m/m and control adult mice at the indicated times post 3 Gy IR.

B. Quantification of IHC for intestine phospho-histone H3 in panel A.

C-

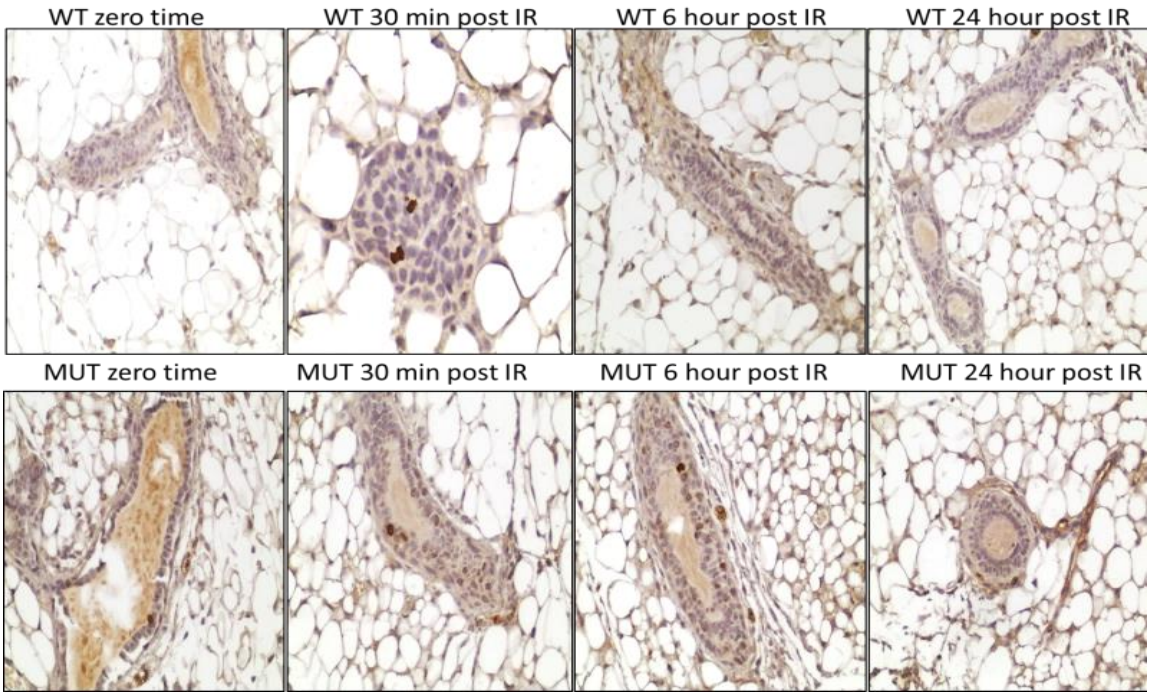

D-

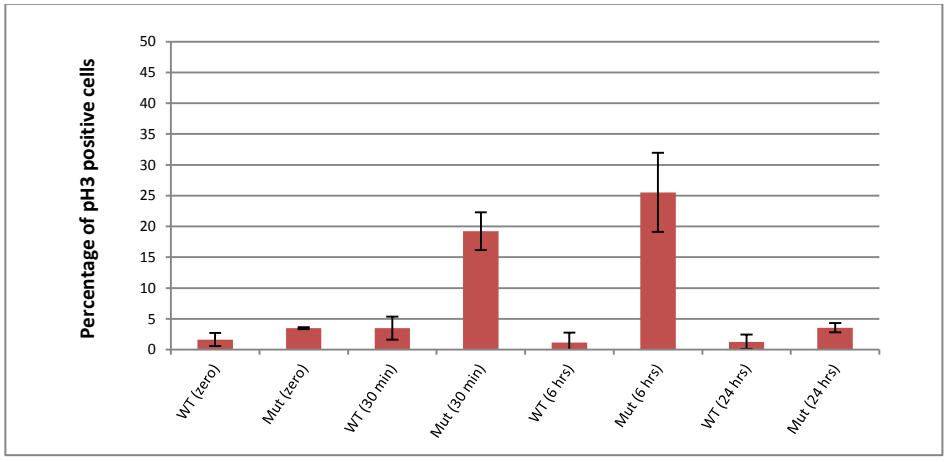

Figure 2-8 G2/M checkpoint activation defect in *Palb*2 MUT tissues. (A-D)

C. Representative IHC images for phospho-histone H3 in the mammary glands of 8 weeks old *Palb*2 m/m and control female mice at the indicated times post 3 Gy IR.

D. Quantification of IHC for mammary gland phospho-histone H3 in panel C.

Apoptosis regulates and controls immune system maturation and cell death through receptor selection (145). Therefore, apoptosis plays a fundamental role in regulation of maturation and growth of lymphocytes. Failure of these cells to undergo apoptosis after DNA damage might result in high mutation rate with survival of these damaged cells, ultimately leading to transformation.

To test for apoptosis in the tissues, we performed the TUNEL assay. As shown in Fig 2.9 A and B, mutant tissues showed less apoptosis than wt control. Mutant intestine and mammary gland showed less apoptotic signal compare to wt tissues (12% and 6% versus 18% and 17% at 30 min post IR, and 14% and 6% versus 20% and 18% at 6 hr post IR), indicating that mutant cells are defective for apoptosis (Fig. 2-9). Furthermore, mutant intestine and mammary gland showed higher IHC staining of phospho-H3, a marker for mitotic cells, post irradiation. This enables the cells to continue to proliferate in spite of the existence of DNA damage, which may lead to further genetic changes and tumor development. Taken together with results of phospho-H3 IHC and BrdU incorporation, these results imply that a significant number of wt cells arrest in S and G2 phases and/or undergo apoptosis, while mutant cells were defective in both, providing a possible mechanism for increased tumor development.

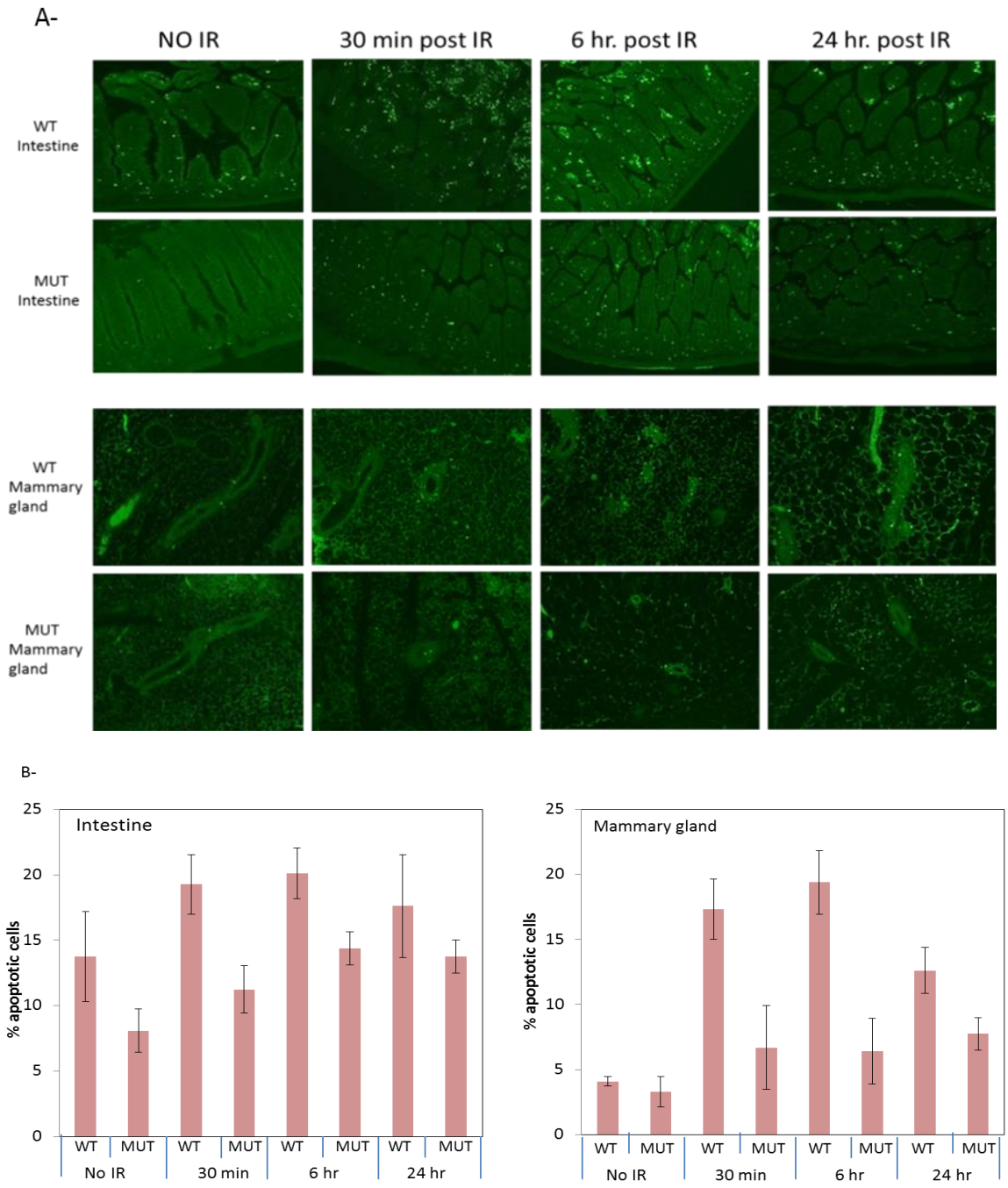

Figure 2-9 Failure of *Palb*2 MUT tissues to undergo apoptosis after DNA damage.

A. Representative TUNEL assay images of the tissue sections from 8 weeks old *Palb*2 m/m and control mice at the indicated times post 3 Gy IR. Upper panels show intestines and lower panels show mammary glands.

B. Quantification of TUNEL assay for intestine (left) and mammary gland (right) in panel A.

2.4.6 Mutant tissues show higher p53 and p21 expression than control

Given the critical role of p53 in the regulation of cell apoptosis, we checked the status of p53 and its downstream target p21 in this context. P53 induction after IR in MUT tissues was found to be more than that in wt tissues (Fig. 2-10). Similar observation was made with respect to p21 (Fig. 2-11). These findings suggest a possibility that the apoptotic function of p53 is blocked or overcome by an anti-apoptotic factor, such as (NF-κB), as will be shown later. That fact that p21 was induced suggest that a G1/S checkpoint could be activated at least transiently, although this needs to investigated further.

A-

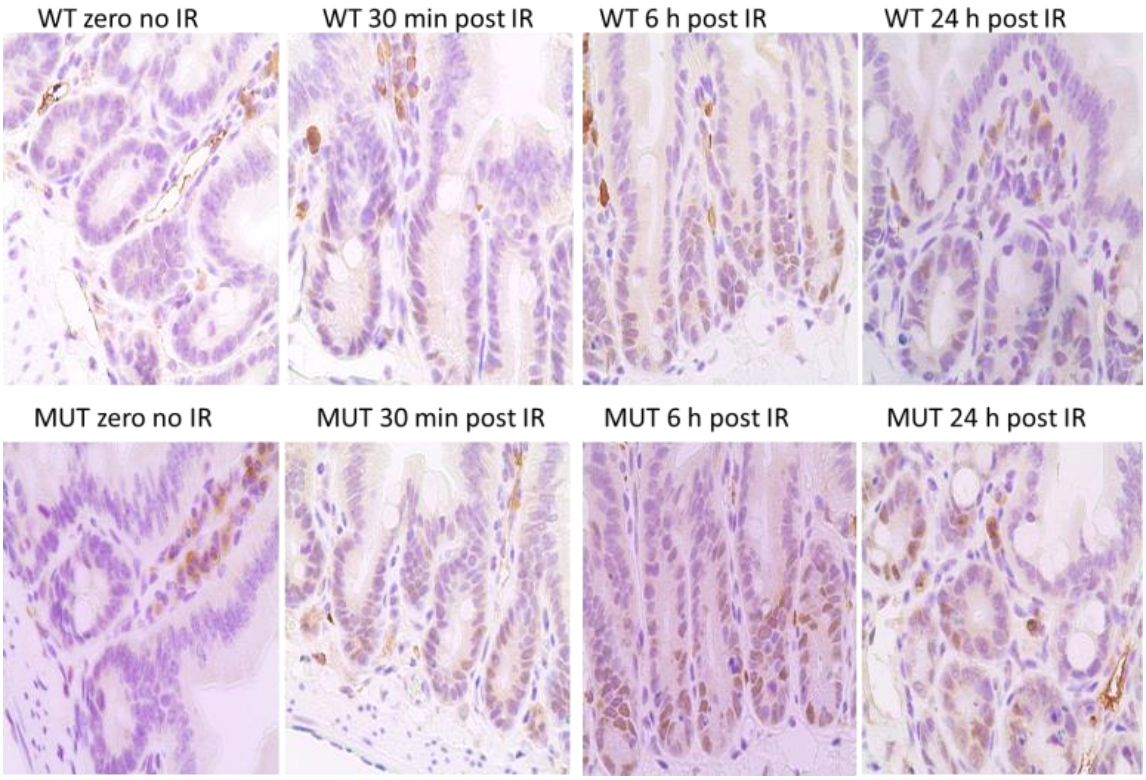

B-

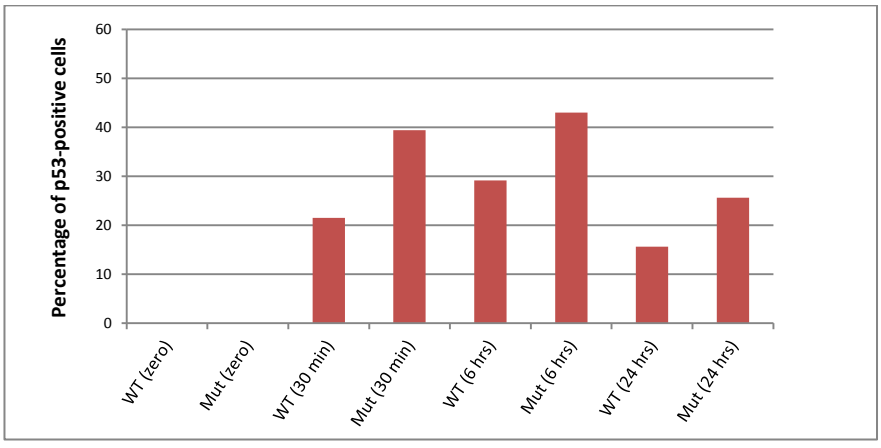

Figure 2-10 Induction of p53 after IR is higher in mutant than in wt mice. (A-D)

A. Representative IHC images for p53 in the intestinal sections from 8 weeks old *Palb*2 m/m and wt mice at the indicated times post 3 Gy IR.

B. Quantification of IHC for intestine p53 in panel A above.

C-

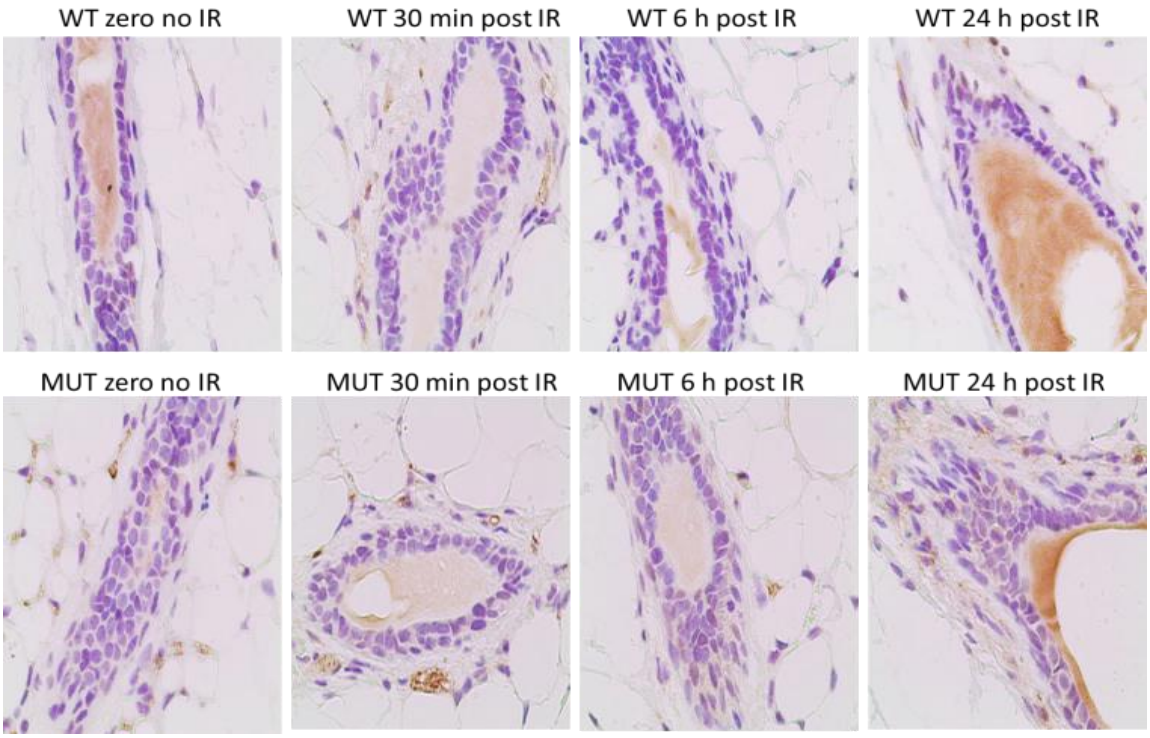

D-

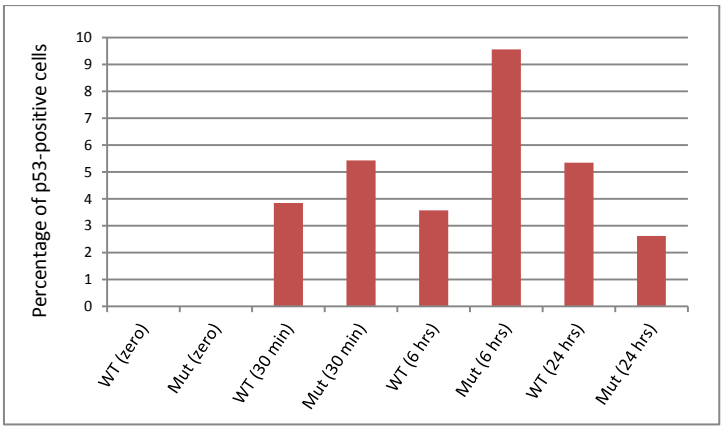

Figure 2-10 Induction of p53 after IR is higher in mutant than in wt mice. (A-D)

C. Representative IHC images for p53 of the mammary gland sections from 8 weeks old *Palb*2 m/m and wt control mice at the indicated times post 3 Gy IR.

D. Quantification of IHC for mammary gland p53 in panel C above.

A-

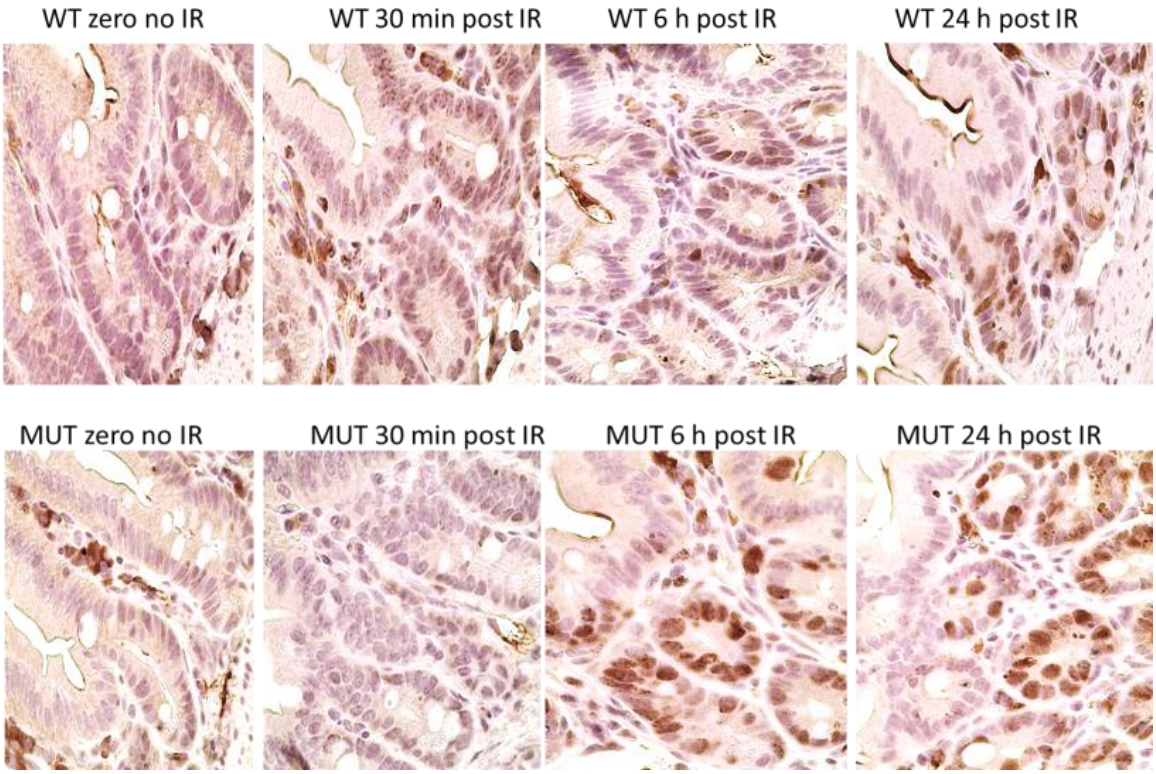

B-

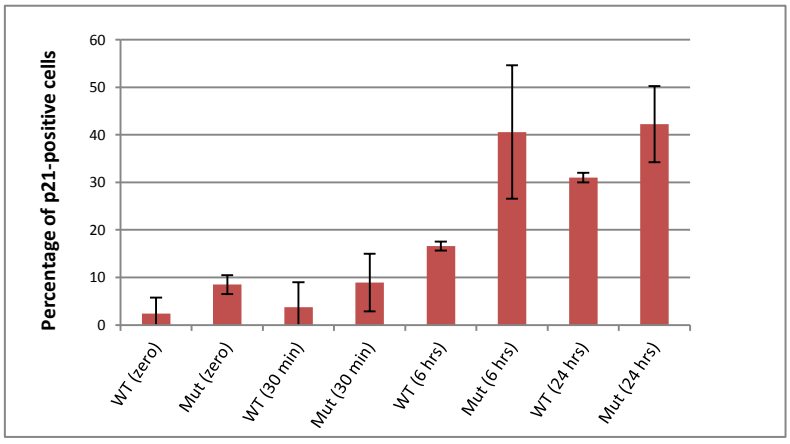

Figure 2-11 Induction of p21 after IR is higher in mutant than in wt mice. (A-D)

A. Representative IHC images for p21 of the intestinal sections from 8 weeks old *Palb*2 m/m and wt control mice at the indicated times post 3 Gy IR.

B. Quantification of IHC for intestine p21 in panel A above.

C-

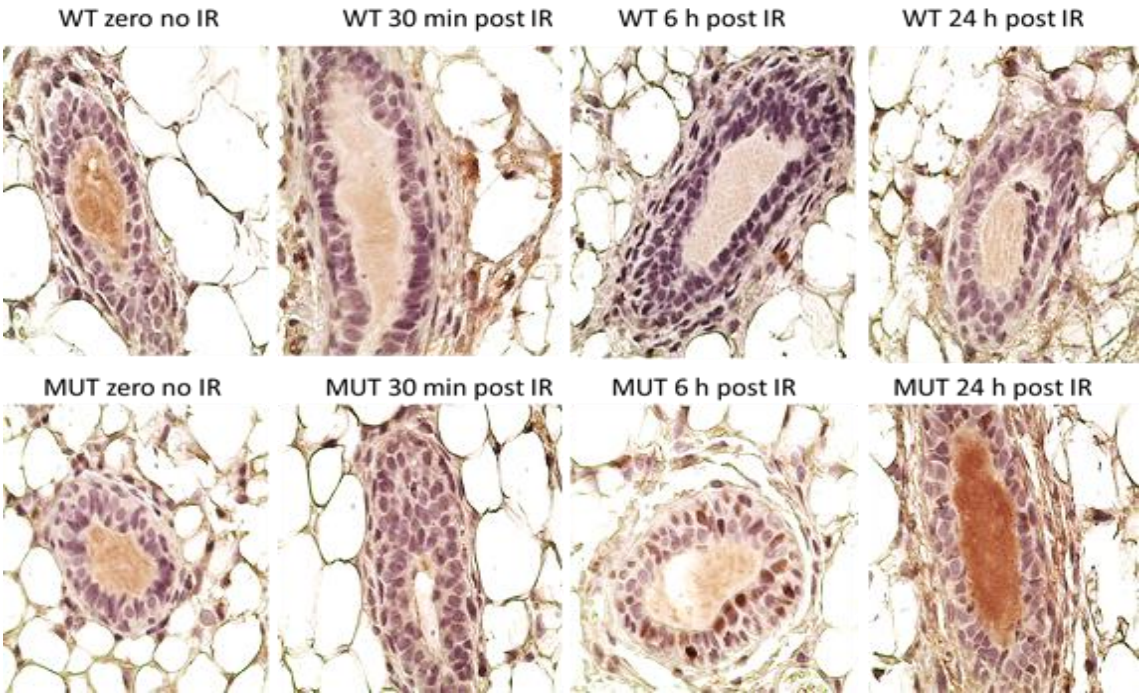

D-

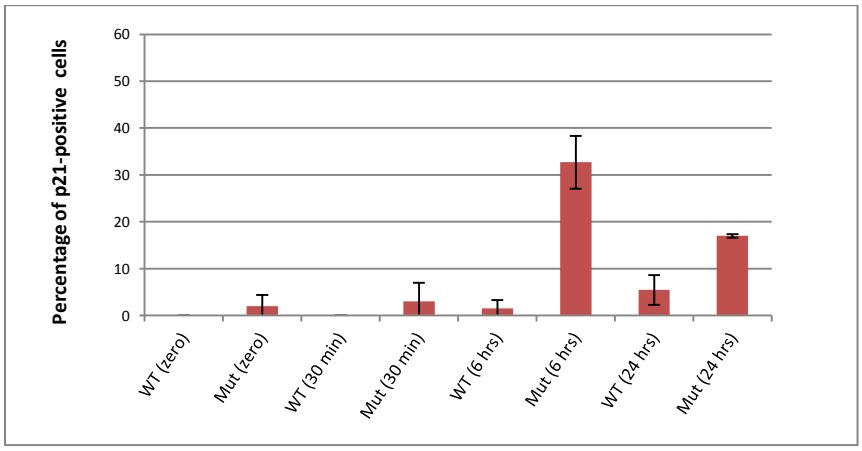

Figure 2-11 Induction of p21 after IR is higher in mutant than in wt mice. (A-D)

C. Representative IHC images for p21 of the mammary gland sections from 8 weeks old *Palb*2 m/m and wt control adult mice at the indicated times post 3 Gy IR.

D. Quantification of IHC for mammary gland p21 in panel C above.

2.4.7 Mutant thymic tissue shows impaired DNA damage repair but increased DNA synthesis and reduced apoptosis after radiation

Since the vast majority of irradiated mice developed thymic lymphoma, we further examined the thymic gland by IHC to detect γH2AX, BrdU incorporation, caspase 3, and the pro-survival factor NF-κB (p65), as well as by TUNEL assay to analyze apoptosis (Fig. 2-12A-E). Similar to the situation with mammary glands and intestines, we found more γH2AX induction in the mutant thymus, yet it showed higher levels of BrdU incorporation, less caspase 3 and less TUNEL staining (Fig. 2-12). Importantly, increased NF-κB expression was detected in the mutant thymus, suggesting that it may attenuate radiation-induced apoptosis and allow accumulation of mutations in mutant thymocytes, ultimately leading to the formation of thymic lymphoma.

A-

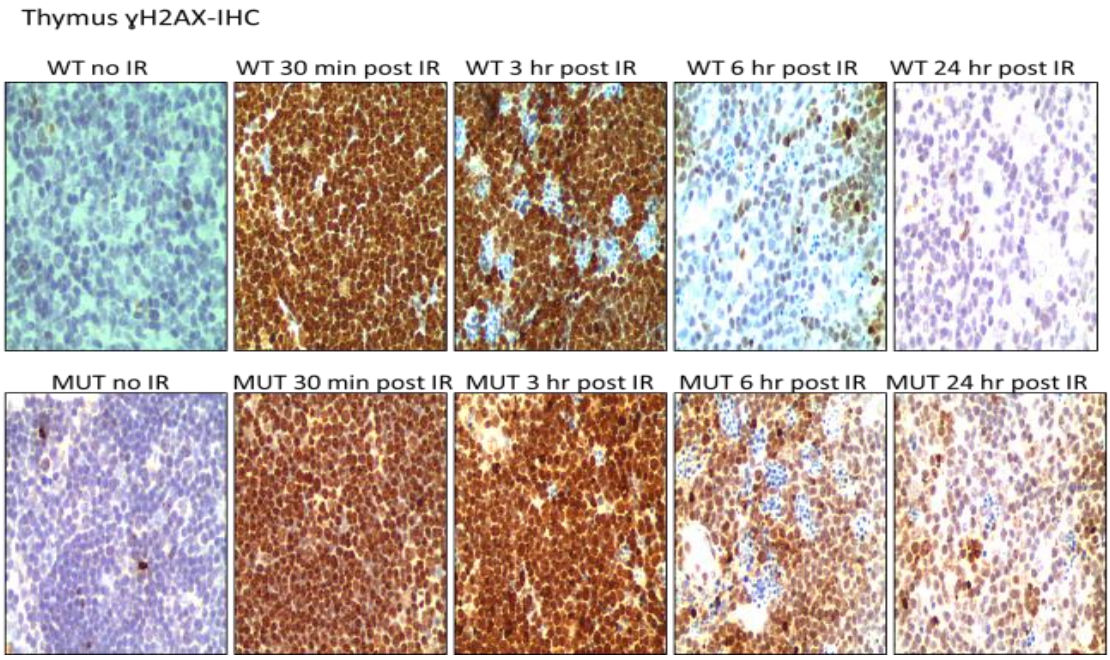

B-

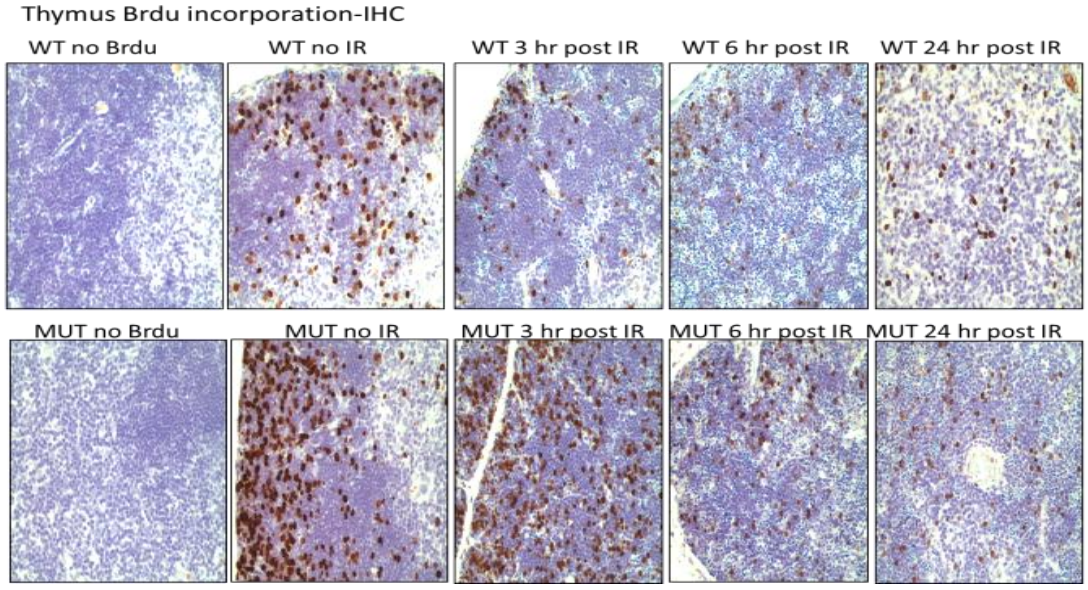
Thymus Brdu incorporation-IHC
WT no Brdu
WT no IR
WT 3 hr post IR
WT 6 hr post IR
WT 24 hr post IR
MUT no Brdu
MUT no IR
MUT 3 hr post IR
MUT 6 hr post IR
MUT 24 hr post IR

C-

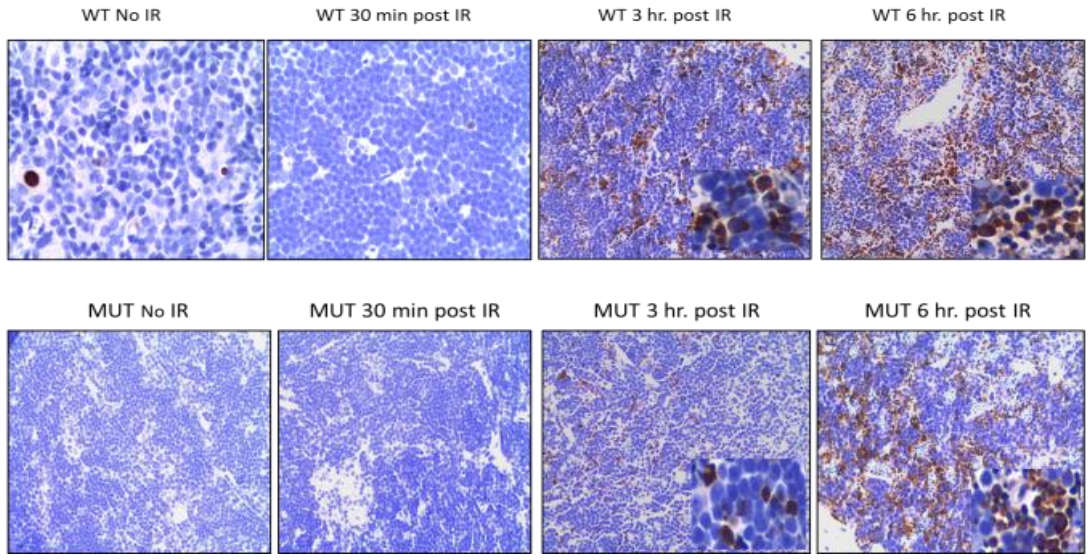
Thymus Caspase-3 IHC
WT No IR
WT 30 min post IR
WT 3 hr. post IR
WT 6 hr. post IR
MUT No IR
MUT 30 min post IR
MUT 3 hr. post IR
MUT 6 hr. post IR

D-

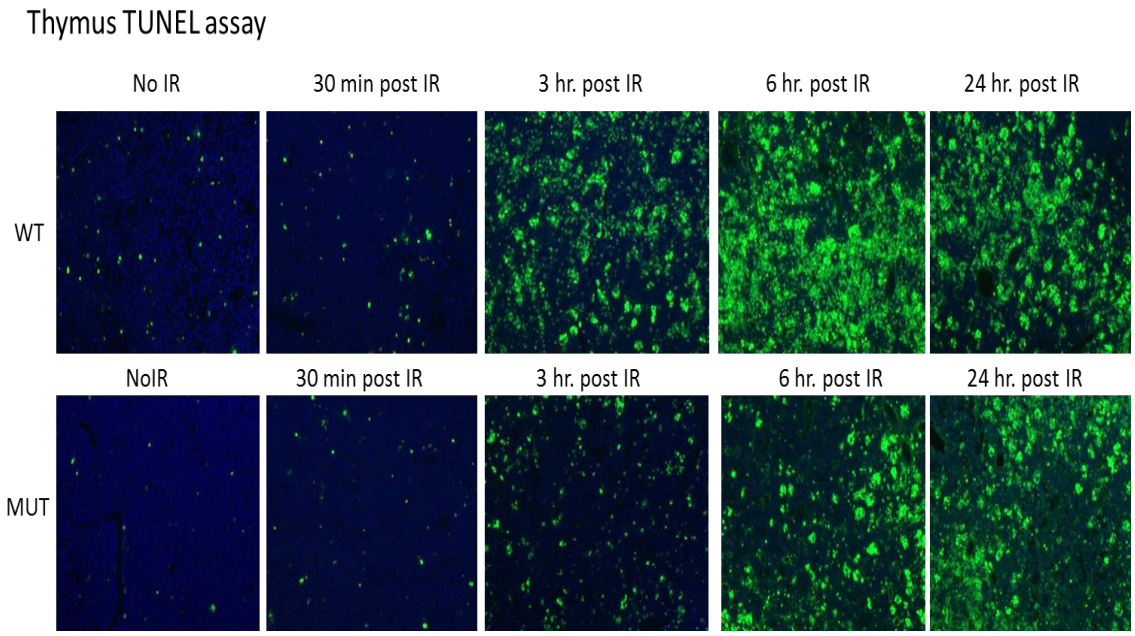

E-

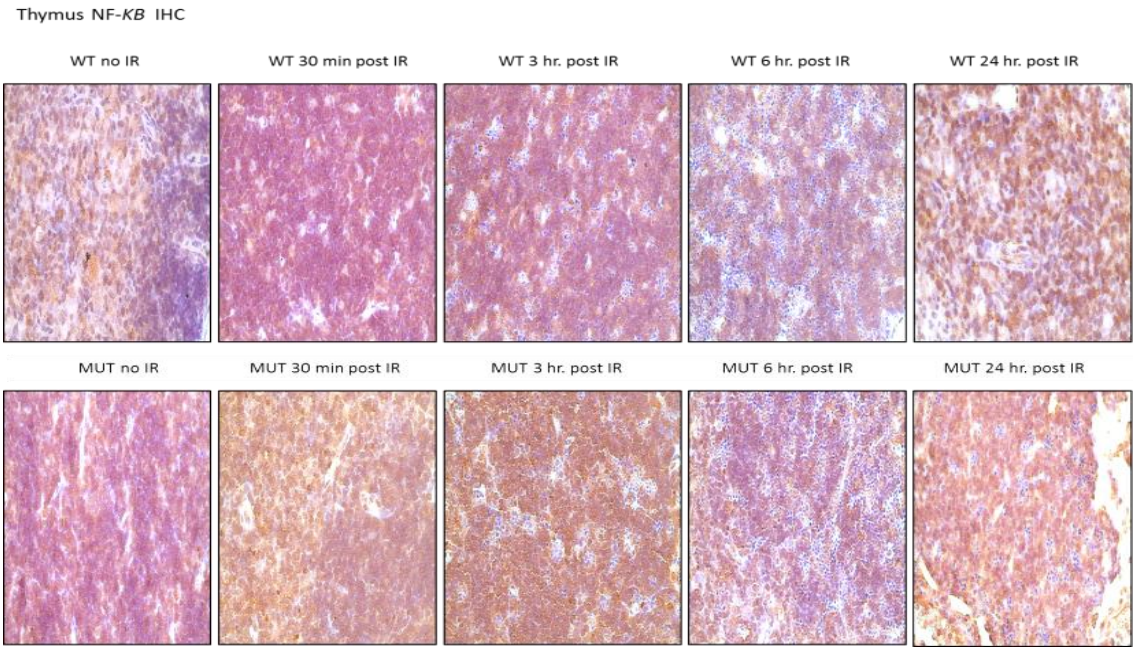

Figure 2-12 Comparative analyses of mutant vs wt thymus tissues before and after radiation. (A-E)

Representative IHC images from 8 weeks old *Palb*2 m/m and wt mice at the indicated times post 3 Gy IR. A. γH2AX; B, BrdU incorporation; C, Caspase 3, D. TUNEL assay; and E, NF-κB (p65).

Next, to explore the status of DNA damage response in the thymic lymphomas, we did γH2Ax and 53BP1 IHC in these tumors. Our findings are higher levels of γH2AX and 53BP1 foci in the mutant than control wt thymic tumors (Fig. 2-13 A and B). These observations suggest that mutant thymic lymphomas remain inefficient to repair and continue to generate more DSBs than do wt tumors. Since the lymphocytes have a high rate of cellular turnover and proliferation, they likely have a higher dependence and needs for DNA damage repair. Collectively, the above data suggest that compromised BRCA1-PALB2-BRCA2 pathway could be a potential mechanism for thymic lymphoma development. In consistent with this notion, a recent report showed for the first time two patients presented with non-Hodgkin lymphoma carrying biallelic *PALB2* mutations (139). These two patients have biallelic *PALB2* mutations, one being a truncating mutation and the second a deletion of exon 6, underscoring a fundamental role of PALB2 in lymphoma suppression (139).

A- (γH2AX)

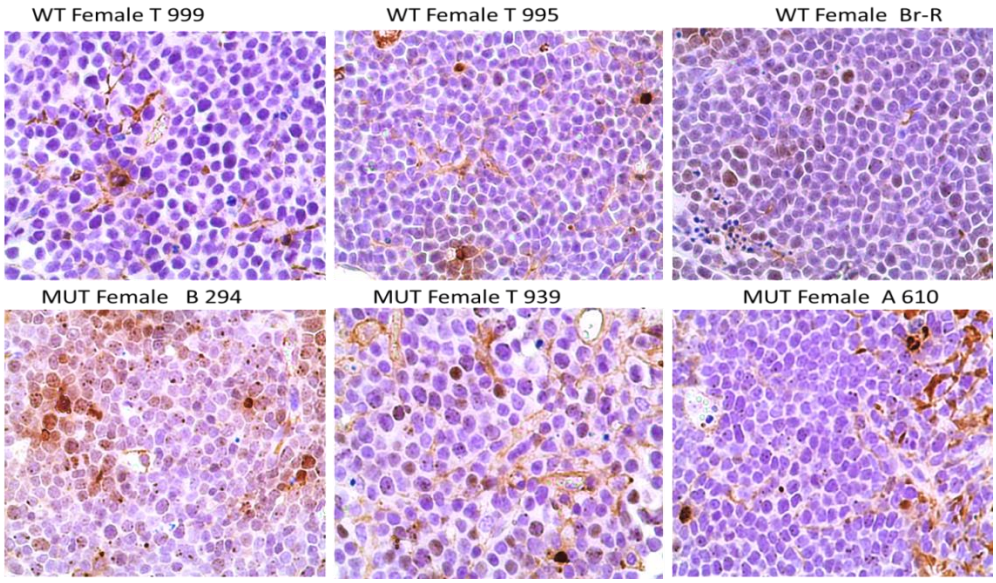

B- (53BP1)

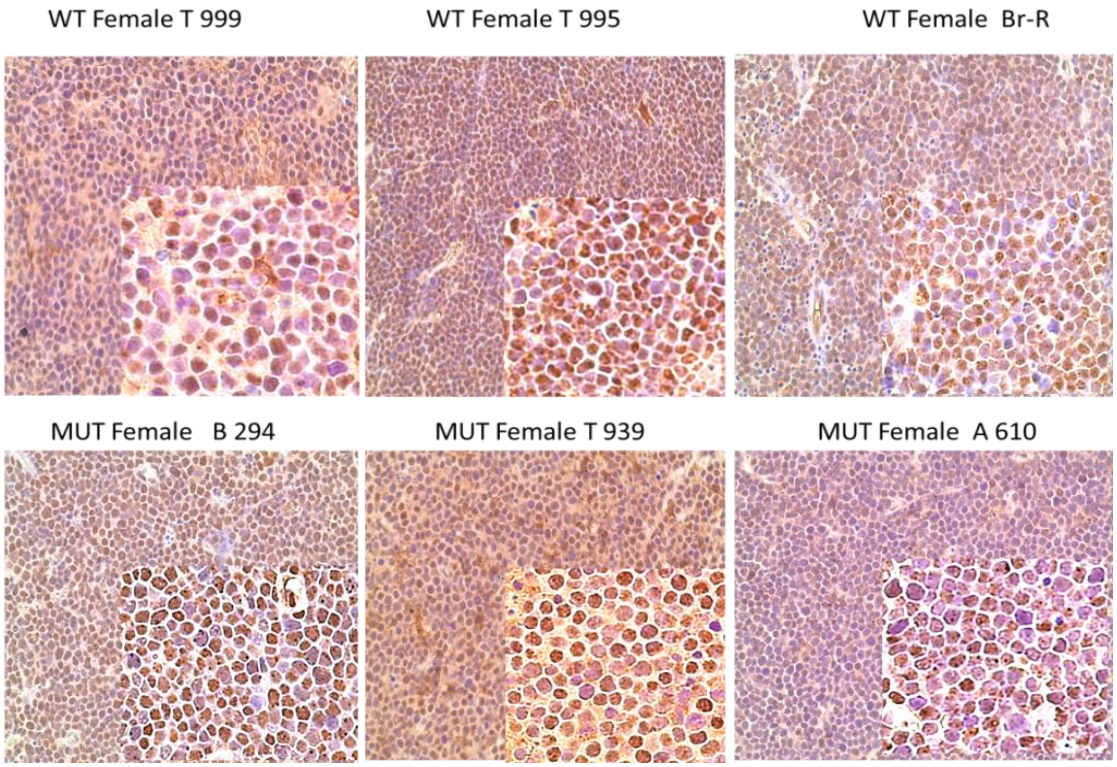

Figure 2-13 γH2AX and 53BP1 foci in thymic lymphomas arising from *Palb2* mutant and wt mice.

A. Representative IHC images for γH2AX in tumors from ~250 days old *Palb*2 m/m and wt mice.

B. Representative IHC images for 53 BP1 in tumors from ~250 days old *Palb*2 m/m and wt mice.

2.4.8 DMBA treatment accelerates breast cancer development in *Palb2* mutant mice with shift in tumor histological characteristics

Since our mutant mice did not develop mammary tumors after IR challenge, possibly due to early development of thymic lymphomas, we next challenged them with carcinogen 7,12-dimethylbenz(a)anthracene (DMBA), which has been shown to induce mammary tumor formation in mice. (See the introduction about its properties and mechanism of actions).

Generation of high levels of reactive oxygen species (ROS) and DNA adducts is a well known mechanism of action for DMBA. Therfore, it is not surprising that our mutant mice were more sensitive to the toxicity of the drug than wt mice (70% of mutant mice died from toxcicity vs 20% for wt mice, T_{50}= 60 Vs T_{50}= 150 days,respectively, when treated with a single dose of 1 mg DMBA). Then, we reduced the dosage to fractionated 0.5 mg (2 X 0.25 mg, one week apart). Again the mutant mice showed higher sensitivity as shown in Kaplan-Meier survival curve (Fig. 2-14 A) (56% for mutant vs 0% for wt control, with T_{50}=80 vs 150 days, respectively). Finally, we treated the mice with 0.1 mg for WT and 0.08 mg for MUT of DMBA, which was well tolerated by both mutant and wt mice in term of toxcicity. Wt and mutant mice treated with 0.1 mg DMBA exhibited similar incidence of mammary gland tumors between (55% vs 50%, respectively) (Fig. 2-14B). However, there are clear differece in tumor latency (T_{50}= 256 vs 388 days for mutant and wt mice, respectively) (Fig. 2-14 A). Moroever, tumors that developed in the mutant mice consisted of 90% spindle neoplasm and 10% sequamous neoplasm, while among those arising from wt

mice 50% were spindle neoplasm, 40% sequamous and 10% mixed (Fig. 2-15B). Tumors from the mutant mice were of higher grade, with sarcoma-like appearance, spindle-shaped cells with prominant nuclei, and high mitotic index with significant necrosis. A previous study showed that spindle cells neoplasm have poor prognosis with high rate of metastasis and were almost always triple negative (146). These results indicate a difference in gene expression profiles between the two groups of tumors resulting in different histological subtypes (Fig.2-15 B).

A-

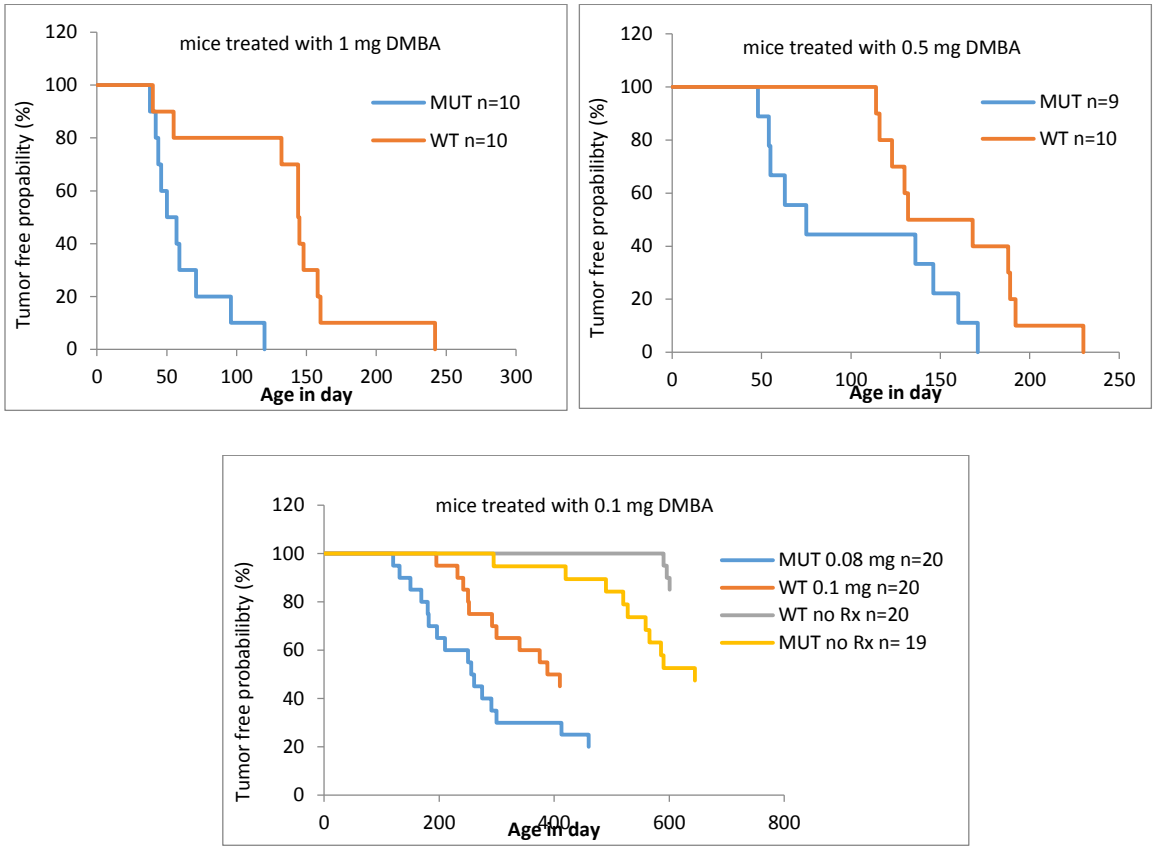

Figure 2-14 Tumor formation in DMBA treated *Palb*2 knockin and wt control mice. (A-B)

A. Kaplan-Meier tumor free survival curve of DMBA treated *Palb*2 m/m and control adult female mice (at DMBA dosages indicated with each curve).

B-

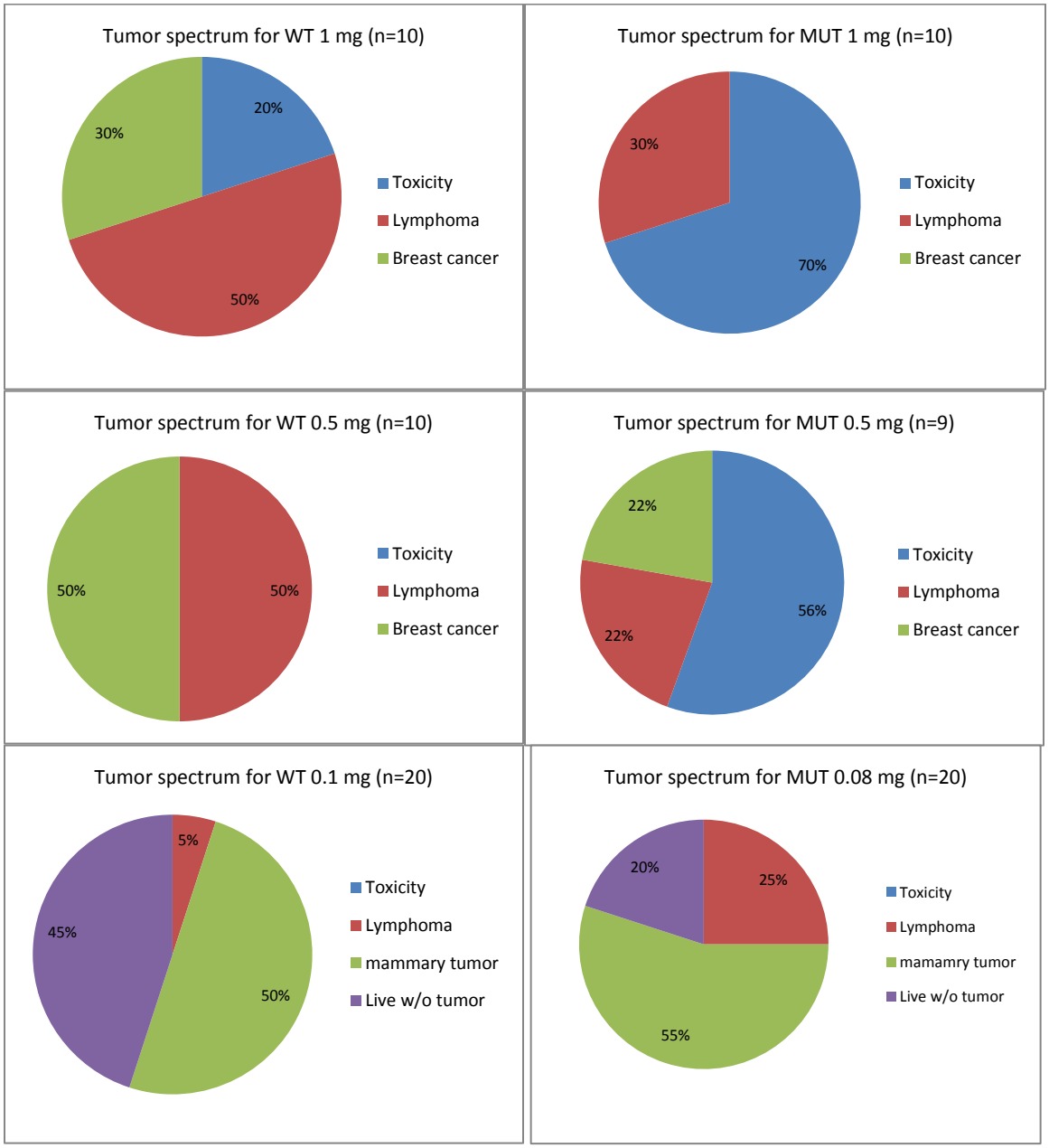

Figure 2-14 Tumor formation in DMBA treated *Palb*2 knockin and wt control mice. (A-F)

B. Tumor spectrums of DMBA treated adult female mice (at DMBA dosages indicated with each spectrum).

A-

B-

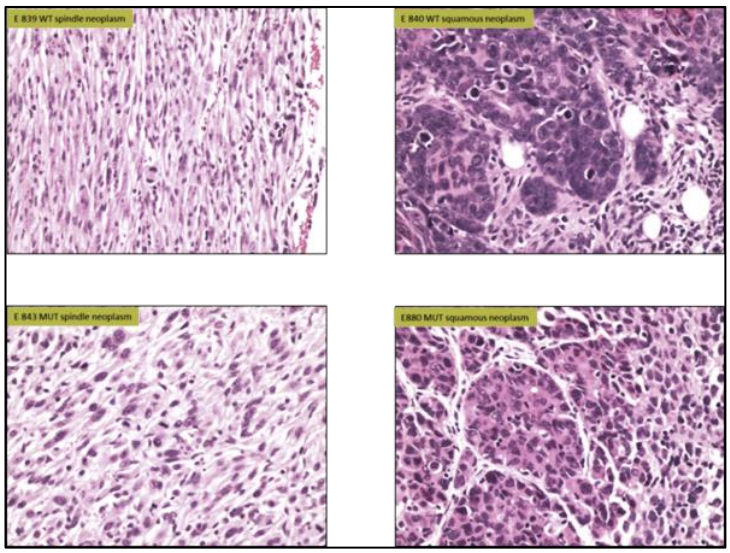

C-

Slide #	Latency(day)	Tag	Genotype	Tissue	Histologic review	Tubule	Nuclear grade	Mitosis	Grade	Differentiation	Necrosis
WT											
Xia-839	269	E 955	WT	MG	Spindle cell neoplasm	3	2	3	8	Poor	Moderate
Xia-840	199	E 987	WT	MG	Squamous cell carcinoma mixed adenosequamous	2	3	3	9	Poor	Mild
Xia-841	289	E 993	WT	MG	Squamous cell carcinoma mixed glandular	2	3	2	7	Moderate	Extensive
Xia-842	269	E 809	WT	MG	Spindle cell neoplam epithelial cell	3	3	2	8	Poor	Moderate
Xia-871	398	E 985	WT	MG	Spindle cell neoplasm	3	3	3	9	Poor	Moderate
Xia-872	370	E 991	WT	MG	Squamous cell and glandular	3	3	3	9	Poor	Extensive
Xia-873	296	E 829	WT	MG	Spindle cells and squamous mixed	3	2	2	7	Moderate	Extensive
Xia-874	391	R lost	WT	MG	Spindle cell neoplasm	3	3	3	9	Poor	Moderate
Xia-875	247	E 954	WT	MG	Spindle cell neoplasm	3	3	3	9	Poor	Moderate
Xia-876	308	E 810	WT	MG	Sequamous with glandular arrangment	2	3	3	8	Poor	Extensive
	Mean 303.6				Spindle neoplasm 50%, squamous 40%, mixed 10%						
MUT											
Xia-843	195	E 997	MUT	MG	Spindle cell neoplasm	3	3	3	9	Poor	Mild focal
Xia-844	238	E 984	MUT	MG	Spindle cell neoplasm	3	3	3	9	Poor	Moderate
Xia-845	241	E 973	MUT	MG	Spindle cell neoplasm	3	2	2	7	Moderate	Extensive
Xia-846	162	E 812	MUT	MG	Spindle cell neoplasm	3	2	2	7	Moderate	Extensive
Xia-847	273	E 969	MUT	MG	Spindle cell neoplasm	3	3	3	9	Poor	Moderate
Xia-848	174	E 999	MUT	MG	Spindle cell neoplasm	3	3	2	8	Poor	Moderate
Xia-877	370	E 1000	MUT	MG	Spindle cell neoplasm	2	3	2	7	Moderate	Extensive
Xia-878	148	No cut	MUT	MG	Spindle cell neoplasm	3	3	3	9	Poor	Extensive
Xia-879	298	E 976	MUT	MG	Spindle cell neoplasm	3	3	3	9	Poor	Moderate
Xia-880	110	E 998	MUT	MG	Squamous cell	3	3	2	8	Poor	Moderate
	Mean 220.9				spindle neoplasm 90%, squamous 10%						

Figure 2-15 Mammary gland tumor development after DMBA treatment and histopathological characterization of the tumors. (A-C)

(A).*Palb*2 mutant mice images with breast cancer. (B).Histopathology of breast cancer. (C).Summary of tumor histopathology, grades and classifications.

Similar to radiation, DMBA-treated mutant tissues exhibited higher levels of γH2AX foci at 24 and 48 hr after DMBA than controls, indicating more DNA damage and inefficient repair in these tissues (Fig. 2-16 A for intestine and B for mammary gland).

A-

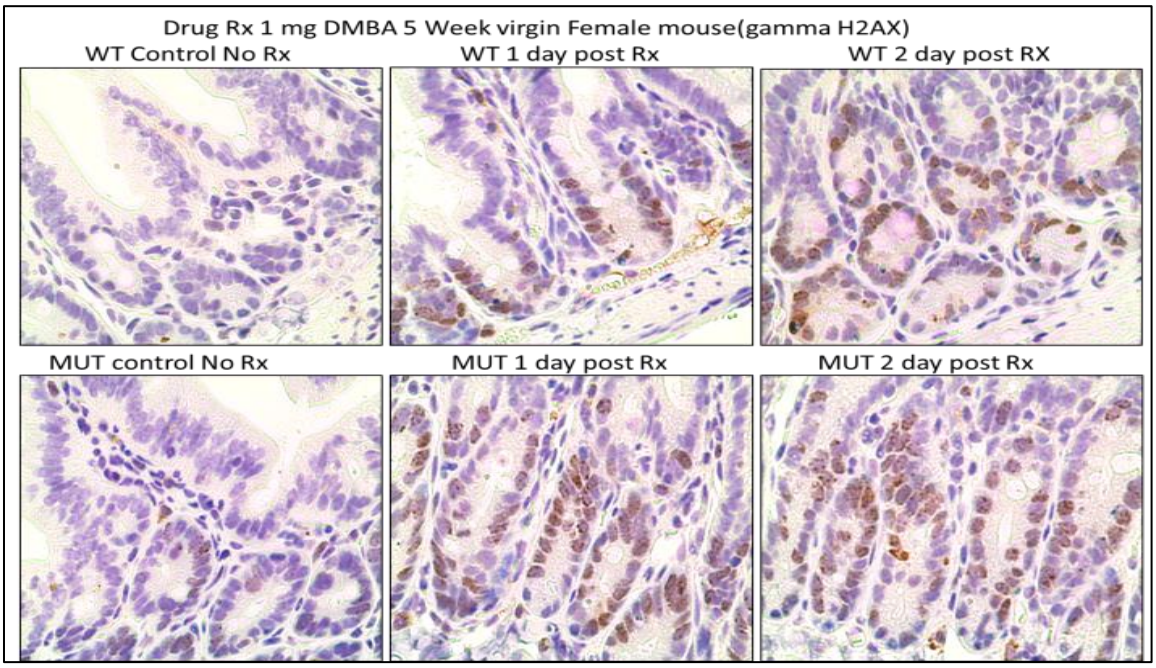

B-

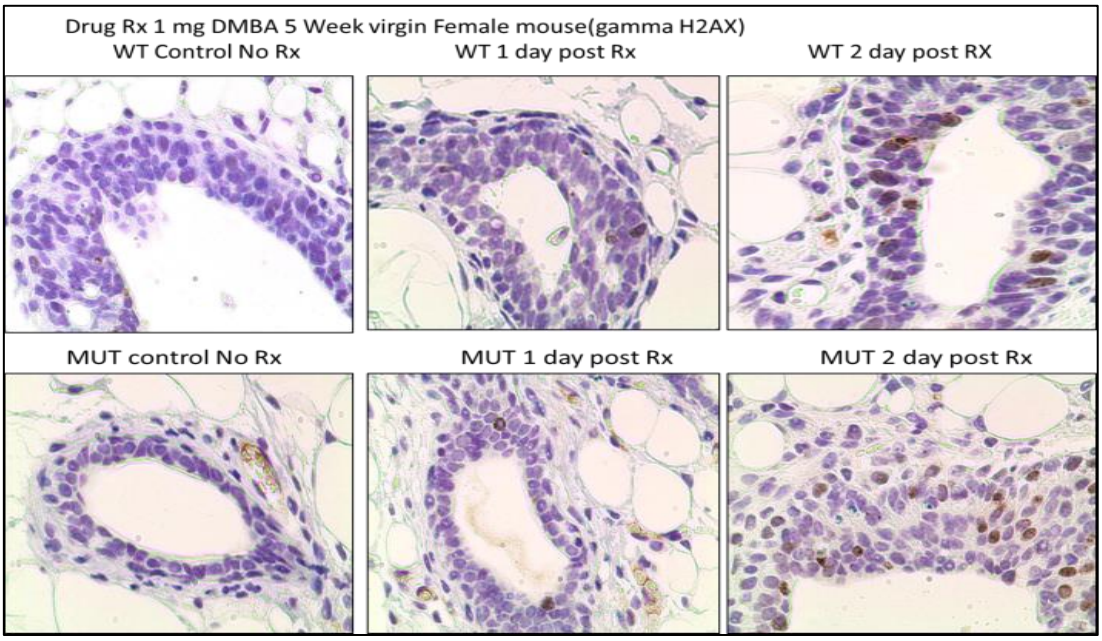

Figure 2-16 DMBA-induced DNA damage is higher in MUT mice tissues. (A-D)

A. Representative γH2AX IHC images for intestinal and sections from 8 weeks old *Palb*2 m/m and wt control mice at the indicated times post 1 mg DMBA treatment.

B. Representative γH2AX IHC images for mammary gland sections from 8 weeks old *Palb*2 m/m and wt control mice at the indicated times post 1 mg DMBA treatment.

2.4.9 *Palb2* mutant mice exhibit anemia phenotype when challenged with 1 mg DMBA within one day after treatment

Bi-allelic germline mutation in *PALB2* result in Fanconi anemia (FA), subtype N (131). To test potential FA phenotype in our mice we administered DMBA to both wt and mutant mice by oral gavage and then collected blood and bone marrow 24 hr after. In the absent of challenge, both wt and mutant mice showed normal red blood cell (RBC) morphology and population density. However, 24 hr after of 1 mg DMBA treatment, the mutant mice showed severe pallor (Figure 2-17A). Peripheral blood film showed fewer RBC population with a large number of hemolysized RBCs with spiky appearance (acanthocytosis) (Fig. 2-17B), suggesting these RBCs are more vulnerable to rupture, which could be due to lipid peroxidation by high ROS tension in mutant mice leading to a change in cell membrane permeability and physical property (147, 148).

Furthermore, to test whether this anemia was due to peripheral cell destruction or a central hematopoietic insult, we conducted bone marrow smear and H&E staining, As shown in Fig. 2-17 C-D, there was no obvious difference between wt and mutant either before or after Rx except for excessive erythropoiesis in mutant than wt marrow. This excessive erythropoiesis in mutant mice indicates a compensatory reactive mechanism of the bone marrow precursor cells to replace peripheral blood loss. This phenotype is consistent with the notion that increased NF-κB in the mutant mice upregulates the expression of glutathione (L-gamma-glutamyl-L-cysteinylglycine, GSH) and other antioxidants that protect cell membrane under basal condition (149). However, when these

cells are exposed to high oxidative environment after DMBA treatment, their membrane integrity would be lost probably through lipid peroxidation.

A-

B-

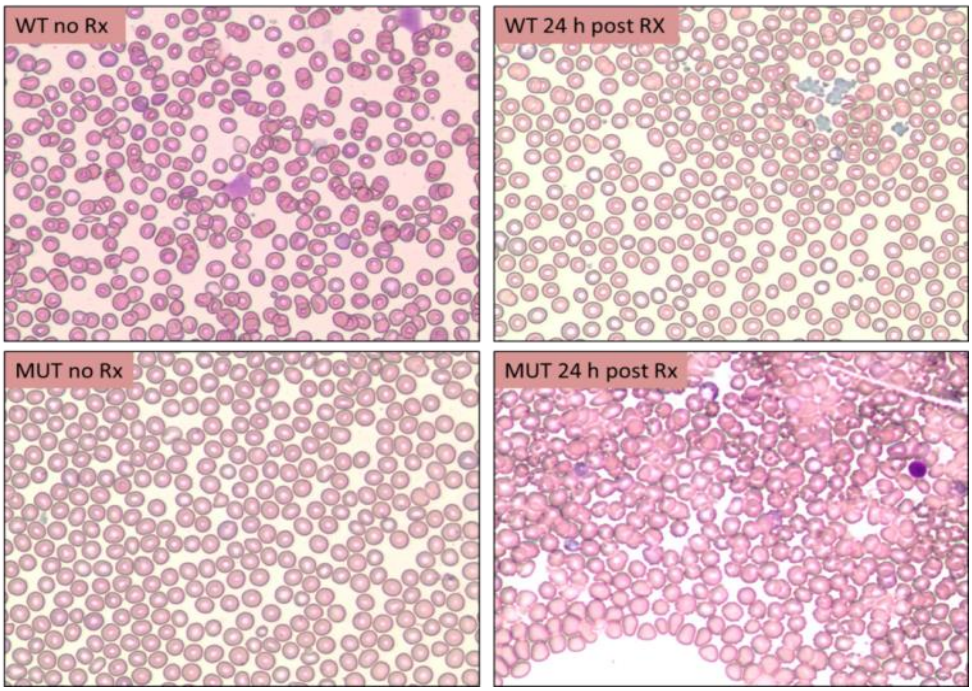

Figure 2-17 *Palb*2 mutant mice exhibit hemolytic anemia upon DMBA treatment. (A-D)

- **A.** Representative *Palb*2 m/m (left) and wt control (right) mice at one week after 2 rounds of 0.25 mg DMBA treatment (at week 5 and week 6, one-week part).
- **B.** Representative images of peripheral blood films from *Palb*2 m/m and wt mice either untreated or at 24 hr after 1mg DMBA treatment.

C-

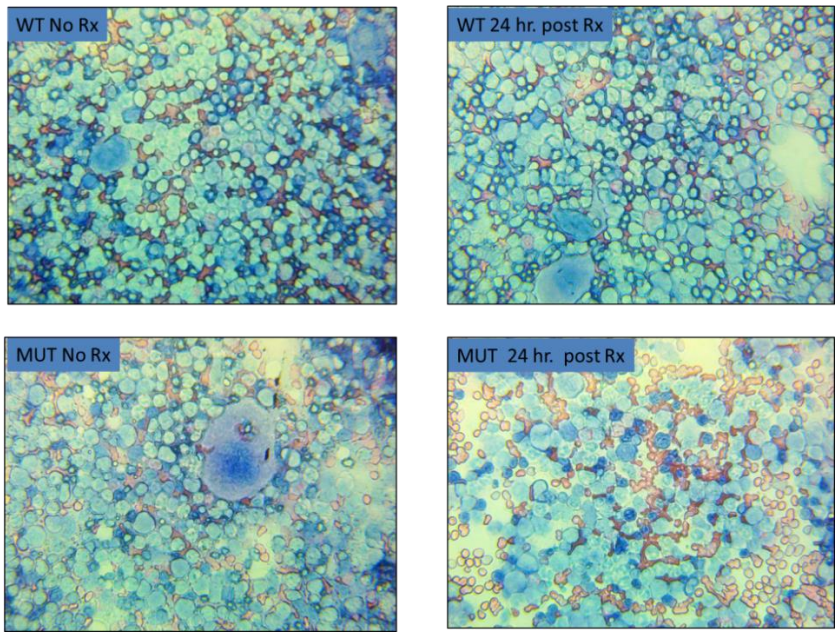

D-

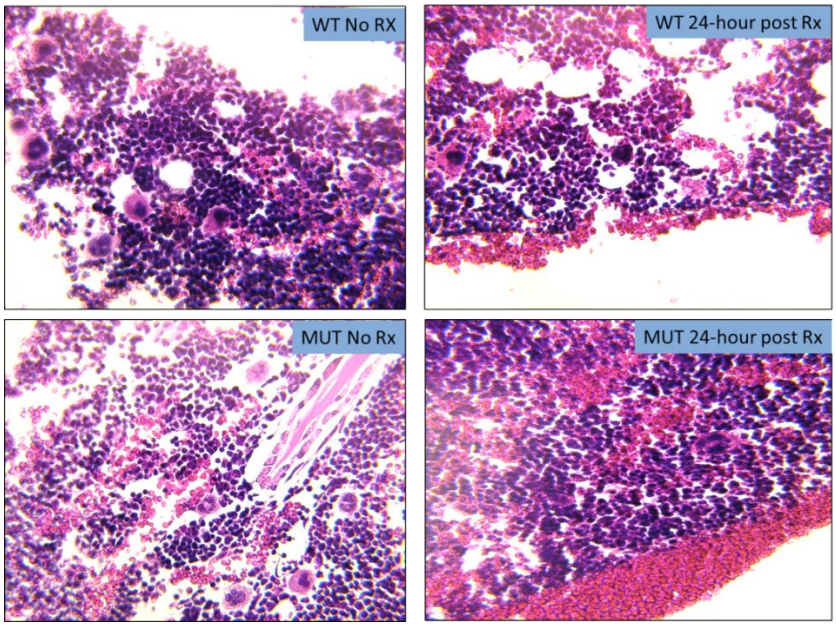

Figure 2-17 *Palb*2 mutant mice exhibit hemolytic anemia upon DMBA treatment. (A-D)

A. Representative bone marrow smear (stained with Geimsa and Wright stains).
B. Representative bone marrow H&E staining at the indicated time for the same mice in C.

CHAPTER 3

The PALB2-BRCA1 Interaction Is Critical for Suppressing p53-associated Spontaneous Tumor Development

3.1 Summary

It has been well established that loss of p53 function is essential for the development of BRCA1 mutant breast cancer. Similarly, our lab has previously shown that p53 acts as a barrier to tumor development upon loss of PALB2. In order to specifically induce or accelerate the development of *PALB2*-associated tumor types, such as mammary, ovarian and pancreatic cancers, we crossed the mice with *Trp53* mutant mice to generate *Palb2* mutant mice with a *Trp53* heterozygous background, which has been shown to be a “sensitizer” for tumor formation. Surprisingly, *Trp53* heterozygosity did not induce formation of the above *PALB2*-associated tumors; rather, the mutation of *Palb2* led to accelerated formation of p53-associated tumors, e.g. lymphomas and sarcomas. Interestingly, almost half of *Palb2*m/m;*Trp*53+/- female mice developed osteosarcoma, whereas the incidence of this tumor type was only 14% among males from the same genotype. Such a pronounced gender difference contradicts the normal male predominance of osteosarcoma in humans, suggesting a major shift in tumor development mechanism in the context of our *Palb*2 mutation. Whole exome sequencing (WES) showed loss of the wild-type allele of *Trp53* in the majority of the tumors, including several cases with what appeared to be a focal deletion of the gene, suggesting that disruption of BRCA1-PALB2/BRCA2 axis promotes regional genomic deletions that may lead to loss of other tumor suppressors such as p53. These results suggest a potentially novel mechanism for BRCA/PALB2-mediated tumor suppression,

which is by preventing *Trp53*/*TP53* loss of heterozygosity (LOH), which allows for tumorigenesis.

3.2 Introduction

Loss of p53 function is associated with a large variety of cancers. This loss of function could be brought about through genetic changes such as deletion, mutation (germline or somatic), insertion, and genomic rearrangement. Germline mutation in p53 is associated with the Li-Fraumeni syndrome (150). These cancer-prone individuals have one mutant and one wt *TP53* allele, and a mutation or loss of the wt allele is required for tumors to develop. *Trp*53-/- transgenic mice show extremely high incidence of thymic lymphoma at early age with median tumor latency about 4.5 months (151). *Trp*53+/- mice also showed a tendency for tumor development but with relatively longer tumor latency of about 1.5 year (152), with a tumor spectrum consisting of mainly osteosarcoma and B cell lymphoma. It has been found that lymphomas arising from *Trp53*+/- mice show a loss of the wt allele at early age, while sarcomas may retain the wt allele even at later age (153), suggesting p53 haploinsufficiency could suffice to promote tumorigenesis in older mice. However, that is not the case for patients with Li-Fraumeni syndrome, since most of their tumors have lost the wt *TP*53 allele (154), supporting the two hit model for the cancer development.

The primary bone tumor (osteosarcoma) is an aggressive tumor with childhood and adolescent age of onset (155). The aggressiveness of this tumor comes from the diversity, complexity, and heterogeneity at the level of genomic

and chromosomal rearrangement. This tumor type is characterized by both inter- and intra-tumoural heterogeneity, adding another layer of difficulties in both treatment and prognosis for patients (156). Epidemiological studies showed males are more frequently affected than females with average male: female ratio of 1.2:1 (157, 158). Defective DNA repair and genome stability maintenance has been implicated in pathogenesis of osteosarcoma, as mutations or inactivation of *TP53, RB1, RECQL4, BLM, WRN, BRCA2* and other DNA damage response genes have been found to be mutated in the tumors (150, 159-162). Furthermore, many oncogenes such as c-MYC and c-FOS, and other signaling pathways such as the NF-κB pathway also have a role in osteosarcoma pathogenesis (163). NF-κB has been shown to be downregulated in osteosarcoma and play a critical role not only in osteoclast maturation and differentiation but also in radio resistance of this tumor (164). Thereby, targeting it through its Receptor Activator of NF-κB Ligand (RANKL) is a promising therapeutic approach for osteolytic bone tumors such as osteosarcoma (165). Since most of tumors show aneuploidy, an early defect in DNA repair appears to be an underlying mechanism for pathogenesis of osteosarcoma and its consequences (166). Moreover, dysregulation of G1 and S-phase checkpoint genes such as *RB*, *TP53* and the *INK4/ARF* locus have been reported to be associated with poor prognosis (167).

3.3 Material and methods

3.3.1 Mice

*Trp*53 Knockout strain used in this study was originally generated in Tyler Jacks lab, carrying a mutant allele in which a neomycin cassette replaces exons 2-6, including the start codon (168).

A neomycin cassette replaces exons 2-6, including the start codon, of *Trp53*. About 40% of the p53 coding region is deleted in this strain. These animal had been maintained on 129/SV background.

Palb2 knock-in mutant mice were crossed with *Trp53*-/- mice to obtain a *Trp53*+/- background in order to sensitize the *Palb2* mutant mice for potential spontaneous tumor development. Littermates of 6 different genotypes (*Palb2w/w;Trp53*+/+, *Palb2m/m*; *Trp53*+/+, *Palb*2w/w;*Trp53*+/-, *Palb2m/m*;*Trp53*+/-, *Palb2m/m*;*Trp53*-/-, *and Palb2w/w*; *Trp53*-/-) were generated and observed for spontaneous tumor development for up to 800 days.

Genotyping was performed on tail DNA upon weaning. Genotyping for *Palb2* was performed as decribed before *Trp*53 genotyping was through amplification of the region surrounding exons 6 and 7 using a mixture of 3 primers (2 forward and 1 reverse). The forward primers are neo F (5-GCCTTCTATGCCTTCTTGACG) and exo 6 F (5-GTACCCGAGTATCTGGAAGACA), and the reverse primer is exo 7 RN (5-AAGGATAGGTCGGCGGTTCATGC). This primer combination would give a 500 bp PCR product for the WT and a 600 bp one for the MUT alleles.

The reaction mix for a single reaction consisted of:

Hotmaster Taq DNA polymerase	0.2 μl
dNTP 5mM (promega)	0.8 μl
10X HotMaster Taq buffer	2.0 μl
Neo F primer 20 mM	0.3 μl
Exo 6 F 20 mM primer	0.3 μl
Exo 7 RN 20 mM primer	0.3 μl
DNA	1.0 μl
H2O	15.0 μl

The PCR cycling were: 94 °C 5 min; 94 °C 1 min, 66 °C 1 min, 72 °C 1 min X 34 cycles; 72 °C 10 min; 4 °C forever.

3.3.2 Whole exome sequencing (WES)

Genomic DNA extraction and WES were both performed by RUCDR Infinite Biologics. WES library was prepared using Agilent SureSelect chemistry. Sequencing was performed on Illumina NextSeq, 2x150bp paired-end reads, ~50M reads per sample.

3.3.3 Histology

Animals with tumor were sacrificed and subjected to dissection. Tumor samples were fixed in 10% formalin solution. Specimens were processed for histology, embedded in paraffin, sectioned at 4 μm, and stained with hematoxylin and eosin.

3.4 Results and discussion

3.4.1 Combined *Palb*2 mutant and *Trp*53 leads to accelerated tumor development compared with either mutation alone.

To gain insight into how PALB2-BRCA1 interaction participates in tumor suppression, we crossed our mutant mice with *Trp*53 knockout mice to sensitize our mutant for spontaneous tumor development. In addition, the rationale behind such crossing is that most of *BRCA1* and *PALB2* mutant human breast cancers contain somatic mutations in p53, suggesting p53 is a barrier to cell proliferation and tumorigenesis after the loss of BRCA1 and PALB2. A cohort of about 20 mice of each of the following genotypes (*Palb2*w/w;*Trp*53+/+, *Palb2*m/m;*Trp53*+/+, *Palb*2w/w;*Trp*53+/- and *Palb*2m/m;*Trp*53+/-, *Palb*2w/w;*Trp*53-/- both gender and *Palb*2m/m;*Trp*53-/- males only) were generated and then monitored for tumor development. Strikingly, combined mutation of *Palb*2 and *Trp*53 led to greatly accelerated tumor development compared with either mutation alone (Fig. 3-1A). The median tumor latency for *Palb*2m/m;*Trp*53+/- mice was 253 days versus 586 days and 482 days for *Palb2*m/m;*Trp53*+/+ and *Palb*2w/w;*Trp*53+/- mice, respectively, indicating that *Palb*2 synergize with *Trp*53 to suppress tumor formation, particularly sarcomas. Moreover, median tumor latency for *Palb*2m/m;*Trp*53-/- (double mutant) mice was 85 days, while for *Palb*2w/w;*Trp*53-/- mice it was 155 days, again showing synergistic acceleration of tumor development (Fig. 3-1A).

Interestingly, 48% of *Palb*2m/m;*Trp*53+/- females developed osteosarcoma, whereas only 14% of the males of the same genotype developed

this tumor, and the incidence was even lower in *Palb*2w/w;*Trp*53+/- mice (Fig. 3-1C-D). This gender bias contradicts the normally male predominant osteosarcoma in humans, suggesting a clear shift in gender bias in the context of our *Palb*2 mutation. Another surprising finding was that more than 40% *Palb2*m/m;*Trp53*+/+ males developed liver tumor (Fig. 3-1B) , suggesting a potential role of PALB2, and perhaps also BRCA1, in the pathogenesis of hepatic tumor as will be discussed later.

A-

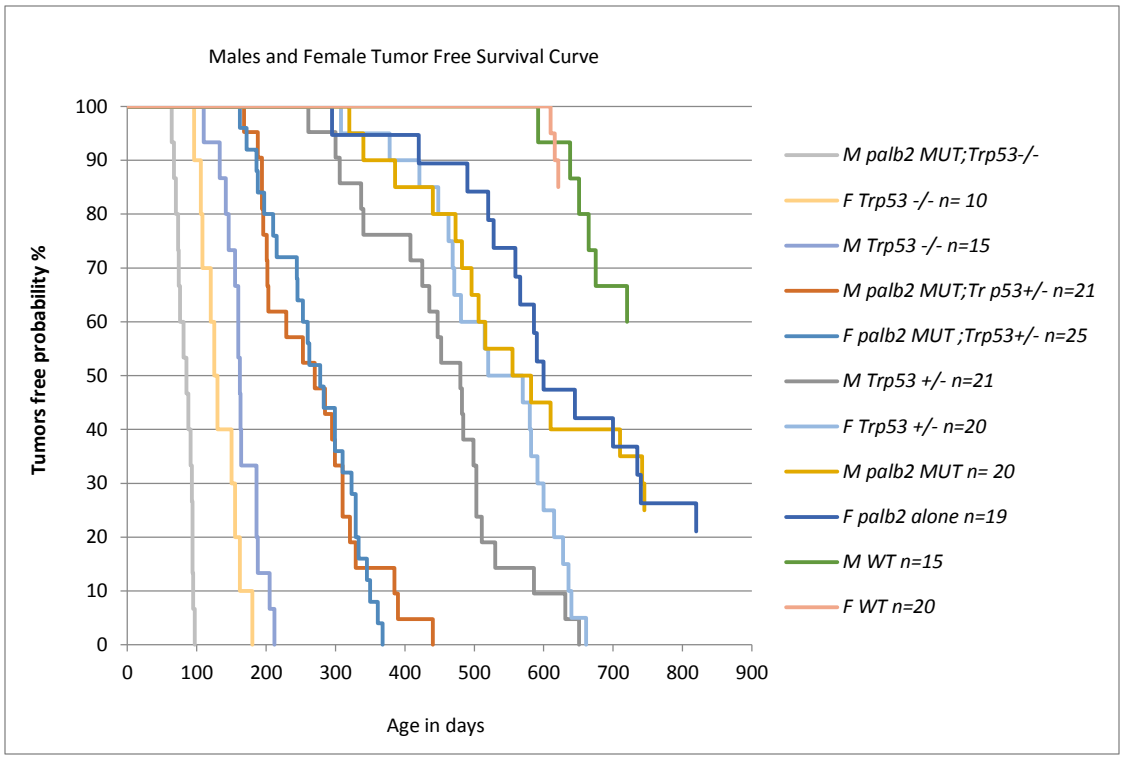

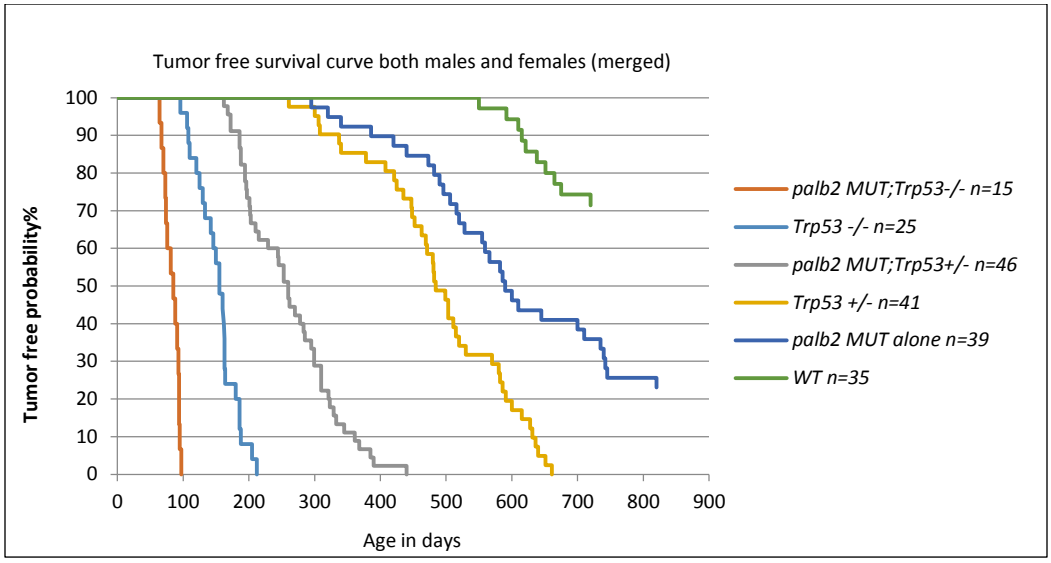

Figure 3-1 Tumor formation in *Palb*2 knockin and *Trp*53 mice with different crossing.

A. Kaplan-Meier tumor free survival curve for *Palb2* and *Trp53* single and double mutant mice. Top, male and female separated; bottom, male and females combined.

B-

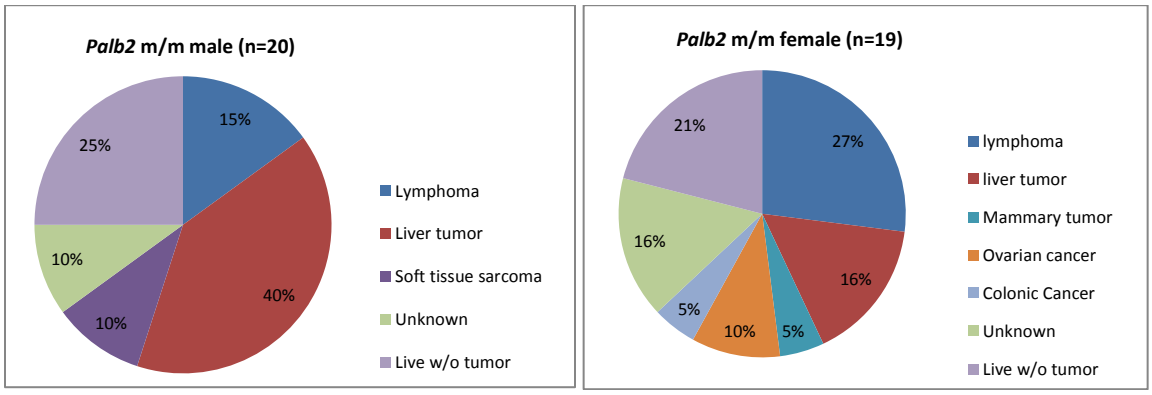

C-

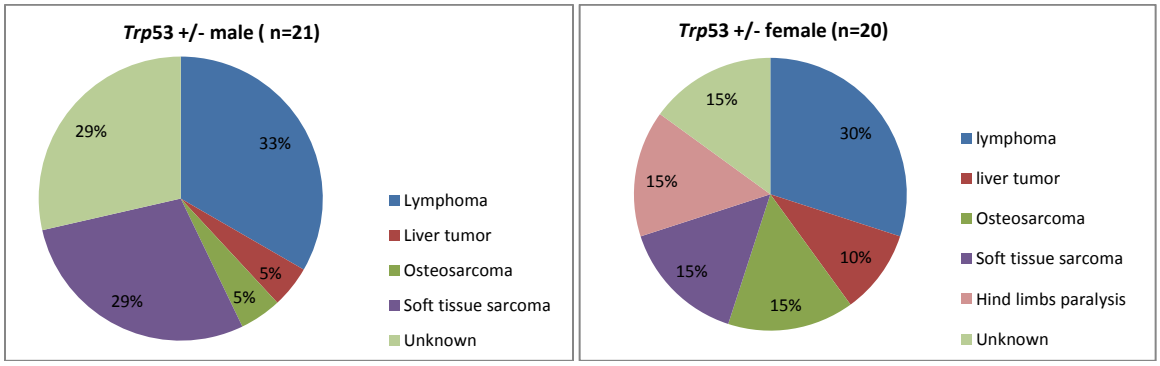

D-

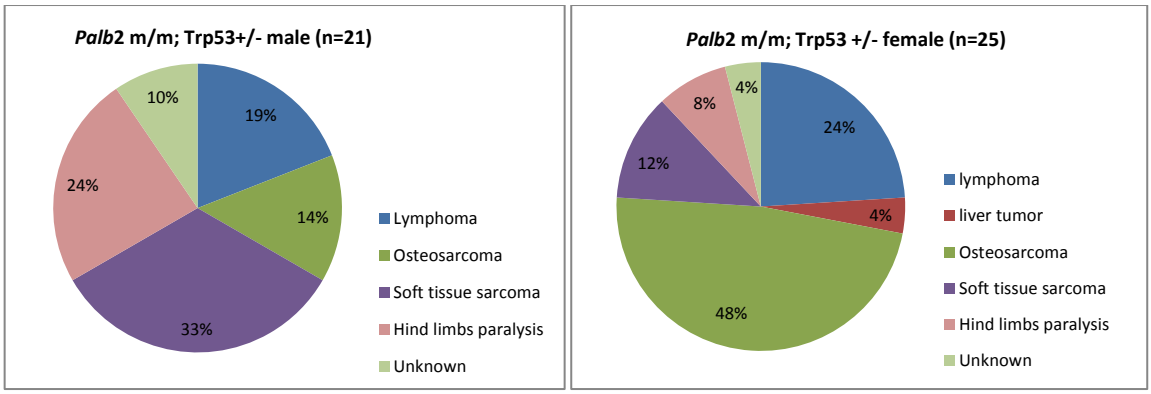

Figure 3-1 Tumor spectrum of mice with single or combined *Palb*2 and *Trp*53 mutations.

B. Tumor spectrum for *Palb*2 m/m;*Trp*53+/+ mice (male on the right and female left).

C. Tumor spectrum for *Palb*2 w/w;*Trp*53+/- mice (male on the right and female left).

D. Tumor spectrum for *Palb*2 m/m;*Trp*53+/- mice (male on the right and female left).

As shown in Fig. 3-1B-D, *Palb*2m/m;*Trp*53+/- mice develop multiple types of tumor, including osteosarcoma, thymic lymphoma, colonic obstruction (intestinal lymphoma), liver tumor, and soft tissue sarcoma. All tumor types shown in the spectrum were confirmed by H&E histopathology (Fig 3-2).

Osteosarcoma tumors taken from distal end of the femur bone exhibited fibroblastic cells, high mitotic index osteoblastic cells with eosinophilic osteoid matrix (pink stained) and a lot of bone necrosis (higher magnification). They also showed multinucleated giant osteoblastic cell producing bone.

Thymic lymphoma tumors showed sheets of lymphocytes, closely packed, high mitotic index with deeply basophilic polychromatic nucleus.

Colonic obstruction with lymphoplasmocytic infiltration of mesenteric lymph node showed reactive changes, well defined multiple nodules, lymphocytes infiltration of colonic mucosa with distortion of intestinal epithelia causing obstruction.

Liver tumor showed discohesive hepatocyte, fatty infiltration and pleomorphic nuclei.

The soft tissue sarcoma (fibrosarcoma), a malignant neoplasm of mesenchymal origin, shown in Fig. 3-2 was located subcutaneously on the back of a 480 days old mouse. It consists of fibroblastic type of cells with spindle shaped, elongated nuclei, abundant mitotic figure, and infiltrating subcutaneous fat tissue (inset).

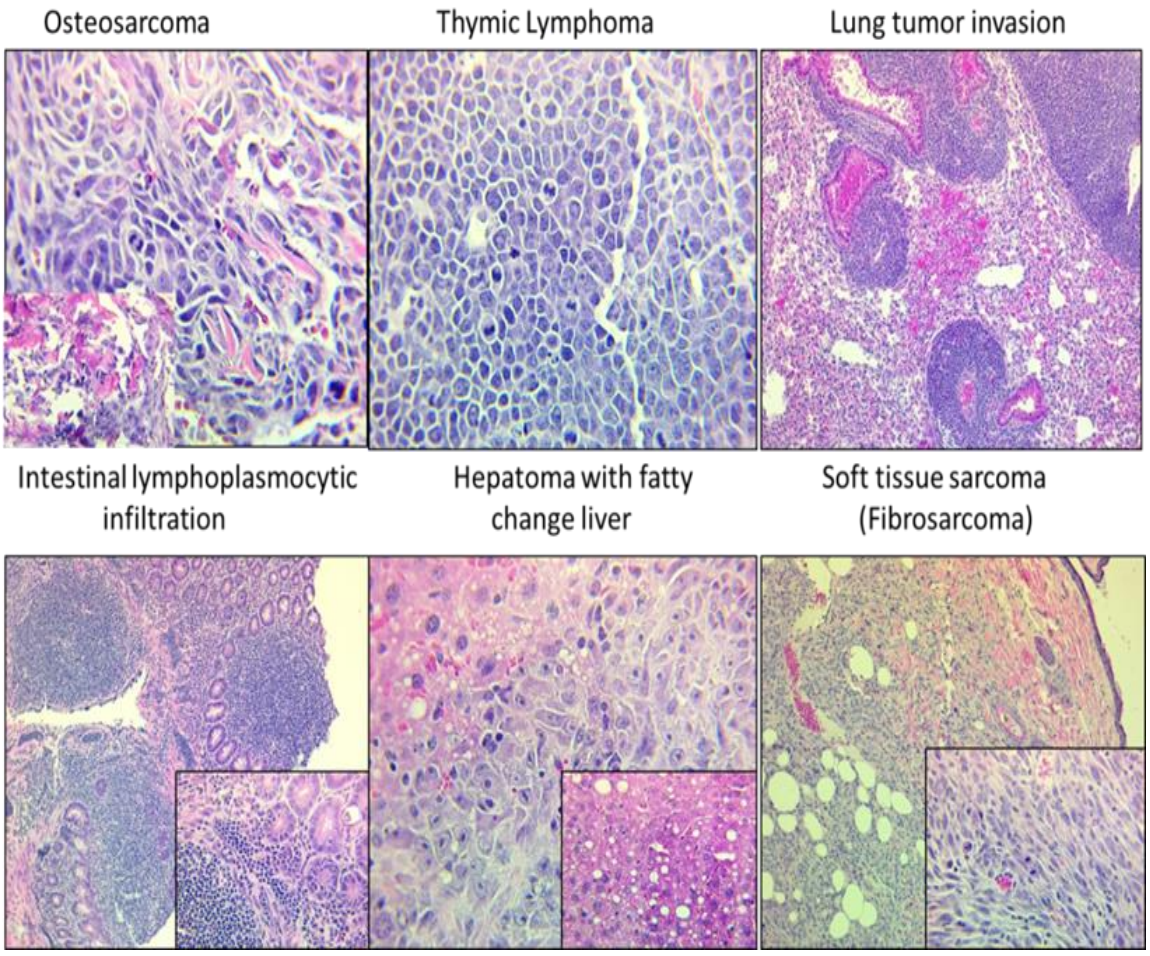

Figure 3-2 Histopathology for different tumors from *Palb2*m/m;*Trp*53+/- mice.

3.4.2 Recurrent genomic alterations in tumors from *Palb2*m/m;*Trp53*+/- mice

To understand the consequence of the DNA repair defect in our *Palb2* mutant mice at the genomic level, we conducted whole exome sequencing (WES) analysis of the tumors arising from the *Palb2m*/*m*;*Trp53*+/- mice. As shown in Fig. 3-3, apparent genome instability was observed in both thymic lymphoma and osteosarcoma. Comparative analysis of the 14 tumors sequenced identified 2 recurring focal deletions and 1 recurring focal amplification in chromosome 1, 2 and 14, respectively. The 2 deletions occurred in all thymic lymphomas and 6 out of 8 sarcomas (both osteo- and soft tissue), and the amplification showed up in most of both thymic lymphomas and osteosarcomas (but not soft tissue sarcomas). The details of the loci are: a deletion in chromosome 1 encompassing Gm29216, Gm28439, Gm28438, Gm28437, Gm10925, Gm28661, Gm10222 (always together); a deletion in chromosome 2 encompassing Gm13340 and Gm13339 (always together, and sometimes Gm13341 as well); an amplification of Gm21738 on chromosome 14 (extremely focal, neighbors almost never co-amplified). In Fig. 3-3, the red ovals denote the above 3 events, and the green ones denote the deletion/rearrangement of T cell receptor (TCR) alpha/delta locus on chromosome 14 and TCR beta locus on chromosome 6 that are expected in thymic lymphomas. In depth sequence analyses are currently underway.

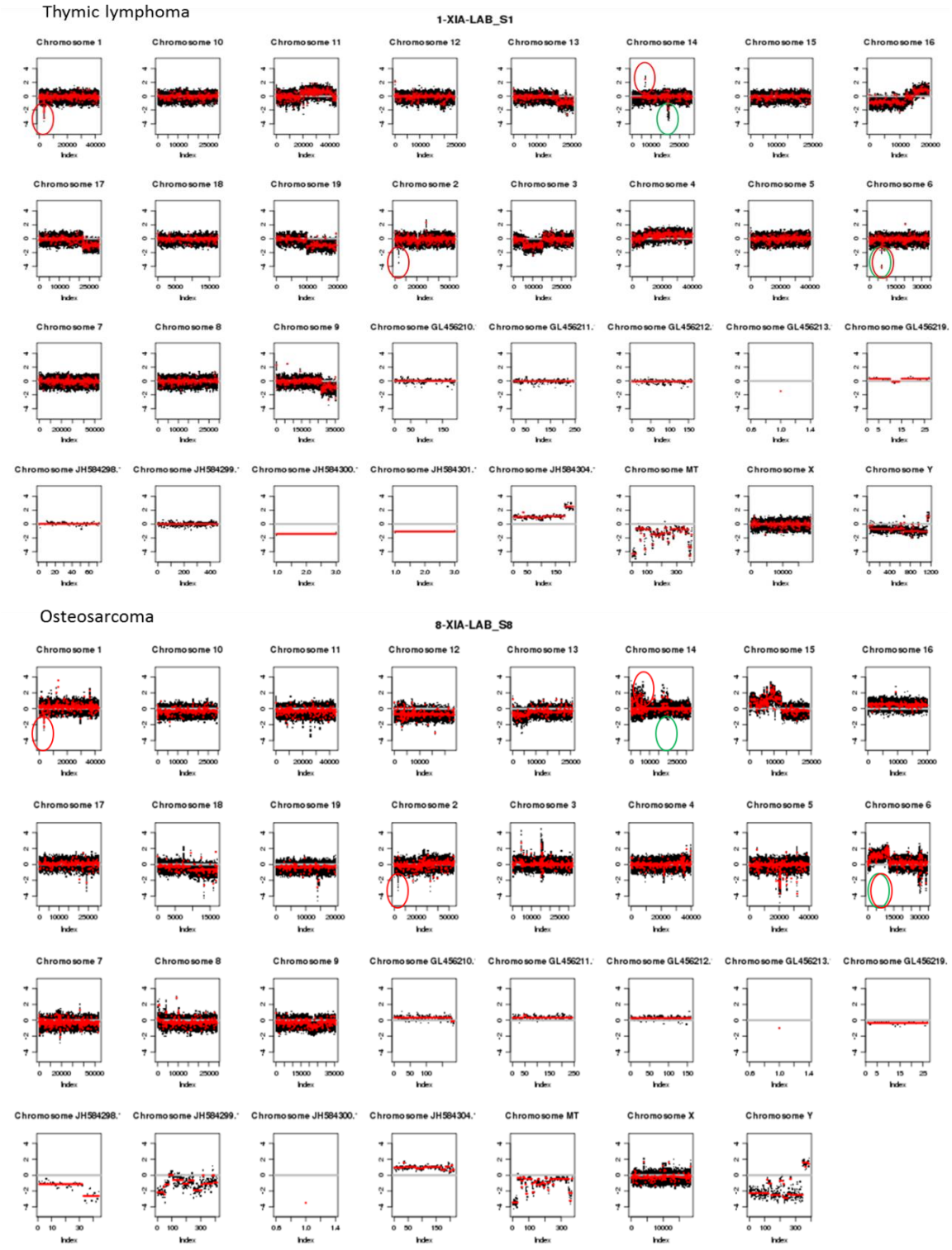

Figure 3-3 Chromosomal abnormalities in a representative thymic lymphoma (top) and a representative osteosarcoma (bottom) arising from the *Palb2*m/m;*Trp53*+/- mice. Green ovals indicate T cell receptor loci, and red indicate recurring changes.

3.4.3 Deletion of the wt *Trp53* allele in tumors from *Palb2*m/m;*Trp53*+/- mice

Tumors arising from *Trp53*+/- mice typically show loss of the wt allele. When we analyzed the bam files of the tumors using the Integrative Genomics Viewer (IGV) (Fig. 3-4), it was evident that the majority of the 14 tumors analyzed had lost exons 2-7, which represent the wt allele. Note that the mutant allele contains a neomycin cassette in place of exons 2-7 so that following a loss of the wt allele these exons will be completely absent in tumor cells. Some of the tumors do not show a complete loss of exons 2-7, likely due to the presence of significant amount of normal cells. Combined with the accelerated tumor development in *Palb2*m/m;*Trp53*+/- vs *Trp53*+/- mice, these results indicate that disruption of the BRCA1-PALB2/BRCA2 axis promote *Trp53*/*TP53* loss of heterozygosity (LOH), which then greatly facilitates tumor development

.

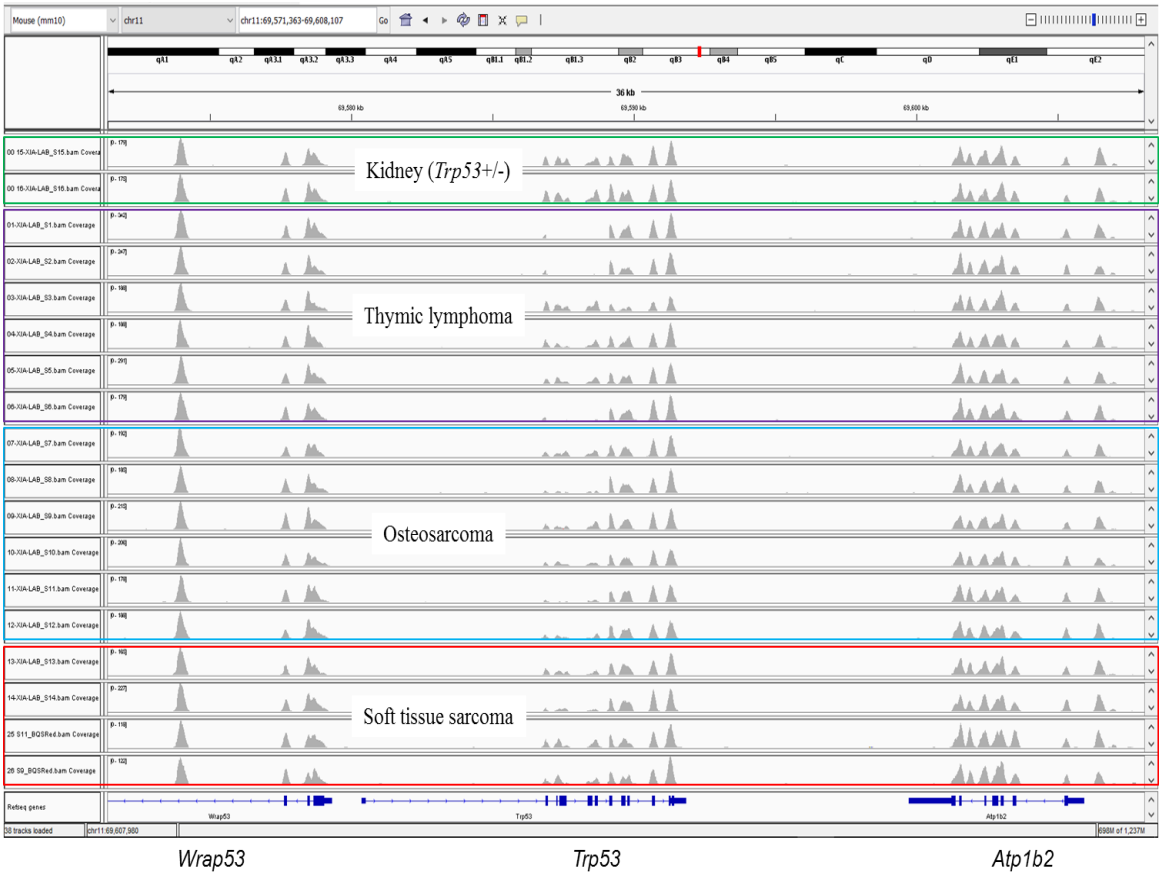

Figure 3-4 Status of the *Trp53* locus in tumors obtained from *Palb2*m/m;*Trp53+/-* mice visualized by aligning the WES bam files in the IGV.

CHAPTER 4

Activation of the NF-κB pathway in *Palb2* mutant mice and its potential therapeutic significance

4.1 Summary

The NF-κB signaling pathway is a well-established pathway that promotes cell survival. In this part of the study, we found increased ROS levels and constitutive activation of NF-κB in mutant cells and tissues in vitro and in vivo compared to wt controls. These findings suggest a key role of this pro-survival factor in tumorigenesis when the BRCA1-PALB2 axis is disrupted (or following the loss of PALB2 or BRCA1).

To test the role of NF-κB in tumor development in the *Palb2* mutant mice, we established a cohort to investigate the effect of an NF-κB inhibitor. Strikingly, after inhibitor treatment, we found a dramatic induction of apoptosis in irradiated mutant mice that more than restored the afore-mentioned reduced apoptosis in the mutant mice without the treatment. Importantly, p53 and p21 protein expression levels were still higher in the mutant than control mice, suggesting that the inhibition of apoptosis seen before inhibitor treatment was counterbalanced by NF-κB pro-survival function. Therefore, our findings demonstrated a potentially novel role of NF-κB in enabling the survival of PALB2 and BRCA1 mutant cells in the presence of DNA damage, thereby promoting tumor development. A separate cohort of irradiated mice (NF-κB inhibitor-treated and untreated) are currently being monitored for tumor development.

4.2 Introduction

4.2.1 NF-κB pathway's pro-survival effect

It has been shown that BRCA1 and PALB2 play a role in transcriptional regulation through two signaling pathways: retinoic acid (RA) and NF-κB, which play crucial roles in development and tumorigenesis (169). The authors observed a significant reduction in the activity of NF-κB and retinoic acid responsiveness after depletion of BRCA1 and PALB2, and they suggested that mutations in *BRCA1* and *PALB2* may cause an inability of cells to respond to incoming stimuli. NF-κB has been shown to cause cellular senescence and promote DNA repair (170, 171). While RA, vitamin A derivatives, have been reported to stimulate differentiation, growth and development of tissues through three different RA receptors: alpha, beta and gamma (172). Moreover, studies have demonstrated that RA signaling can stimulate tissue differentiation and exert anti-proliferative effects in breast tumor development (173). Therefore, RA could have selective roles for cellular differentiation and growth (174) through downstream IGF1 regulation. RA inhibits IGF1 (a stimulator and activator for AKT) thereby inhibiting tumor cell growth in MCF7 breast cancer cells (18). Therefore, reduced RA signaling upon loss of PALB2 function may represent another possible novel mechanism of PALB2 in tumor suppression.

The prosurvival transcription factors NF-κB is a family of five genes, NF-κB1 (p50/p105), NF-κB2 (p52/p100), RELA (p65), REL, and RELB. These five genes give rise to two types of NF-κB proteins (Fig. 4-1A). The first class (RelA (p65), c-Rel, and RelB) is synthesized in a mature form that have a

transactivation domain that enables it to interact with transcriptional apparatus. The second class (NF-κB1 and NF-κB2) is synthesized in a precursor form (175). These precursor forms (p105 and p100) are partially degraded by the proteasome forming the mature proteins (p50, and p52). All of these proteins share a Rel Homology Domain (RHD) that mediates their dimerization forming homo- or hetero-dimers (176). These dimers are cytoplasmic in the majority of cells and transcriptionally inactive due to their binding to the inhibitors of NF-κB (IkBs) . The IkBs, composed of IkBα, IKBβ, and IkBε, contain Ankyrin repeats that, bind NF-κB proteins through their RHD domains. The IκBs can be phosphorylated by the IKB kinase (IKKs) at its two conserved serine residues. After phosphorylation, IkBs are ubiquiinated and degraded by the proteasome (175). The IKK consists of two catalytic subunits (IKKα or IKK1 and IKKβ or IKK2) and one regulatory IKKγ (or NEMO for NF-κB essential modifier) (177).

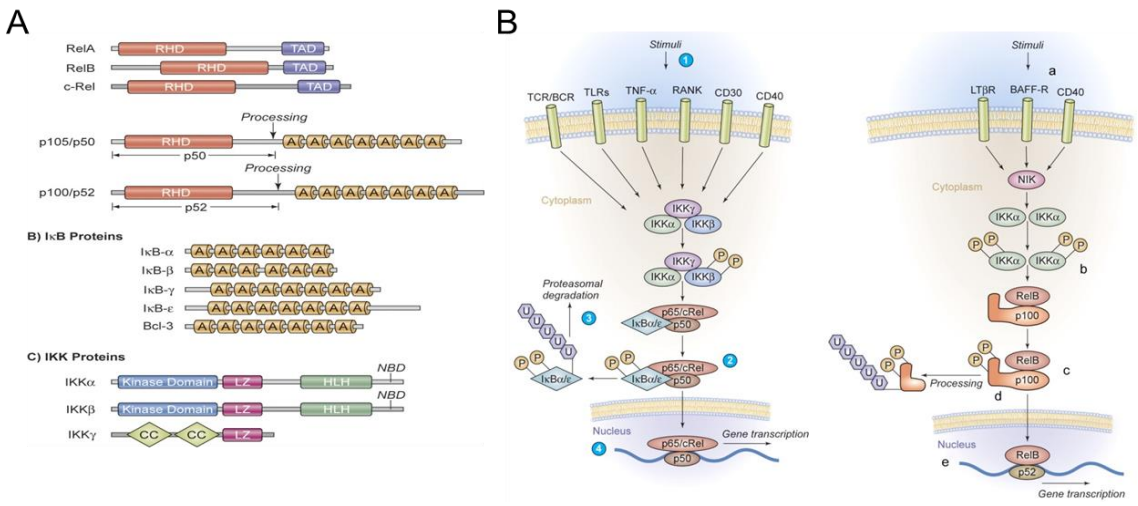

Figure 4-1 Canonical and alternative pathway of NF-κB activation. (A) Structure of NF-κB proteins. (B) NF-κB pathways. Adapted from Philipp J. Jost, 2006 (178).

There are many different signals that can stimulate the NF-κB pathway through a diverse set of cytokines, pI3K/Akt, Ras/MAPK, cytotoxic drugs, reactive oxygen species (ROS), and ionizing radiation (179, 180). In the classical or canonical pathway, dimers composed of p50 together with either p65 or c-Rel are kept inactive in the cytoplasm through binding of IκB proteins (181). Upon activation by external stimuli such as lipopolysaccharide (LPS), TNFα, IL1, or other cytokines, IκB kinases (IKKβ) phosphorylate IκBα at it two serine residues and induce IκBα polyubiquitinylation and subsequent degradation by the proteasome (178, 182). This event allows the translocation of the p65/p50 complex to the nucleus where it regulates the transcription of its target genes (Fig. 4-1B).

In the alternative or non-canonical pathway, the dimers are composed of p100 and RelB subunits (183), in an inactive form in the cytoplasm. A set of stimuli such as CD40 and B-cell activating factor beyond the TNF family activate IKKα, which then phosphorylates p100 leading to its processing at proteasome ending with transcriptional active dimer p52/RelB formation (184). Then this dimer will translocate to the nucleus for gene transcription (178, 185).

The IKKβ subunit activation will phosphorylate IKB in serine residues. Upon phosphorylation, IKB proteins degraded by the proteasome allowing translocation of NF-κB to the nucleus, where it binds to DNA response element (RE) (176). It has been well known that NF-κB activation is responsible for cell resistant to death through upregulation of anti-apoptotic genes, leading to radio- and chemo-resistance of cancer cells (186, 187).

Knockout of other essential NF-κB genes including IKK, IKB produce somewhat different phenotypes. *RelA*-/- mice die early during embryogenesis, with abnormally small embryos detected at embryonic day 7.5 showing massive liver cell death (50).

4.2.2 NF-κB and Cancer

NF-κB can either suppress or promote tumor development. On one hand, NF-κB plays an essential role in preventing tumor initiation and ROS accumulation by transcriptional upregulation of SOD2, an antioxidant enzyme (188). On the other hand, NF-κB is critical not only to maintain cancer cells growth and survival but also to assist the resistance to chemotherapy or radiation therapy (187) through upregulation of apoptotic inhibitors such as c-IAPI, c-IAP2, Traf1 and the Bcl2 (189, 190). Thus, the role of NF-κB in cancer is complex and context dependent.

With high and continuous oxidative stress, many cells become adjusted to such oxidative tension through the promotion of endogenous antioxidant pathway, which enables the tumor cells resistant to oxidative damage (191).

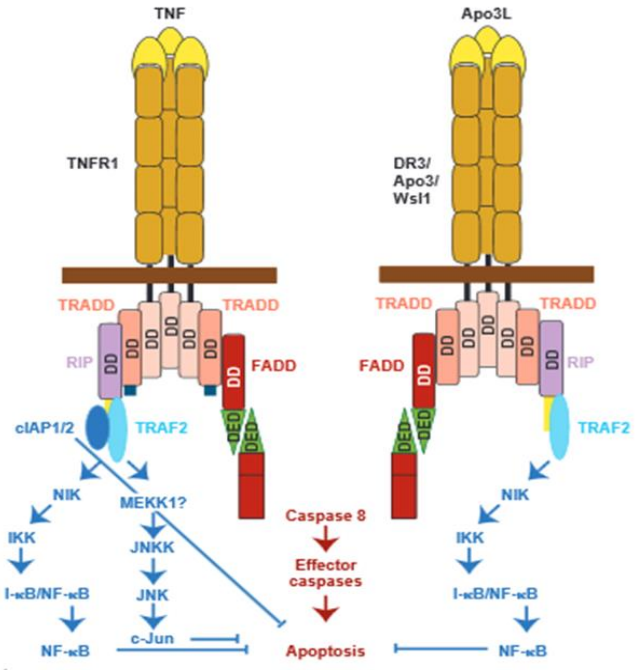

Figure 4-2 Model of anti-apoptotic effect of NF-κB (adapted from Ashkenazi A1, Dixit VM, Science. 1998) (36).

4.3 Material and methods

4.3.1 MEF generation

Mouse embryos at E13.5-14.5 were taken from uterine horn of pregnant mother. After removal of the head and the abdominal content, each embryo was minced with new a razor blade and transferred to falcon tube containing 1 ml of 2X trypsin. The mixture was incubated at 37°C for 20 min and then centrifuged at 1,000 rpm for 5 min. The pellet was finally suspended and cultured in DMEM medium supplemented with 10% heat inactivated FBS, 1% penicillin/streptomycin, and 1% L-glutamine at 37°C in a humidified chamber containing 5% CO_2.

4.3.2 ROS measurement

MEFs were grown in 6-well plates. Cells were washed twice with PBS and then incubated with phenol red-free DMEM containing 10% fetal bovine serum and 25 mM DCF-DA (2′,7′-Dichlorofluorescin diacetate, Sigma Aldrich) at 37°C for 30 min. Cells were washed twice with PBS and trypsinized. Then, harvested cells were resuspended in 300 μl cold PBS. Finally, ROS levels were measured by flow cytometry with excitation at 488 nm and emission at 515 to 545 nm.

4.3.3 TPCA-1 administration and tissue collection

Male mice at 8 weeks of age were treated with intraperitoneal injection of the TPCA-1 (2-[(Aminocarbonyl)amino]-5-(4-fluorophenyl)-3-thiophenecarboxamide) (Selleckchem), a selective inhibitor of IKK2 (IKKB), at 20 mg/kg body weight twice at 12 hr apart. TPCA1 was given in a vehicle composed of 0.9% DMSO (Sigma, D2650), 7% dimethylacetoacetamide (DMA) and 10% Cremophor (both from Sigma-Aldrich). The mammary gland, intestine, thymus and spleen were harvested, fixed in 10% formalin overnight, transferred to 70% ethanol and then submitted to CINJ Histopathology Shared Resources for further processing. All animal studies were carried out in accordance with an institutionally approved protocol.

4.3.4 Western blotting

Mouse PALB2 polyclonal antibody M8 used were raised in rabbits against 1-200 aa of mouse PALB2 and affinity purified at 1:1000 dilution. The following commercial antibodies were used: p21 mouse monoclonal antibody (F5, Santa

Cruz, at 1:200 dilution), GAPDH mouse monoclonal antibody (Cat#, Santa Cruz, at 1:5,000 dilution), p65 (Santa Cruz, Sc109, at 1:200 dilutions).

4.4 Results and discussion

4.4.1 *Palb2* mutant MEFs exhibit a higher ROS levels.

Previously, our lab reported a regulatory role of PALB2 for the expression of the "master antioxidant transcription factor" NRF2 in the control of cellular redox status (192). Therefore, we compared the levels of ROS using the DCFDA assay in *Palb2* mutant and wt MEFs. As shown in Fig. 4-3, ROS levels of *Palb2* mutant MEFs were almost double of those of wt cells in three independent lines for each genotype, indicating a key role of PALB2-BRCA1 interaction in redox regulation in vivo (Fig. 4-3).

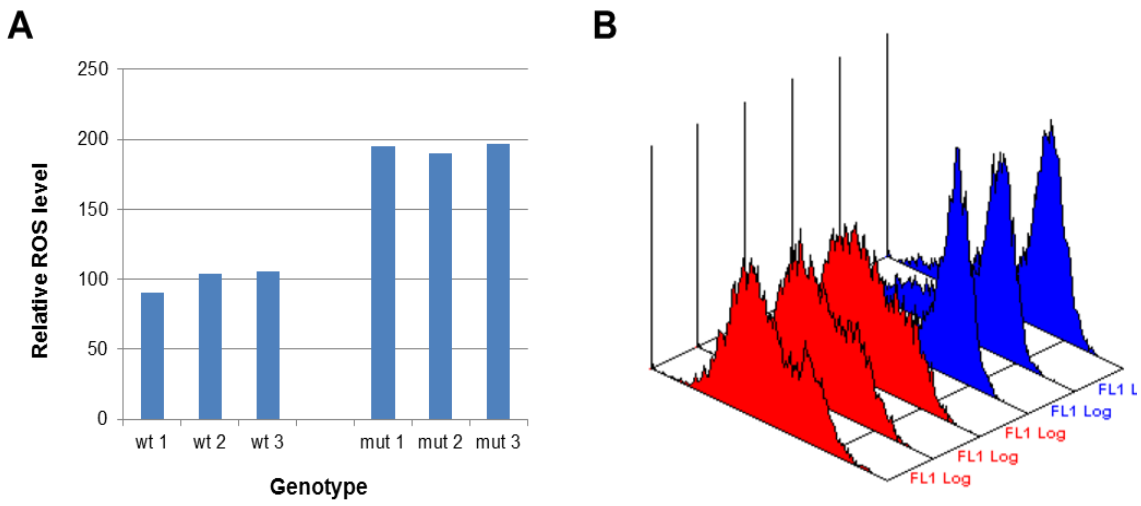

Figure 4-3. ROS levels are higher in *Palb2*m/m than control MEFs (passage #2).

A- Quantification of ROS levels for three independent wt and mut MEFs.

B- Histogram plot the horizontal axis for genotype (the red for 3 different wt and the blue for mut) against the number of events detected (vertical axis ROS levels) for the same MEFs in A.

4.4.2 Mutant mice tissues exhibit more oxidized DNA than corresponding control

When the ROS production surpasses the capacity of the antioxidant defense system, the resulting oxidative stress can cause different kinds of DNA damage, including oxidized DNA, single strand or even double strand breaks (193). To determine the levels of oxidative stress in vivo, we measured, 8-oxo-2'-deoxyguanosine (8-oxo-dG), a marker of oxidative DNA damage, by IHC. As shown in Fig. 4-4, in both intestine and the mammary gland, *Palb*2 mutant cells showed higher basal levels of 8-oxo-dG before IR. Following DMBA ingestion, 8-oxo-dG levels were induced in both wt and mutant tissues; however, the levels in the mutant tissues remained higher. These results further underscore the importance of PALB2 and the BRCA1-PALB2 interaction for cellular redox homeostasis. Furthermore, as 8-oxo-dG can lead to G to T transversion (113) and therefore accumulation of point mutations during DNA replication, this could represent a significant mechanism for neoplastic transformation upon mutation or loss of PALB2 and BRCA1.

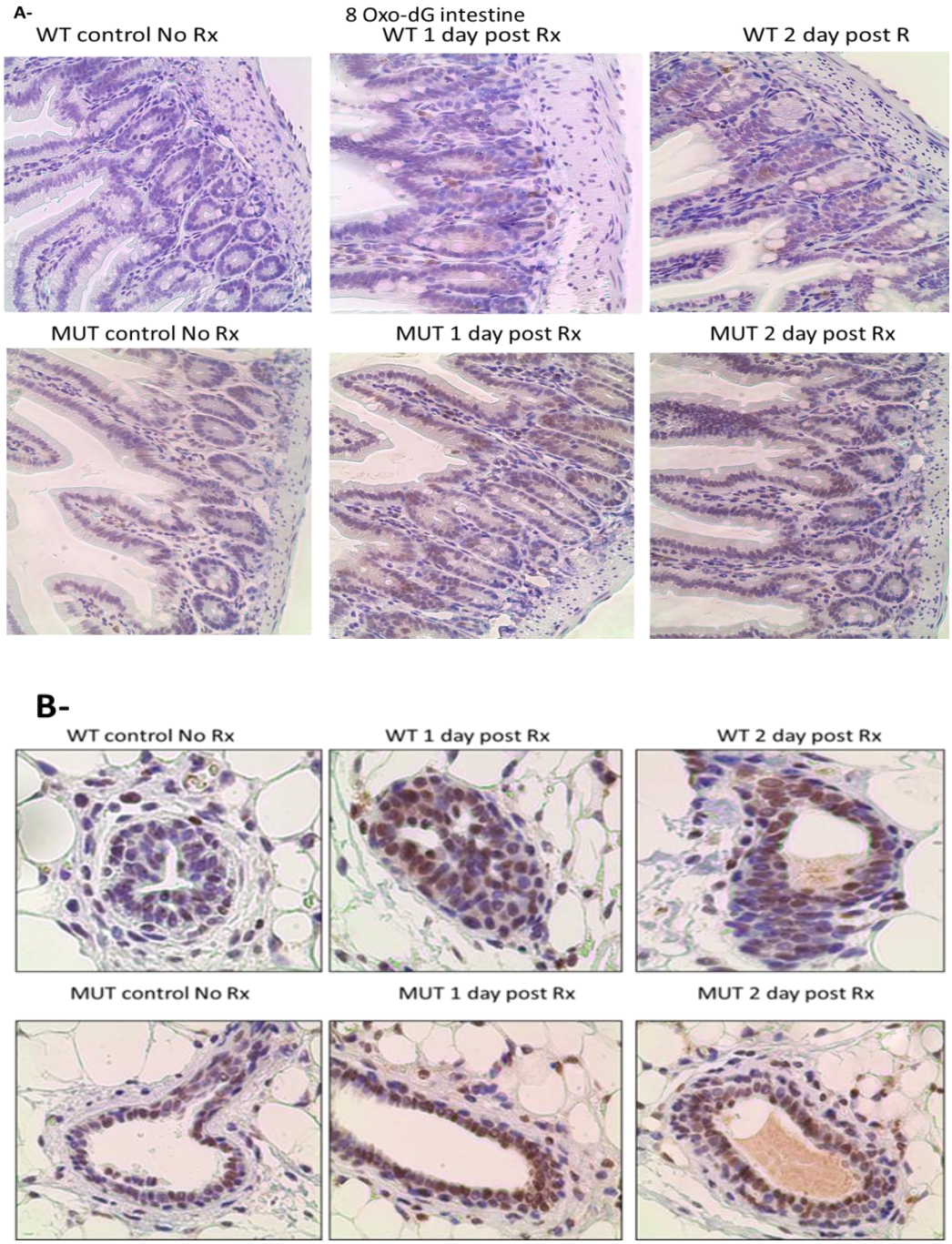

Figure 4-4 DNA oxidation levels are higher in *Palb2* mutant tissues.

A- Representative 8-oxo-dG IHC images for intestinal sections from 8 weeks old *Palb2m/m* and wt control mice at the indicated times post 1 mg DMBA treatment.

B- **B**- Representative 8-oxo-dG IHC images for mammary gland sections from 8 weeks old *Palb2m/m* and wt control mice at the indicated times post 1 mg DMBA treatment.

4.4.3 p53 and NF-κB induction in *Palb2* mutant MEFs

Given the importance of p53 in BRCA1- and PALB2-mediated tumor suppression, we tested the levels of p53 and its key downstream effector p21 in *Palb2* mutant MEFs. As expected, at passage 2 basal p53 level was higher in the mutant than in the wt cells (Fig. 4-5A). Strikingly, p21 level was at least 10 times higher in the mutant cells at the same time. After IR, p21 levels further increased in both cells, but the induction was stronger in the mutant than in the wt cells. The overall trend was similar at passage 4, albeit the induction of p21 showed a faster buildup (between 30 min and 6 hr post IR) and earlier attenuation (compare 6 and 24 hr post IR) in the wt cells than at passage 2. These results are in most part consistent with the higher levels of DNA damage and oxidative stress in the mutant cells. Faint band of PALB2 mutant indicate hypomorphic expression of this protein in mutant MEFs or instability of it.

It is believed that high levels of ROS can lead to cell death, while moderate increase of ROS can induce a variety of responses such as cell survival and inflammation (194). NF-κB pathway can be activated by ROS-responsive mediators such as phosphatidylinositol 3-kinase (PI3K) and mitogen activated protein kinase (MAPK) (195, 196). Others have proposed that ROS can regulate NF-κB through phosphorylation of IkBα leading to its degradation and nuclear translocation of NF-κB (197). Upregulation of NF-κB can lead to increased expression of SOD2, catalase, GSH and other antioxidant pathway molecules. Moreover, it can also alter cell death factors like caspase enabling cell survival and resistance to death (198). We have discovered a consistent NF-κB

overexpression in mutant MEFs compared with wild MEFs at both passage 2 and passage 5 (Fig. 4-5B). It is currently not clear whether this was due to an upregulation of its transcription by PALB2 or protein stabilization due to ROS-mediated activation of IKKs. Higher basal expression of NF-κB was also observed in the spleen, and a further induction was seen at 30 min after IR (3 Gy) (Fig. 4-5C). By 6 hr post IR, however, NF-κB was almost completely lost in both wt and mutant tissues. The mechanisms that underlie these observations remain to be investigated.

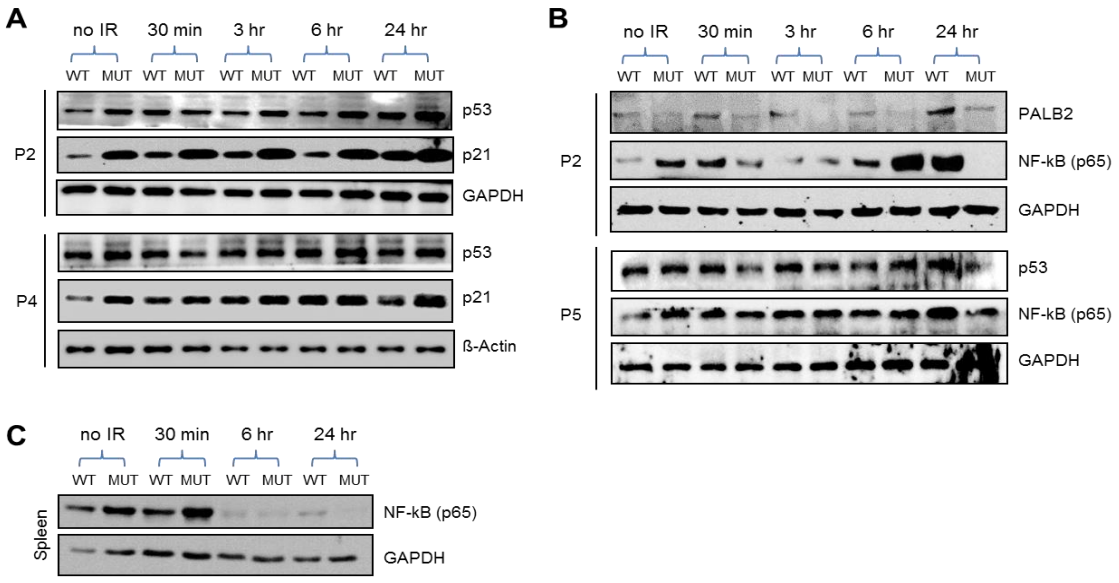

Figure 4-5 Western blotting for MEFs both *palb2* m/m and control.

A- Western blotting showing p53 and p21 proteins in wt and *Palb2* mutant MEFs (passage 2 and passage 4) at indicated time points post 3Gy IR. GAPDH and β actin serve as loading controls.

B- Western blotting showing PALB2, NF-κB (p65) or p53 levels in wt and *Palb2* mutant MEFs (passage 2 and passage 5) at indicated time points after 3 Gy IR. GAPDH serves a protein loading control.

C- Western blotting showing NF-κB (p65) levels in the spleens of wt and *Palb2* mutant mice at indicated time points after 3 Gy IR. GAPDH serves as a protein loading control.

4.4.4 Inhibition of NF-κB restores radiation–induced apoptosis in *Palb*2 mutant tissues

Since overexpression of NF-κB can enhance tumorigenesis and metastatic aptitude and at the same time reduce radio or chemo sensitivity, we asked whether inhibition of NF-κB using TPCA1, a selective inhibitor of IKK2 (IKKβ), would re-establish radiation-induced apoptosis in these knock-in mice. For this purpose, wt and mutant males were irradiated with 3 Gy of IR, and tissues were collected at different time points to examine the rate of apoptosis. Indeed, unlike tissues from mutant mice untreated with TPCA1 (Fig 2-9) both intestine and mammary gland from TPCA1 treated mutant mice showed high levels of apoptosis as revealed by TUNEL staining (Fig. 4-6A-B). In fact, the rate of apoptosis was higher in both tissues of the mutant mice than in their wt counterparts at 3 and 6 hr after IR (Fig. 4-6 C-D). This observation suggests that these mutant cells are highly dependent on NF-κB activity for their survival after radiation.

In addition to directly promoting the expression of anti-apoptotic genes, NF-κB can also reduce p53 protein stability by promoting the expression of MDM2 (E3 ubiquitin ligase) thereby providing a permissive environment for the cells to proliferate (199). Therefore, by targeting NF-κB, we can potentially restore the apoptotic function of p53, which remains to be tested in the settings used.

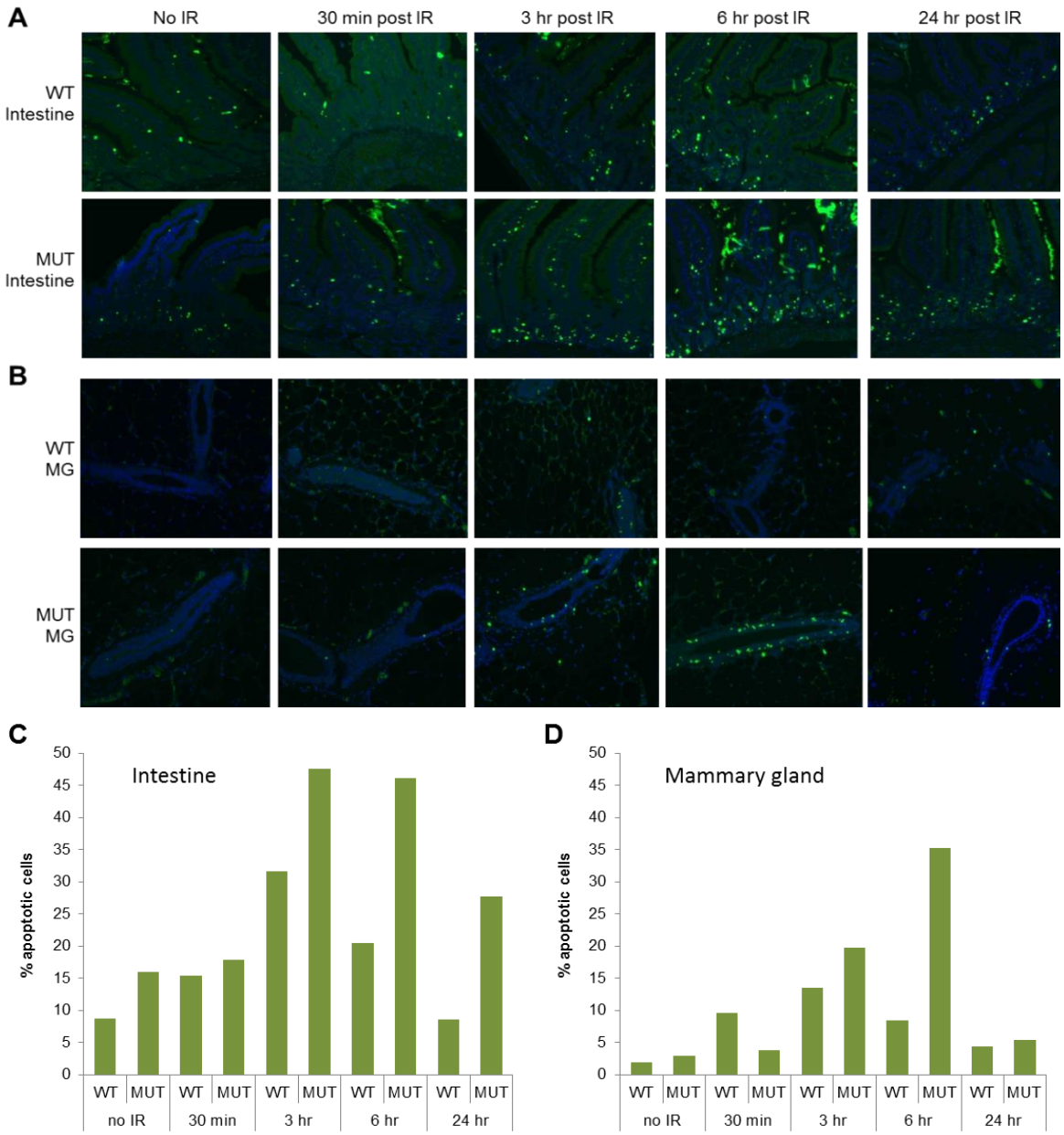

Figure 4-6 NF-κB inhibitor treatment restores radiation-induced apoptosis in *Palb2* mutant mice.

A-B. Representative TUNEL assay images of the intestines (**A**) and mammary glands (**B**) of TPCA 1-treated wt and *Palb2* mutant mice at the indicated time points post 3 Gy IR.

C-D. Quantification of TUNEL assay results for the intestines (**A**) and mammary glands (**B**) of wt and *Palb2* mutant mice treated as above.

4.4.5 Basal and radiation-induced γH2AX, p53 and p21 in mice treated with the NF-κB inhibitor

To gain insight into the mechanism behind the restored apoptosis following TPCA-1 treatment, we analyzed the levels of γH2AX, p53 and p21 in the intestines and mammary glands of TPCA-1 treated wt and mutant mice by IHC before and after radiation. As were in mice untreated with TPCA-1 (Fig.2-5), γH2AX foci were virtually undetectable before radiation in TPCA-1 treated wt mice but clearly visible in the mutant mice, albeit at low levels (Fig. 4-7A-B). After radiation, γH2AX was dramatically induced at 30 min and progressively repaired in both wt and mutant tissues. However, compared with wt mice not treated with TPCA-1 (Fig.2-5), the treated wt mice appeared to have a slower repair kinetics, as significant amount of γH2AX remained in both intestine and mammary glands, particularly the latter (Fig. 4-7A and B). In contrast, repair kinetics in the mutant mice was found to be similar with and without TPCA-1 treatment.

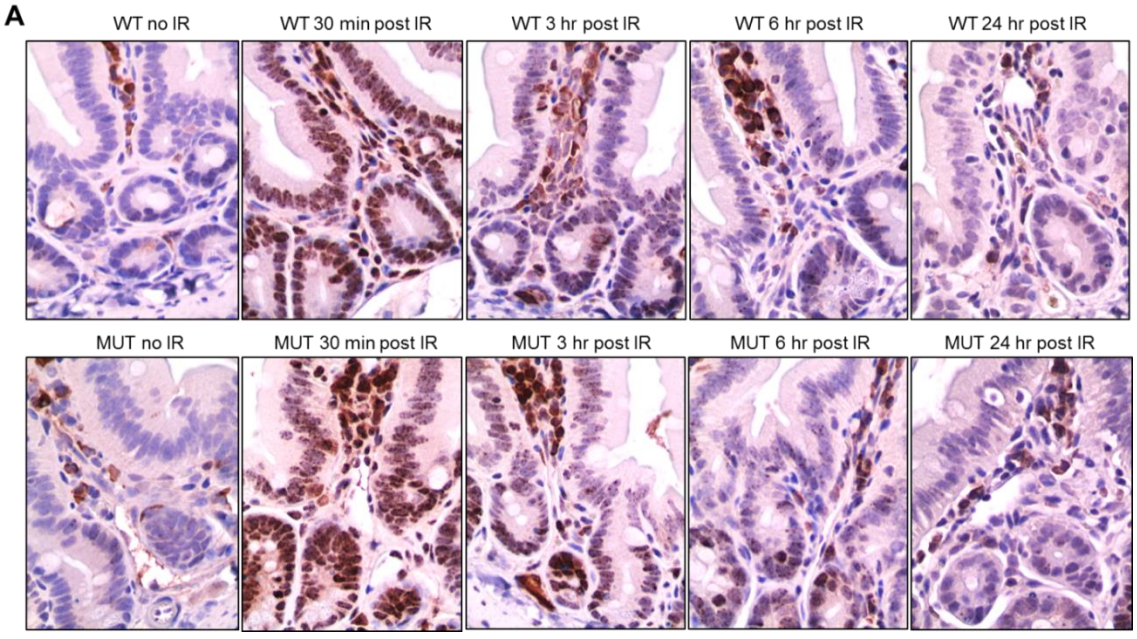

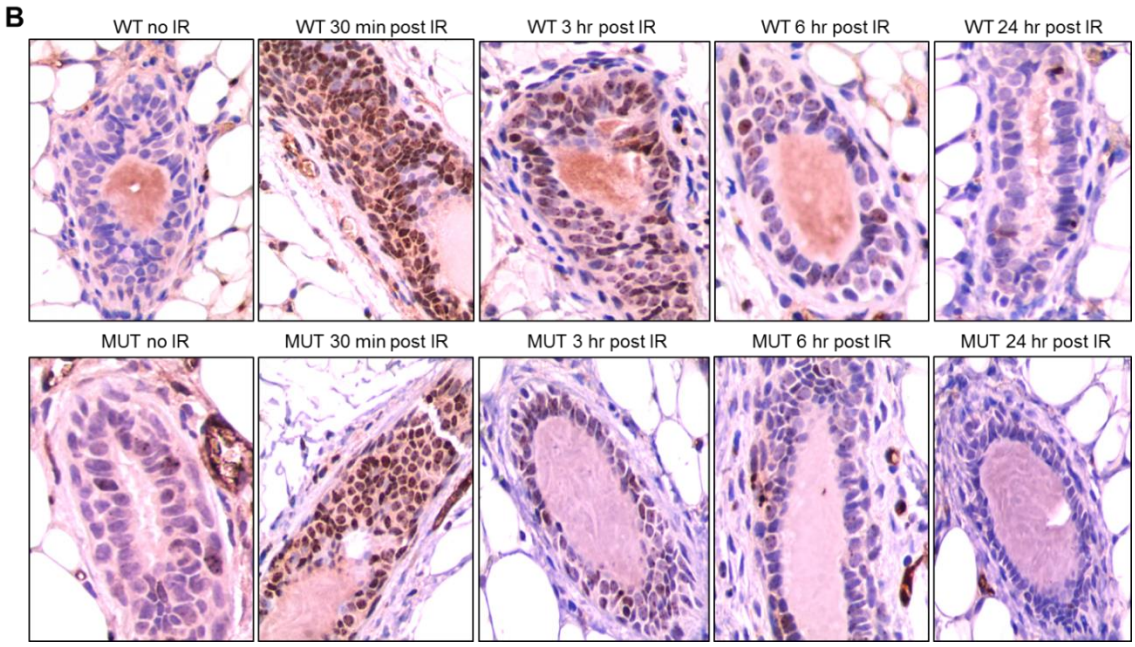

Figure 4-7 Basal and radiation-induced γH2AX levels in NF-κB inhibitor treated wt and *Palb2* mutant mice.

A. Representative IHC images for γH2AX in the intestinal sections from 8 weeks old wt and *Palb2m/m* mice at the indicated time points post 3 Gy IR.

B. Representative IHC images for γH2AX in the mammary gland sections from 8 weeks old wt and *Palb2m/m* mice at the indicated time points post 3 Gy IR.

Next, we examined the levels of p53 in the same tissues as above. Before radiation, no staining signal was seen in wt tissues, and the mutant tissues showed weak but appreciable staining (Fig. 4-8A and B). After radiation, p53 was quickly induced, within 30 min, in both tissues in both wt and mutant mice. In the intestine, the post-induction level was still higher in the mutant than in the wt, which was most evident at 6 and 24 hr after radiation (Fig. 8A). In the mammary gland, p53 level was higher in the mutant at 3 hr but then decreased (to a new steady level). Although p53 level in wt mammary glands was lower initially, by 24

hr after radiation it was at least similar, if not higher, than that in the mutant glands (Fig. 4-8B).

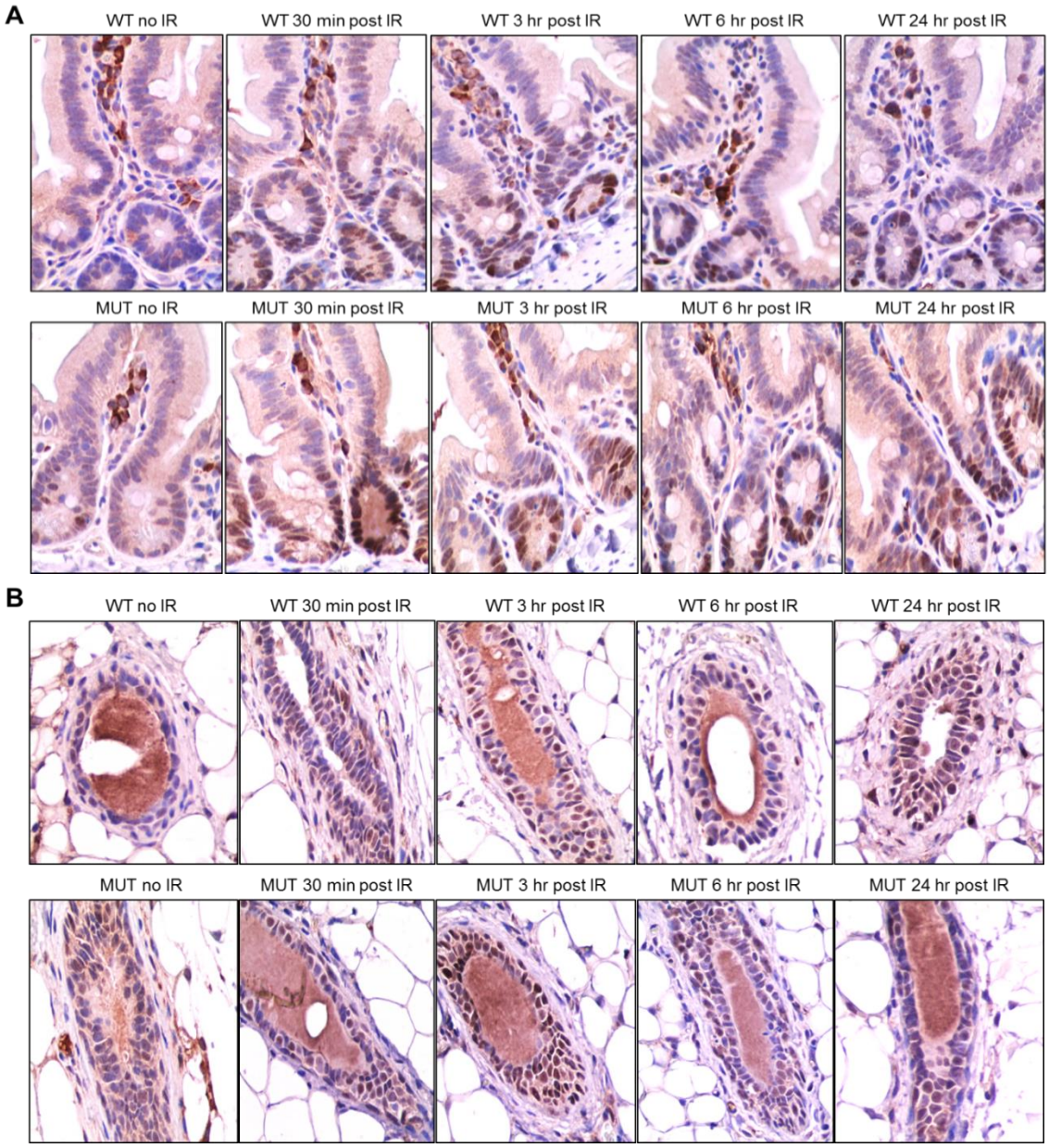

Figure 4-8. p53 induction in wt and mutant mice irradiated after NF-κB inhibitor treatment.

A. Representative IHC images of p53 in the intestines of 8 weeks old wt and mutant mice at the indicated time points post 3 Gy IR.

B. Representative IHC images of p53 in the mammary glands of 8 weeks old wt and mutant mice at the indicated time points post 3 Gy IR.

Finally, the levels of p21 were determined. As shown in Fig. 4-9, p21 induction was barely detectable at 30 min but was evident in the intestine by 3 hr after radiation of both wt and mutant mice. From then on, p21 levels appeared to be consistently higher in the mutant intestine, although the difference was modest. In the mutant mammary gland, p21 was strongly induced in a subset of epithelial cells by 3 hr and was largely maintained through at least 6 hr after radiation. In contrast, very few p21-positive cells were detected throughout the time course, which is reminiscent of the largely lack of induction of p21 in the mammary gland of TPCA-1 untreated wt mice (Fig.2-11) and suggests a tissue specificity of p21 induction following DNA damage in vivo.

Overall, results from this set of studies demonstrate higher levels of NF-κB in *Palb2* mutant mice, which is likely due to increased ROS level. Upregulation of NF-κB in turn appears to promote resistance to apoptosis of mutant cells after DNA damage, leading increased survival in the presence of DNA damage, which may drive genome instability leading to tumor development. As p53 and p21 are both induced to similar extents in the mutant mice regardless of TPCA-1 treatment, our data suggest that NF-κB may counteract the pro-apoptotic function of p53 by inducing the expression of anti-apoptotic genes, which will be tested in future studies.

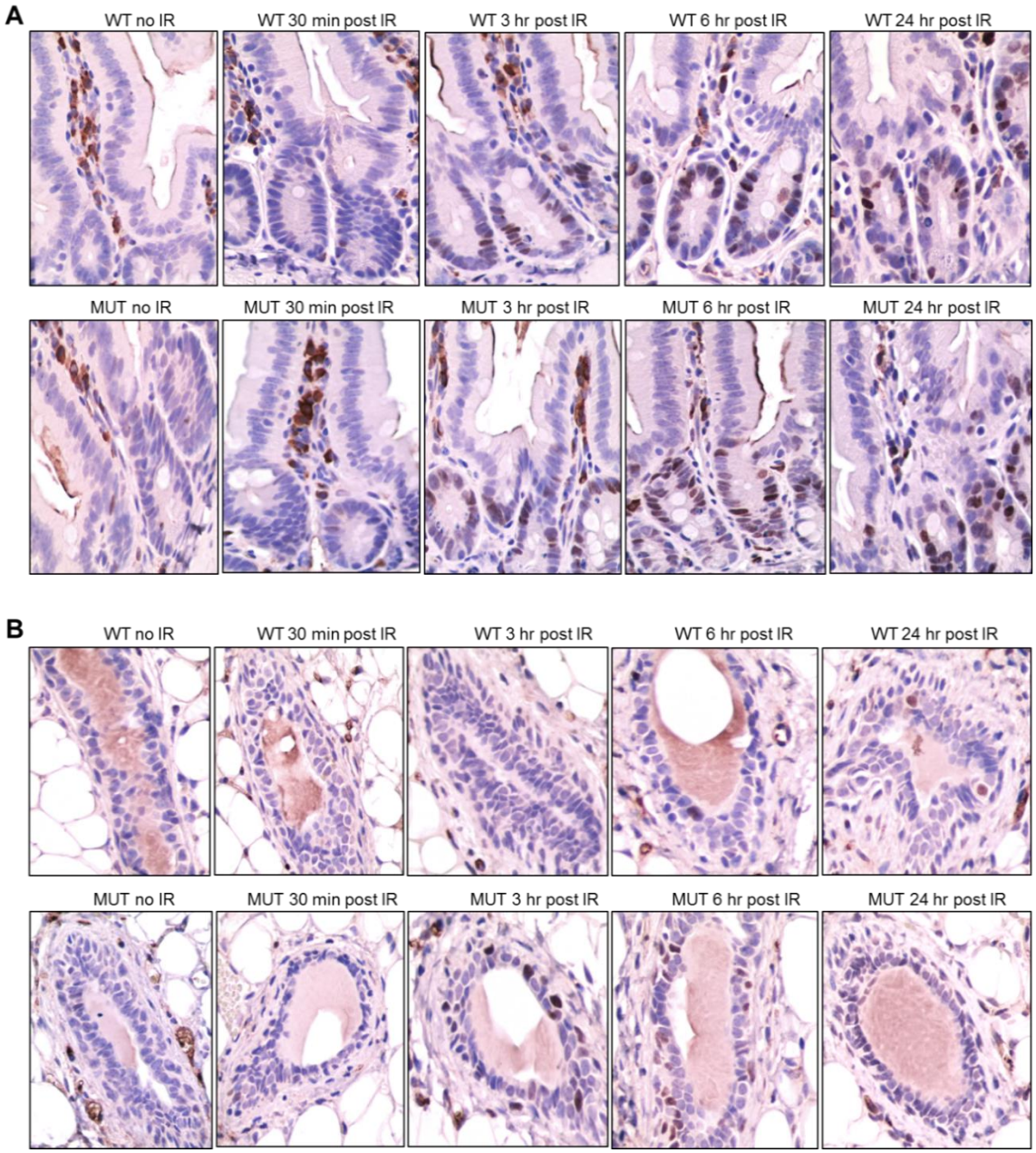

Figure 4-9 p21 induction in wt and mutant mice irradiated after NF-κB inhibitor treatment.

A. Representative IHC images of p53 in the intestines of 8 weeks old wt and *Palb2*m/m mice at the indicated time points post 3 Gy IR.

B. Representative IHC images of p21 in the mammary glands of 8 weeks old wt and *Palb2*m/m mice at the indicated time points post 3 Gy IR.

CHAPTER 5

Conclusions and Perspectives

In this study, we characterized the tumor susceptibility of our *Palb2* knockin mice under different conditions. When aged normally, the mice showed increased tumor development compared with wt mice, indicating that the interaction between PALB2 and BRCA1 plays an important role in tumor suppression. Surprisingly, liver cancer was overall the major tumor type that developed, and it preferentially affected males. In females, we did observe one case of mammary tumor and two cases of ovarian tumor among 19 animals during an 800-day observation period. As none of the wt females developed either tumor, this result suggests that the interaction between the two proteins is important for suppressing tumorigenesis in the mammary gland and ovary, which are the sites susceptible to tumor development in human *BRCA1* and *PALB2* mutation carriers. Therefore, this model recapitulates at least some aspects of the *PALB2* and *BRCA1*-associated tumorigenesis in humans.

Given the long latency of tumor development in our mutant mice, we challenged them with two DNA damaging agents, IR and DMBA. In both cases, overall tumor development was greatly accelerated. More importantly, the mutant mice developed tumors faster than did wt mice, underscoring the key role of the BRCA1-PALB2 interaction in DNA repair and tumor suppression.

In light of high frequency of p53 mutations in human breast cancers arising from *BRCA1* mutation carriers and the now established role of p53 as a critical barrier to *BRCA1*- and *PALB2*-associated tumor development, we crossed our mutant mice with *Trp53*-/- mice to generate mice with the *Palb2* mutation in a *Trp53*+/- background to “sensitize” the mice for tumor development.

Palb2m/m;*Trp53*+/- mice developed tumors much faster than either single mutant mice, again demonstrating the tumor suppressive role of the BRCA1-PALB2 interaction. Interestingly, the major tumors types affecting the *Palb2m/m*;*Trp53*+/- mice were lymphomas and sarcomas, which are commonly associated with p53 mutations, rather than mammary, pancreatic or ovarian tumors typically associated with PALB2 mutations in humans. Moreover, whole exome sequencing revealed that a majority of the tumors from the compound mutant mice had lost the wt *Trp53* allele. These results strongly suggest that a key mechanism of tumor suppression mediated by the BRCA1/PALB2 complex is to prevent the loss of p53 through genome instability.

Interestingly, cells and tissues of our mutant mice showed constitutively increased ROS levels and NF-κB expression, which is known to be responsive to oxidative stress. The increased ROS levels can be at least partially attributed to the role of PALB2 in promoting the function of NRF2, a master antioxidant transcription factor (192). Interestingly, it has recently been reported that ROS can induce NF-κB activity in BRCA1 deficient cells which in turn drive aberrant cell growth and accumulation of DNA damage (180, 200). It would be interestingly to test whether NF-kB is also overexpressed in human cancers with various, mostly truncating, *PALB2* or *BRCA1* mutations. If so, NF-κB would represent a potential molecular target therapy for the cancers.

Chronic inflammation contributes to accumulation of mutations that can initiate cancer and promote tumor progression (201). Therefore, constitutively high NF-κB activity may accelerate tumor development from chronic tissue

damage and inflammation as in hepatocellular carcinoma (202). As such, inhibition of NF-κB may be beneficial for cancer prevention. However, manipulating NF-κB for the prevention or treatment of cancers is not without any risk, as defects or over-suppression of NF-κB leads to impaired immunity (203, 204). It is well known that NF-κB activity decreases bone density and skeleton development (205). On the other side, inhibition of NF-κB has a promoter effect on bone tumor development through osteoblast and osteoclast activity regulation (206). Therefore, NF-κB inhibitors should be used for short periods and intermittent in order to avoid its immunosuppressive effect with longer and continuous usage.

Notably, there is an inverse correlation between estrogen hormone level and NF-κB activity, as the former exerts multi-level effects on NF-kB through either inhibition of IKK activity, degradation of IkB, and compete for DNA binding sites or through its competition and binding with coactivators of NF-κB (207-209). Decreased activity of NF-κB secondary to estrogen hormone in females not only promotes osteoblast activation and bone formation, but also inhibits osteoclast function to limit bone loss, resulting in a gain of bone formation (206, 210). Consistent with this notion, higher estrogen levels could be explaining why we observed about 3.5 times more osteosarcoma in females at their reproductive age (first year) than in males (48% female versus 14% male) (Fig.5-1). As it has been well documented that in humans osteosarcoma has higher incidence in males (211), our results suggest a shift in gender preference due possibly to the mutation in PALB2. In such genetic context with the abrogation of PALB2-BRCA1

interaction (or even loss of BRCA1 or PALB2 function), NF-κB inhibitors could potentially be used as an adjuvant to other cancer therapies such as radiotherapy or chemotherapy.

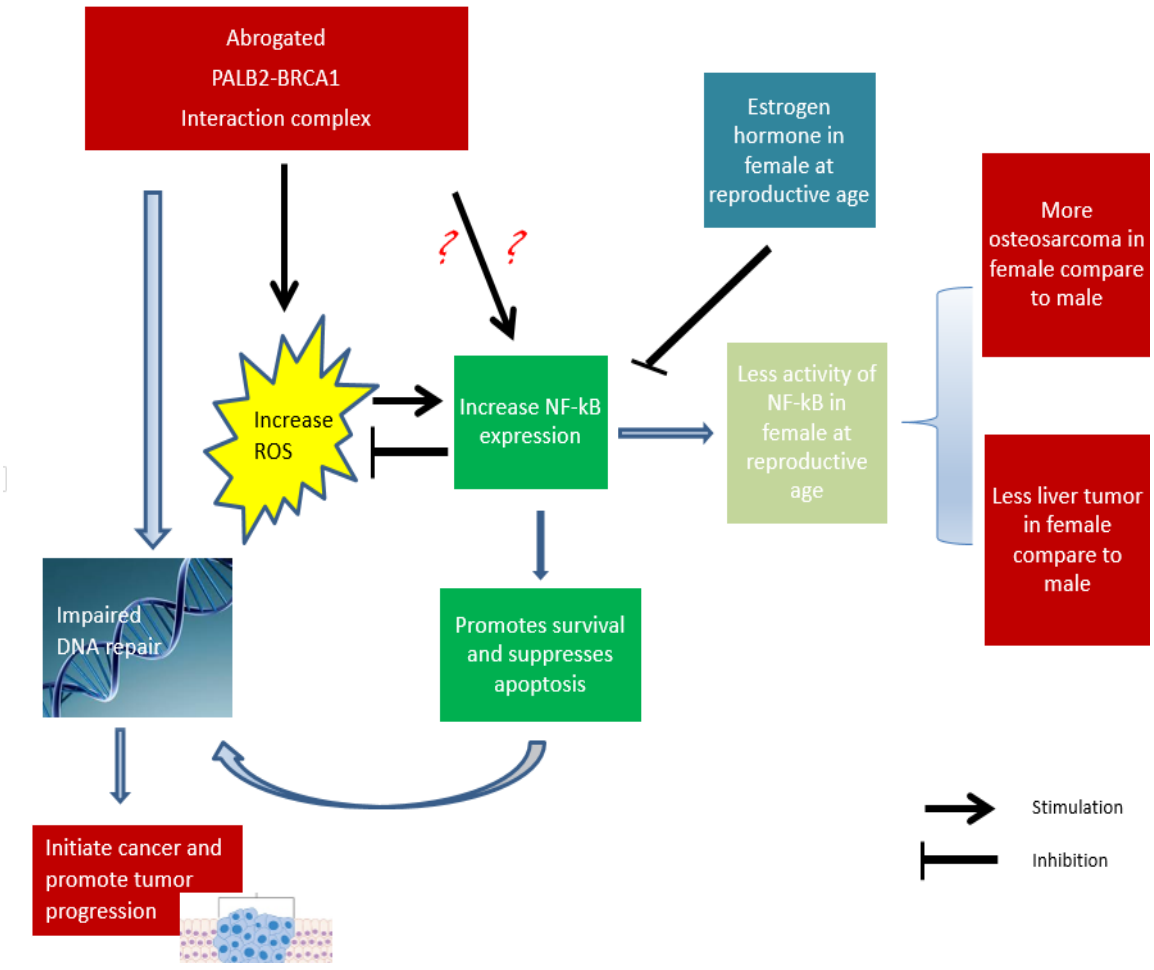

Figure 5-1. Proposed model depicting mechanism of PALB2-BRCA1 interaction and tumorigenesis.

REFERENCES

1. Moynahan ME & Jasin M (2010) Mitotic homologous recombination maintains genomic stability and suppresses tumorigenesis. *Nature reviews. Molecular cell biology* 11(3):196-207.

2. Roy R, Chun J, & Powell SN (2011) BRCA1 and BRCA2: different roles in a common pathway of genome protection. *Nature reviews. Cancer* 12(1):68-78.

3. Xia B*, et al.* (2006) Control of BRCA2 cellular and clinical functions by a nuclear partner, PALB2. *Molecular cell* 22(6):719-729.

4. Oliver AW, Swift S, Lord CJ, Ashworth A, & Pearl LH (2009) Structural basis for recruitment of BRCA2 by PALB2. *EMBO reports* 10(9):990-996.

5. Zhang F*, et al.* (2009) PALB2 links BRCA1 and BRCA2 in the DNA-damage response. *Current biology : CB* 19(6):524-529.

6. Sy SM, Huen MS, & Chen J (2009) PALB2 is an integral component of the BRCA complex required for homologous recombination repair. *Proceedings of the National Academy of Sciences of the United States of America* 106(17):7155-7160.

7. Lee AS & Ang P (2014) Breast-cancer risk in families with mutations in PALB2. *The New England journal of medicine* 371(17):1650-1651.

8. Malone KE*, et al.* (2006) Prevalence and predictors of BRCA1 and BRCA2 mutations in a population-based study of breast cancer in white and black American women ages 35 to 64 years. *Cancer research* 66(16):8297-8308.

9. Turner N, Tutt A, & Ashworth A (2004) Hallmarks of 'BRCAness' in sporadic cancers. *Nature reviews. Cancer* 4(10):814-819.

10. Wei M*, et al.* (2005) BRCA1 promoter methylation in sporadic breast cancer is associated with reduced BRCA1 copy number and chromosome 17 aneusomy. *Cancer research* 65(23):10692-10699.

11. Birgisdottir V*, et al.* (2006) Epigenetic silencing and deletion of the BRCA1 gene in sporadic breast cancer. *Breast cancer research : BCR* 8(4):R38.

12. Walsh T*, et al.* (2011) Mutations in 12 genes for inherited ovarian, fallopian tube, and peritoneal carcinoma identified by massively parallel sequencing. *Proceedings of the National Academy of Sciences of the United States of America* 108(44):18032-18037.

13. Rustgi AK (2014) Familial pancreatic cancer: genetic advances. *Genes & development* 28(1):1-7.

14. Li D, Kumaraswamy E, Harlan-Williams LM, & Jensen RA (2013) The role of BRCA1 and BRCA2 in prostate cancer. *Frontiers in bioscience (Landmark edition)* 18:1445-1459.

15. Tischkowitz M & Xia B (2010) PALB2/FANCN: recombining cancer and Fanconi anemia. *Cancer research* 70(19):7353-7359.

16. Buisson R & Masson JY (2012) PALB2 self-interaction controls homologous recombination. *Nucleic acids research* 40(20):10312-10323.

17. Xia B*, et al.* (2007) Fanconi anemia is associated with a defect in the BRCA2 partner PALB2. *Nature genetics* 39(2):159-161.

18. Evers B & Jonkers J (2006) Mouse models of BRCA1 and BRCA2 deficiency: past lessons, current understanding and future prospects. *Oncogene* 25(43):5885-5897.

19. Bouwman P*, et al.* (2011) Loss of p53 partially rescues embryonic development of Palb2 knockout mice but does not foster haploinsufficiency of Palb2 in tumour suppression. *The Journal of pathology* 224(1):10-21.

20. Ludwig T, Chapman DL, Papaioannou VE, & Efstratiadis A (1997) Targeted mutations of breast cancer susceptibility gene homologs in mice: lethal phenotypes of Brca1, Brca2, Brca1/Brca2, Brca1/p53, and Brca2/p53 nullizygous embryos. *Genes & development* 11(10):1226-1241.

21. Ludwig T, Fisher P, Murty V, & Efstratiadis A (2001) Development of mammary adenocarcinomas by tissue-specific knockout of Brca2 in mice. *Oncogene* 20(30):3937-3948.

22. Shakya R*, et al.* (2008) The basal-like mammary carcinomas induced by Brca1 or Bard1 inactivation implicate the BRCA1/BARD1 heterodimer in tumor suppression. *Proceedings of the National Academy of Sciences of the United States of America* 105(19):7040-7045.

23. Huo Y*, et al.* (2013) Autophagy opposes p53-mediated tumor barrier to facilitate tumorigenesis in a model of PALB2-associated hereditary breast cancer. *Cancer discovery* 3(8):894-907.

24. Holstege H*, et al.* (2009) High incidence of protein-truncating TP53 mutations in BRCA1-related breast cancer. *Cancer research* 69(8):3625-3633.

25. Erkko H*, et al.* (2007) A recurrent mutation in PALB2 in Finnish cancer families. *Nature* 446(7133):316-319.

26. Greenblatt MS, Chappuis PO, Bond JP, Hamel N, & Foulkes WD (2001) TP53 mutations in breast cancer associated with BRCA1 or BRCA2 germ-line mutations: distinctive spectrum and structural distribution. *Cancer research* 61(10):4092-4097.

27. Simhadri S*, et al.* (2014) Male fertility defect associated with disrupted BRCA1-PALB2 interaction in mice. *The Journal of biological chemistry* 289(35):24617-24629.

28. Rantakari P*, et al.* (2010) Inactivation of Palb2 gene leads to mesoderm differentiation defect and early embryonic lethality in mice. *Human molecular genetics* 19(15):3021-3029.

29. Kerr JF, Wyllie AH, & Currie AR (1972) Apoptosis: a basic biological phenomenon with wide-ranging implications in tissue kinetics. *British journal of cancer* 26(4):239-257.

30. Majno G & Joris I (1995) Apoptosis, oncosis, and necrosis. An overview of cell death. *The American journal of pathology* 146(1):3-15.

31. Elmore S (2007) Apoptosis: a review of programmed cell death. *Toxicologic pathology* 35(4):495-516.

32. Wong RS (2011) Apoptosis in cancer: from pathogenesis to treatment. *Journal of experimental & clinical cancer research : CR* 30:87.

33. Hengartner MO (2001) Apoptosis: corralling the corpses. *Cell* 104(3):325-328.

34. Peng L & Liu JJ (1997) A novel method for quantitative analysis of apoptosis. *Laboratory investigation; a journal of technical methods and pathology* 77(6):547-555.

35. Lavrik IN, Golks A, & Krammer PH (2005) Caspases: pharmacological manipulation of cell death. *The Journal of clinical investigation* 115(10):2665-2672.

36. Ashkenazi A & Dixit VM (1998) Death receptors: signaling and modulation. *Science (New York, N.Y.)* 281(5381):1305-1308.

37. Schneider P & Tschopp J (2000) Apoptosis induced by death receptors. *Pharmaceutica acta Helvetiae* 74(2-3):281-286.

38. Kroemer G, Galluzzi L, & Brenner C (2007) Mitochondrial membrane permeabilization in cell death. *Physiological reviews* 87(1):99-163.

39. Saelens X*, et al.* (2004) Toxic proteins released from mitochondria in cell death. *Oncogene* 23(16):2861-2874.

40. Bouchier-Hayes L, Lartigue L, & Newmeyer DD (2005) Mitochondria: pharmacological manipulation of cell death. *The Journal of clinical investigation* 115(10):2640-2647.

41. Kovacsovics M*, et al.* (2002) Overexpression of Helicard, a CARD-containing helicase cleaved during apoptosis, accelerates DNA degradation. *Current biology : CB* 12(10):838-843.

42. Gross A, McDonnell JM, & Korsmeyer SJ (1999) BCL-2 family members and the mitochondria in apoptosis. *Genes & development* 13(15):1899-1911.

43. Szegezdi E, Fitzgerald U, & Samali A (2003) Caspase-12 and ER-stress-mediated apoptosis: the story so far. *Annals of the New York Academy of Sciences* 1010:186-194.

44. Sos ML*, et al.* (2009) Identifying genotype-dependent efficacy of single and combined PI3K- and MAPK-pathway inhibition in cancer. *Proceedings of the National Academy of Sciences of the United States of America* 106(43):18351-18356.

45. Dashzeveg N & Yoshida K (2015) Cell death decision by p53 via control of the mitochondrial membrane. *Cancer letters* 367(2):108-112.

46. Levine AJ (1997) p53, the cellular gatekeeper for growth and division. *Cell* 88(3):323-331.

47. Green DR & Kroemer G (2009) Cytoplasmic functions of the tumour suppressor p53. *Nature* 458(7242):1127-1130.

48. Chipuk JE, Bouchier-Hayes L, Kuwana T, Newmeyer DD, & Green DR (2005) PUMA couples the nuclear and cytoplasmic proapoptotic function of p53. *Science (New York, N.Y.)* 309(5741):1732-1735.

49. Cimmino A*, et al.* (2005) miR-15 and miR-16 induce apoptosis by targeting BCL2. *Proceedings of the National Academy of Sciences of the United States of America* 102(39):13944-13949.

50. Beg AA, Sha WC, Bronson RT, Ghosh S, & Baltimore D (1995) Embryonic lethality and liver degeneration in mice lacking the RelA component of NF-kappa B. *Nature* 376(6536):167-170.

51. Karin M & Lin A (2002) NF-kappaB at the crossroads of life and death. *Nature immunology* 3(3):221-227.

52. Deveraux QL*, et al.* (1998) IAPs block apoptotic events induced by caspase-8 and cytochrome c by direct inhibition of distinct caspases. *The EMBO journal* 17(8):2215-2223.

53. Irmler M*, et al.* (1997) Inhibition of death receptor signals by cellular FLIP. *Nature* 388(6638):190-195.

54. Wang CY, Guttridge DC, Mayo MW, & Baldwin AS, Jr. (1999) NF-kappaB induces expression of the Bcl-2 homologue A1/Bfl-1 to preferentially suppress chemotherapy-induced apoptosis. *Molecular and cellular biology* 19(9):5923-5929.

55. Ren X*, et al.* (2016) Activator protein 1 promotes gemcitabine-induced apoptosis in pancreatic cancer by upregulating its downstream target Bim. *Oncology letters* 12(6):4732-4738.

56. Natoli G*, et al.* (1997) Activation of SAPK/JNK by TNF receptor 1 through a noncytotoxic TRAF2-dependent pathway. *Science (New York, N.Y.)* 275(5297):200-203.

57. De Smaele E*, et al.* (2001) Induction of gadd45beta by NF-kappaB downregulates pro-apoptotic JNK signalling. *Nature* 414(6861):308-313.

58. Ebrahimi S*, et al.* (2017) Targeting the Akt/PI3K signaling pathway as a potential therapeutic strategy for the treatment of Pancreatic Cancer. *Current medicinal chemistry*.

59. Hao J*, et al.* (2017) Targeting NF-kappaB/AP-2beta signaling to enhance antitumor activity of cisplatin by melatonin in hepatocellular carcinoma cells. *American journal of cancer research* 7(1):13-27.

60. Kerr JF, Winterford CM, & Harmon BV (1994) Apoptosis. Its significance in cancer and cancer therapy. *Cancer* 73(8):2013-2026.

61. Lowe SW, Ruley HE, Jacks T, & Housman DE (1993) p53-dependent apoptosis modulates the cytotoxicity of anticancer agents. *Cell* 74(6):957-967.

62. Harris CC (1996) Structure and function of the p53 tumor suppressor gene: clues for rational cancer therapeutic strategies. *Journal of the National Cancer Institute* 88(20):1442-1455.

63. Lowe SW & Lin AW (2000) Apoptosis in cancer. *Carcinogenesis* 21(3):485-495.

64. Tsujimoto Y, Cossman J, Jaffe E, & Croce CM (1985) Involvement of the bcl-2 gene in human follicular lymphoma. *Science (New York, N.Y.)* 228(4706):1440-1443.

65. Knudsen ES & Wang JY (2010) Targeting the RB-pathway in cancer therapy. *Clinical cancer research : an official journal of the American Association for Cancer Research* 16(4):1094-1099.

66. Lin WC, Lin FT, & Nevins JR (2001) Selective induction of E2F1 in response to DNA damage, mediated by ATM-dependent phosphorylation. *Genes & development* 15(14):1833-1844.

67. Singh N (2007) Apoptosis in health and disease and modulation of apoptosis for therapy: An overview. *Indian journal of clinical biochemistry : IJCB* 22(2):6-16.

68. Goolsby C, Paniagua M, Tallman M, & Gartenhaus RB (2005) Bcl-2 regulatory pathway is functional in chronic lymphocytic leukemia. *Cytometry. Part B, Clinical cytometry* 63(1):36-46.

69. Pepper C, Hoy T, & Bentley DP (1997) Bcl-2/Bax ratios in chronic lymphocytic leukaemia and their correlation with in vitro apoptosis and clinical resistance. *British journal of cancer* 76(7):935-938.

70. Devarajan E*, et al.* (2002) Down-regulation of caspase 3 in breast cancer: a possible mechanism for chemoresistance. *Oncogene* 21(57):8843-8851.

71. Friesen C, Fulda S, & Debatin KM (1997) Deficient activation of the CD95 (APO-1/Fas) system in drug-resistant cells. *Leukemia* 11(11):1833-1841.

72. Reesink-Peters N*, et al.* (2005) Death receptors and ligands in cervical carcinogenesis: an immunohistochemical study. *Gynecologic oncology* 96(3):705-713.

73. Fadeel B & Orrenius S (2005) Apoptosis: a basic biological phenomenon with wide-ranging implications in human disease. *Journal of internal medicine* 258(6):479-517.

74. Olivier M*, et al.* (2002) The IARC TP53 database: new online mutation analysis and recommendations to users. *Human mutation* 19(6):607-614.

75. Stoll R*, et al.* (2001) Chalcone derivatives antagonize interactions between the human oncoprotein MDM2 and p53. *Biochemistry* 40(2):336-344.

76. Vazquez A, Bond EE, Levine AJ, & Bond GL (2008) The genetics of the p53 pathway, apoptosis and cancer therapy. *Nature reviews. Drug discovery* 7(12):979-987.

77. Vassilev LT (2007) MDM2 inhibitors for cancer therapy. *Trends in molecular medicine* 13(1):23-31.

78. Sasaki H, Sheng Y, Kotsuji F, & Tsang BK (2000) Down-regulation of X-linked inhibitor of apoptosis protein induces apoptosis in chemoresistant human ovarian cancer cells. *Cancer research* 60(20):5659-5666.

79. Tamm I*, et al.* (2003) Peptides targeting caspase inhibitors. *The Journal of biological chemistry* 278(16):14401-14405.

80. Schimmer AD*, et al.* (2004) Small-molecule antagonists of apoptosis suppressor XIAP exhibit broad antitumor activity. *Cancer cell* 5(1):25-35.

81. LaCasse EC*, et al.* (2008) IAP-targeted therapies for cancer. *Oncogene* 27(48):6252-6275.

82. Armstrong JS (2006) Mitochondria: a target for cancer therapy. *British journal of pharmacology* 147(3):239-248.

83. Galluzzi L, Larochette N, Zamzami N, & Kroemer G (2006) Mitochondria as therapeutic targets for cancer chemotherapy. *Oncogene* 25(34):4812-4830.

84. Marcucci G*, et al.* (2005) Phase I study of oblimersen sodium, an antisense to Bcl-2, in untreated older patients with acute myeloid leukemia: pharmacokinetics, pharmacodynamics, and clinical activity. *Journal of clinical oncology : official journal of the American Society of Clinical Oncology* 23(15):3404-3411.

85. Demchenko YN*, et al.* (2014) Novel inhibitors are cytotoxic for myeloma cells with NFkB inducing kinase-dependent activation of NFkB. *Oncotarget* 5(12):4554-4566.

86. Daniel PT, Wieder T, Sturm I, & Schulze-Osthoff K (2001) The kiss of death: promises and failures of death receptors and ligands in cancer therapy. *Leukemia* 15(7):1022-1032.

87. Nicholson DW (2000) From bench to clinic with apoptosis-based therapeutic agents. *Nature* 407(6805):810-816.

88. Menzel T*, et al.* (2011) A genetic screen identifies BRCA2 and PALB2 as key regulators of G2 checkpoint maintenance. *EMBO reports* 12(7):705-712.

89. Ghobrial IM, Witzig TE, & Adjei AA (2005) Targeting apoptosis pathways in cancer therapy. *CA: a cancer journal for clinicians* 55(3):178-194.

90. Essers J*, et al.* (2000) Homologous and non-homologous recombination differentially affect DNA damage repair in mice. *The EMBO journal* 19(7):1703-1710.

91. Metzger L & Iliakis G (1991) Kinetics of DNA double-strand break repair throughout the cell cycle as assayed by pulsed field gel electrophoresis in CHO cells. *International journal of radiation biology* 59(6):1325-1339.

92. Wang H, Wang X, Iliakis G, & Wang Y (2003) Caffeine could not efficiently sensitize homologous recombination repair-deficient cells to ionizing radiation-induced killing. *Radiation research* 159(3):420-425.

93. Watanabe S, Shimosato Y, Okita T, Ezaki H, & Shigemitsu T (1972) Leukemia and thyroid carcinoma found among A-bomb survivors in Hiroshima. *Recent results in cancer research. Fortschritte der Krebsforschung. Progres dans les recherches sur le cancer* 39:57-83.

94. Gluzman D*, et al.* (2005) Malignant diseases of hematopoietic and lymphoid tissues in Chernobyl clean-up workers. *The hematology journal : the official journal of the European Haematology Association* 5(7):565-571.

95. Carmichael A, Sami AS, & Dixon JM (2003) Breast cancer risk among the survivors of atomic bomb and patients exposed to therapeutic ionising radiation. *European journal of surgical oncology : the journal of the European Society of Surgical Oncology and the British Association of Surgical Oncology* 29(5):475-479.

96. Rogakou EP, Pilch DR, Orr AH, Ivanova VS, & Bonner WM (1998) DNA double-stranded breaks induce histone H2AX phosphorylation on serine 139. *The Journal of biological chemistry* 273(10):5858-5868.

97. Stiff T*, et al.* (2004) ATM and DNA-PK function redundantly to phosphorylate H2AX after exposure to ionizing radiation. *Cancer research* 64(7):2390-2396.

98. Grabarz A, Barascu A, Guirouilh-Barbat J, & Lopez BS (2012) Initiation of DNA double strand break repair: signaling and single-stranded resection dictate the choice between homologous recombination, non-homologous end-joining and alternative end-joining. *American journal of cancer research* 2(3):249-268.

99. Jasin M (2002) Homologous repair of DNA damage and tumorigenesis: the BRCA connection. *Oncogene* 21(58):8981-8993.

100. Ceccaldi R, Rondinelli B, & D'Andrea AD (2016) Repair Pathway Choices and Consequences at the Double-Strand Break. *Trends in cell biology* 26(1):52-64.

101. Chapman JR, Sossick AJ, Boulton SJ, & Jackson SP (2012) BRCA1-associated exclusion of 53BP1 from DNA damage sites underlies temporal control of DNA repair. *Journal of cell science* 125(Pt 15):3529-3534.

102. Carrasco D*, et al.* (1998) Multiple hemopoietic defects and lymphoid hyperplasia in mice lacking the transcriptional activation domain of the c-Rel protein. *The Journal of experimental medicine* 187(7):973-984.

103. Brownell E*, et al.* (1988) Regional localization of the human c-rel locus using translocation chromosome analysis. *Oncogene* 2(5):527-529.

104. Mathew S, Murty VV, Dalla-Favera R, & Chaganti RS (1993) Chromosomal localization of genes encoding the transcription factors, c-rel, NF-kappa Bp50, NF-kappa Bp65, and lyt-10 by fluorescence in situ hybridization. *Oncogene* 8(1):191-193.

105. El-Serag HB (2011) Hepatocellular carcinoma. *The New England journal of medicine* 365(12):1118-1127.

106. Palmer DH (2008) Sorafenib in advanced hepatocellular carcinoma. *The New England journal of medicine* 359(23):2498; author reply 2498-2499.

107. Sid B*, et al.* (2014) AICAR induces Nrf2 activation by an AMPK-independent mechanism in hepatocarcinoma cells. *Biochemical pharmacology* 91(2):168-180.

108. Trachootham D, Alexandre J, & Huang P (2009) Targeting cancer cells by ROS-mediated mechanisms: a radical therapeutic approach? *Nature reviews. Drug discovery* 8(7):579-591.

109. Ames BN (1983) Dietary carcinogens and anticarcinogens. Oxygen radicals and degenerative diseases. *Science (New York, N.Y.)* 221(4617):1256-1264.

110. Zibara K*, et al.* (2016) ROS mediates interferon gamma induced phosphorylation of Src, through the Raf/ERK pathway, in MCF-7 human breast cancer cell line. *Journal of cell communication and signaling*.

111. Latimer HR & Veal EA (2016) Peroxiredoxins in Regulation of MAPK Signalling Pathways; Sensors and Barriers to Signal Transduction. *Molecules and cells* 39(1):40-45.

112. Liu SL*, et al.* (2002) Reactive oxygen species stimulated human hepatoma cell proliferation via cross-talk between PI3-K/PKB and JNK signaling pathways. *Archives of biochemistry and biophysics* 406(2):173-182.

113. Kawanishi S, Hiraku Y, & Oikawa S (2001) Mechanism of guanine-specific DNA damage by oxidative stress and its role in carcinogenesis and aging. *Mutation research* 488(1):65-76.

114. Delaney S, Jarem DA, Volle CB, & Yennie CJ (2012) Chemical and biological consequences of oxidatively damaged guanine in DNA. *Free radical research* 46(4):420-441.

115. Elchuri S*, et al.* (2005) CuZnSOD deficiency leads to persistent and widespread oxidative damage and hepatocarcinogenesis later in life. *Oncogene* 24(3):367-380.

116. Song FN*, et al.* (2014) RANKL promotes migration and invasion of hepatocellular carcinoma cells via NF-kappaB-mediated epithelial-mesenchymal transition. *PloS one* 9(9):e108507.

117. Kanter EM*, et al.* (2006) Dual modality imaging of a novel rat model of ovarian carcinogenesis. *Journal of biomedical optics* 11(4):041123.

118. Diagaradjane P, Yaseen MA, Yu J, Wong MS, & Anvari B (2006) Synchronous fluorescence spectroscopic characterization of DMBA-TPA-induced squamous cell carcinoma in mice. *Journal of biomedical optics* 11(1):014012.

119. Birtwistle J*, et al.* (2009) The aldo-keto reductase AKR1C3 contributes to 7,12-dimethylbenz(a)anthracene-3,4-dihydrodiol mediated oxidative DNA damage in myeloid cells: implications for leukemogenesis. *Mutation research* 662(1-2):67-74.

120. Russo J & Russo IH (1996) Experimentally induced mammary tumors in rats. *Breast cancer research and treatment* 39(1):7-20.

121. Marion SL*, et al.* (2013) 7,12-dimethylbenz[a]anthracene-induced malignancies in a mouse model of menopause. *Comparative medicine* 63(1):6-12.

122. Lawther PJ & Waller RE (1976) Coal fires, industrial emissions and motor vehicles as sources of environmental carcinogens. *IARC scientific publications* (13):27-40.

123. Miyata M, Furukawa M, Takahashi K, Gonzalez FJ, & Yamazoe Y (2001) Mechanism of 7,12-dimethylbenz[a]anthracene-induced immunotoxicity: role of metabolic activation at the target organ. *Japanese journal of pharmacology* 86(3):302-309.

124. Gelboin HV (1980) Benzo[alpha]pyrene metabolism, activation and carcinogenesis: role and regulation of mixed-function oxidases and related enzymes. *Physiological reviews* 60(4):1107-1166.

125. Todorovic R*, et al.* (1997) Determination of benzo[a]pyrene- and 7,12-dimethylbenz[a]anthracene-DNA adducts formed in rat mammary glands. *Chemical research in toxicology* 10(9):941-947.

126. Devanesan PD*, et al.* (1993) Identification and quantitation of 7,12-dimethylbenz[a]anthracene-DNA adducts formed in mouse skin. *Chemical research in toxicology* 6(3):364-371.

127. Imaoka S*, et al.* (2004) Role of phenobarbital-inducible cytochrome P450s as a source of active oxygen species in DNA-oxidation. *Cancer letters* 203(2):117-125.

128. Dandekar S, Sukumar S, Zarbl H, Young LJ, & Cardiff RD (1986) Specific activation of the cellular Harvey-ras oncogene in dimethylbenzanthracene-induced mouse mammary tumors. *Molecular and cellular biology* 6(11):4104-4108.

129. Cardiff RD*, et al.* (1988) c-H-ras-1 expression in 7,12-dimethyl benzanthracene-induced Balb/c mouse mammary hyperplasias and their tumors. *Oncogene* 3(2):205-213.

130. Hattori-Nakakuki Y*, et al.* (1994) Formation of 8-hydroxy-2'-deoxyguanosine in epidermis of hairless mice exposed to near-UV. *Biochemical and biophysical research communications* 201(3):1132-1139.

131. Auerbach AD (2009) Fanconi anemia and its diagnosis. *Mutation research* 668(1-2):4-10.

132. Walden H & Deans AJ (2014) The Fanconi anemia DNA repair pathway: structural and functional insights into a complex disorder. *Annual review of biophysics* 43:257-278.

133. Duxin JP & Walter JC (2015) What is the DNA repair defect underlying Fanconi anemia? *Current opinion in cell biology* 37:49-60.

134. Sobeck A*, et al.* (2006) Fanconi anemia proteins are required to prevent accumulation of replication-associated DNA double-strand breaks. *Molecular and cellular biology* 26(2):425-437.

135. Ishiai M*, et al.* (2008) FANCI phosphorylation functions as a molecular switch to turn on the Fanconi anemia pathway. *Nature structural & molecular biology* 15(11):1138-1146.

136. Li T*, et al.* (2012) Tumor suppression in the absence of p53-mediated cell-cycle arrest, apoptosis, and senescence. *Cell* 149(6):1269-1283.

138. Harvey M*, et al.* (1993) In vitro growth characteristics of embryo fibroblasts isolated from p53-deficient mice. *Oncogene* 8(9):2457-2467.

139. Byrd PJ*, et al.* (2016) A Hypomorphic PALB2 Allele Gives Rise to an Unusual Form of FA-N Associated with Lymphoid Tumour Development. *PLoS genetics* 12(3):e1005945.

140. van Gent DC, Hoeijmakers JH, & Kanaar R (2001) Chromosomal stability and the DNA double-stranded break connection. *Nature reviews. Genetics* 2(3):196-206.

141. Bunting SF*, et al.* (2010) 53BP1 inhibits homologous recombination in Brca1-deficient cells by blocking resection of DNA breaks. *Cell* 141(2):243-254.

142. Hu Y*, et al.* (2014) Regulation of 53BP1 protein stability by RNF8 and RNF168 is important for efficient DNA double-strand break repair. *PloS one* 9(10):e110522.

143. Bothmer A*, et al.* (2011) Regulation of DNA end joining, resection, and immunoglobulin class switch recombination by 53BP1. *Molecular cell* 42(3):319-329.

144. Difilippantonio S*, et al.* (2008) 53BP1 facilitates long-range DNA end-joining during V(D)J recombination. *Nature* 456(7221):529-533.

145. Krammer PH (2000) CD95's deadly mission in the immune system. *Nature* 407(6805):789-795.

146. Carter MR, Hornick JL, Lester S, & Fletcher CD (2006) Spindle cell (sarcomatoid) carcinoma of the breast: a clinicopathologic and immunohistochemical analysis of 29 cases. *The American journal of surgical pathology* 30(3):300-309.

147. Cordeiro RM (2014) Reactive oxygen species at phospholipid bilayers: distribution, mobility and permeation. *Biochimica et biophysica acta* 1838(1 Pt B):438-444.

148. Conte E, Megli FM, Khandelia H, Jeschke G, & Bordignon E (2013) Lipid peroxidation and water penetration in lipid bilayers: a W-band EPR study. *Biochimica et biophysica acta* 1828(2):510-517.

149. Griffith OW (1999) Biologic and pharmacologic regulation of mammalian glutathione synthesis. *Free radical biology & medicine* 27(9-10):922-935.

150. Malkin D*, et al.* (1990) Germ line p53 mutations in a familial syndrome of breast cancer, sarcomas, and other neoplasms. *Science (New York, N.Y.)* 250(4985):1233-1238.

151. Donehower LA (1996) The p53-deficient mouse: a model for basic and applied cancer studies. *Seminars in cancer biology* 7(5):269-278.

152. Venkatachalam S*, et al.* (2001) Is p53 haploinsufficient for tumor suppression? Implications for the p53+/- mouse model in carcinogenicity testing. *Toxicologic pathology* 29 Suppl:147-154.

153. Venkatachalam S*, et al.* (1998) Retention of wild-type p53 in tumors from p53 heterozygous mice: reduction of p53 dosage can promote cancer formation. *The EMBO journal* 17(16):4657-4667.

154. Birch JM*, et al.* (1998) Cancer phenotype correlates with constitutional TP53 genotype in families with the Li-Fraumeni syndrome. *Oncogene* 17(9):1061-1068.

155. Longhi A, Errani C, De Paolis M, Mercuri M, & Bacci G (2006) Primary bone osteosarcoma in the pediatric age: state of the art. *Cancer treatment reviews* 32(6):423-436.

156. Scott MC*, et al.* (2011) Molecular subtypes of osteosarcoma identified by reducing tumor heterogeneity through an interspecies comparative approach. *Bone* 49(3):356-367.

157. Savage SA & Mirabello L (2011) Using epidemiology and genomics to understand osteosarcoma etiology. *Sarcoma* 2011:548151.

158. Mirabello L, Troisi RJ, & Savage SA (2009) Osteosarcoma incidence and survival rates from 1973 to 2004: data from the Surveillance, Epidemiology, and End Results Program. *Cancer* 115(7):1531-1543.

159. Hansen MF*, et al.* (1985) Osteosarcoma and retinoblastoma: a shared chromosomal mechanism revealing recessive predisposition. *Proceedings of the National Academy of Sciences of the United States of America* 82(18):6216-6220.

160. Wang LL*, et al.* (2003) Association between osteosarcoma and deleterious mutations in the RECQL4 gene in Rothmund-Thomson syndrome. *Journal of the National Cancer Institute* 95(9):669-674.

161. Mao FJ, Sidorova JM, Lauper JM, Emond MJ, & Monnat RJ (2010) The human WRN and BLM RecQ helicases differentially regulate cell proliferation and survival after chemotherapeutic DNA damage. *Cancer research* 70(16):6548-6555.

162. Kovac M*, et al.* (2015) Exome sequencing of osteosarcoma reveals mutation signatures reminiscent of BRCA deficiency. *Nature communications* 6:8940.

163. Wang ZQ, Liang J, Schellander K, Wagner EF, & Grigoriadis AE (1995) c-fos-induced osteosarcoma formation in transgenic mice: cooperativity with c-jun and the role of endogenous c-fos. *Cancer research* 55(24):6244-6251.

164. Zuch D*, et al.* (2012) Targeting radioresistant osteosarcoma cells with parthenolide. *Journal of cellular biochemistry* 113(4):1282-1291.

165. Lamoureux F*, et al.* (2008) Therapeutic efficacy of soluble receptor activator of nuclear factor-kappa B-Fc delivered by nonviral gene transfer in a mouse model of osteolytic osteosarcoma. *Molecular cancer therapeutics* 7(10):3389-3398.

166. Stephens PJ*, et al.* (2011) Massive genomic rearrangement acquired in a single catastrophic event during cancer development. *Cell* 144(1):27-40.

167. Lopez-Guerrero JA, Lopez-Gines C, Pellin A, Carda C, & Llombart-Bosch A (2004) Deregulation of the G1 to S-phase cell cycle checkpoint is involved in the pathogenesis of human osteosarcoma. *Diagnostic molecular pathology : the American journal of surgical pathology, part B* 13(2):81-91.

168. Jacks T*, et al.* (1994) Tumor spectrum analysis in p53-mutant mice. *Current biology : CB* 4(1):1-7.

169. Gardini A, Baillat D, Cesaroni M, & Shiekhattar R (2014) Genome-wide analysis reveals a role for BRCA1 and PALB2 in transcriptional co-activation. *The EMBO journal* 33(8):890-905.

170. Wang J*, et al.* (2009) RelA/p65 functions to maintain cellular senescence by regulating genomic stability and DNA repair. *EMBO reports* 10(11):1272-1278.

171. Chien Y*, et al.* (2011) Control of the senescence-associated secretory phenotype by NF-kappaB promotes senescence and enhances chemosensitivity. *Genes & development* 25(20):2125-2136.

172. Amann PM, Eichmuller SB, Schmidt J, & Bazhin AV (2011) Regulation of gene expression by retinoids. *Current medicinal chemistry* 18(9):1405-1412.

173. Donato LJ & Noy N (2005) Suppression of mammary carcinoma growth by retinoic acid: proapoptotic genes are targets for retinoic acid receptor and cellular retinoic acid-binding protein II signaling. *Cancer research* 65(18):8193-8199.

174. del Rincon SV, Rousseau C, Samanta R, & Miller WH, Jr. (2003) Retinoic acid-induced growth arrest of MCF-7 cells involves the selective regulation of the IRS-1/PI 3-kinase/AKT pathway. *Oncogene* 22(22):3353-3360.

175. Karin M & Ben-Neriah Y (2000) Phosphorylation meets ubiquitination: the control of NF-[kappa]B activity. *Annual review of immunology* 18:621-663.

176. Perkins ND (2007) Integrating cell-signalling pathways with NF-kappaB and IKK function. *Nature reviews. Molecular cell biology* 8(1):49-62.

177. Dolcet X, Llobet D, Pallares J, & Matias-Guiu X (2005) NF-kB in development and progression of human cancer. *Virchows Archiv : an international journal of pathology* 446(5):475-482.

178. Jost PJ & Ruland J (2007) Aberrant NF-kappaB signaling in lymphoma: mechanisms, consequences, and therapeutic implications. *Blood* 109(7):2700-2707.

179. Habraken Y & Piette J (2006) NF-kappaB activation by double-strand breaks. *Biochemical pharmacology* 72(9):1132-1141.

180. Buckley NE*, et al.* (2016) A BRCA1 deficient, NFkappaB driven immune signal predicts good outcome in triple negative breast cancer. *Oncotarget* 7(15):19884-19896.

181. Greten FR & Karin M (2004) The IKK/NF-kappaB activation pathway-a target for prevention and treatment of cancer. *Cancer letters* 206(2):193-199.

182. Ducut Sigala JL*, et al.* (2004) Activation of transcription factor NF-kappaB requires ELKS, an IkappaB kinase regulatory subunit. *Science (New York, N.Y.)* 304(5679):1963-1967.

183. Solan NJ, Miyoshi H, Carmona EM, Bren GD, & Paya CV (2002) RelB cellular regulation and transcriptional activity are regulated by p100. *The Journal of biological chemistry* 277(2):1405-1418.

184. Senftleben U*, et al.* (2001) Activation by IKKalpha of a second, evolutionary conserved, NF-kappa B signaling pathway. *Science (New York, N.Y.)* 293(5534):1495-1499.

185. Ghosh S & Hayden MS (2008) New regulators of NF-kappaB in inflammation. *Nature reviews. Immunology* 8(11):837-848.

186. Liu ZG, Hsu H, Goeddel DV, & Karin M (1996) Dissection of TNF receptor 1 effector functions: JNK activation is not linked to apoptosis while NF-kappaB activation prevents cell death. *Cell* 87(3):565-576.

187. Wang CY, Mayo MW, & Baldwin AS, Jr. (1996) TNF- and cancer therapy-induced apoptosis: potentiation by inhibition of NF-kappaB. *Science (New York, N.Y.)* 274(5288):784-787.

188. Sakon S*, et al.* (2003) NF-kappaB inhibits TNF-induced accumulation of ROS that mediate prolonged MAPK activation and necrotic cell death. *The EMBO journal* 22(15):3898-3909.

189. Wang CY, Mayo MW, Korneluk RG, Goeddel DV, & Baldwin AS, Jr. (1998) NF-kappaB antiapoptosis: induction of TRAF1 and TRAF2 and c-IAP1 and c-IAP2 to suppress caspase-8 activation. *Science (New York, N.Y.)* 281(5383):1680-1683.

190. Chu ZL*, et al.* (1997) Suppression of tumor necrosis factor-induced cell death by inhibitor of apoptosis c-IAP2 is under NF-kappaB control. *Proceedings of the National Academy of Sciences of the United States of America* 94(19):10057-10062.

191. Pervaiz S & Clement MV (2004) Tumor intracellular redox status and drug resistance--serendipity or a causal relationship? *Current pharmaceutical design* 10(16):1969-1977.

192. Ma J*, et al.* (2012) PALB2 interacts with KEAP1 to promote NRF2 nuclear accumulation and function. *Molecular and cellular biology* 32(8):1506-1517.

193. Loft S & Poulsen HE (1996) Cancer risk and oxidative DNA damage in man. *Journal of molecular medicine (Berlin, Germany)* 74(6):297-312.

194. Finkel T & Holbrook NJ (2000) Oxidants, oxidative stress and the biology of ageing. *Nature* 408(6809):239-247.

195. Lee SR*, et al.* (2002) Reversible inactivation of the tumor suppressor PTEN by H2O2. *The Journal of biological chemistry* 277(23):20336-20342.

196. Li Q & Engelhardt JF (2006) Interleukin-1beta induction of NFkappaB is partially regulated by H2O2-mediated activation of NFkappaB-inducing kinase. *The Journal of biological chemistry* 281(3):1495-1505.

197. Morgan MJ & Liu ZG (2011) Crosstalk of reactive oxygen species and NF-kappaB signaling. *Cell research* 21(1):103-115.

198. Chen EI*, et al.* (2007) Adaptation of energy metabolism in breast cancer brain metastases. *Cancer research* 67(4):1472-1486.

199. Tergaonkar V, Pando M, Vafa O, Wahl G, & Verma I (2002) p53 stabilization is decreased upon NFkappaB activation: a role for NFkappaB in acquisition of resistance to chemotherapy. *Cancer cell* 1(5):493-503.

200. Sau A*, et al.* (2016) Persistent Activation of NF-kappaB in BRCA1-Deficient Mammary Progenitors Drives Aberrant Proliferation and Accumulation of DNA Damage. *Cell stem cell* 19(1):52-65.

201. Ohnishi S*, et al.* (2013) DNA damage in inflammation-related carcinogenesis and cancer stem cells. *Oxidative medicine and cellular longevity* 2013:387014.

202. Lu S*, et al.* (2016) MicroRNA-4262 activates the NF-kappaB and enhances the proliferation of hepatocellular carcinoma cells. *International journal of biological macromolecules* 86:43-49.

203. Bonizzi G & Karin M (2004) The two NF-kappaB activation pathways and their role in innate and adaptive immunity. *Trends in immunology* 25(6):280-288.

204. Hayden MS, West AP, & Ghosh S (2006) NF-kappaB and the immune response. *Oncogene* 25(51):6758-6780.

205. Krieger NS*, et al.* (2016) Increased bone density in mice lacking the proton receptor OGR1. *Kidney international* 89(3):565-573.

206. Chang J*, et al.* (2009) Inhibition of osteoblastic bone formation by nuclear factor-kappaB. *Nature medicine* 15(6):682-689.

207. Chadwick CC*, et al.* (2005) Identification of pathway-selective estrogen receptor ligands that inhibit NF-kappaB transcriptional activity. *Proceedings of the National Academy of Sciences of the United States of America* 102(7):2543-2548.

208. Kalaitzidis D & Gilmore TD (2005) Transcription factor cross-talk: the estrogen receptor and NF-kappaB. *Trends in endocrinology and metabolism: TEM* 16(2):46-52.

209. Mak P, Li J, Samanta S, & Mercurio AM (2015) ERbeta regulation of NF-kB activation in prostate cancer is mediated by HIF-1. *Oncotarget* 6(37):40247-40254.

210. Luo J*, et al.* (2016) LGR4 is a receptor for RANKL and negatively regulates osteoclast differentiation and bone resorption. *Nature medicine* 22(5):539-546.

211. Anfinsen KP*, et al.* (2011) Age-period-cohort analysis of primary bone cancer incidence rates in the United States (1976-2005). *Cancer epidemiology, biomarkers & prevention :*

a publication of the American Association for Cancer Research, cosponsored by the American Society of Preventive Oncology 20(8):1770-1777.